



Ancestral Grapes with Resistance against Dieback:
Molecular and Functional Analysis of Plant-pathogen Crosstalk in the Context of
***Botryosphaeriaceae* Related Dieback**

Zur Erlangung des akademischen Grades eines
DOKTORS DER NATURWISSENSCHAFTEN
(Dr. rer. nat.)

von der KIT-Fakultät für Chemie und Biowissenschaften
des Karlsruher Instituts für Technologie (KIT) genehmigte

DISSERTATION

von

Islam Maged Abdelazeem Khattab

aus

Ägypten

Dekan: Prof. Dr. Reinhard Fischer

Referent: Prof. Dr. Peter Nick

Korreferent: Prof. Dr. Eva Zyprian

Tag der mündlichen Prüfung: 09. Februar 2021



This document is licensed under a Creative Commons Attribution-NonCommercial-ShareAlike 4.0 International License (CC BY-NC-SA 4.0):
<https://creativecommons.org/licenses/by-nc-sa/4.0/deed.en>

“Printed out with the support of the German Academic Exchange service”

Die vorliegende Dissertation wurde am Botanischen Institut des Karlsruher Instituts für Technologie (KIT), Abteilung für molekulare Zellbiologie, im Zeitraum von April 2017 bis Februar 2021 angefertigt.

Eidesstattliche Erklärung

Hiermit erkläre ich, dass ich die vorliegende Dissertation, abgesehen von der Benutzung der angegebenen Hilfsmittel, selbständig verfasst habe. Alle Stellen, die gemas Wortlaut oder Inhalt aus anderen Arbeiten entnommen sind, wurden durch Angabe der Quelle als Entlehnungen kenntlich gemacht.

Diese Dissertation liegt in gleicher oder ähnlicher Form keiner anderen Prüfungsbehörde vor.

Zudem erkläre ich, dass ich mich beim Anfertigen dieser Arbeit an die Regeln zur Sicherung guter wissenschaftlicher Praxis des KIT gehalten habe, einschlieslich der Abgabe und Archivierung der Primardaten, und dass die elektronische Version mit der schriftlichen übereinstimmt.

Karlsruhe, Januar 2021

Islam Khattab

Table of contents

Table of contents

Acknowledgements	I
Abbreviations.....	III
Zusammenfassung.....	VI
Abstract	IX
1. Introduction	1
1.1. Worldwide consequences of Grapevine Trunk Diseases.....	1
1.2. Botryosphaeria dieback lifestyle; a silent killer.....	2
1.3. Virulence and symptoms of Botryosphaeria Dieback in grapevine.....	3
1.4. Plant defense mechanisms against intruders.....	6
1.5. Fungal signals manipulating <i>Vitis</i> responses	10
1.6. Defense mechanisms in the context of Grapevines trunk diseases.....	10
1.7. . Chemical control; A classical approach to avoid in favor of sustainable viticulture.....	12
1.8. The scope of the studies	13
2. Methodology	18
2.1. Screening wild grapes population for resistance against Botryosphaeria dieback.....	18
2.1.1. Phylogenetic analysis based on genome-wide SNPs	18
2.1.2. Plant material	18
2.1. 3. fungal material and inoculation.....	19
2.1.4. Changes of wood anatomy following inoculation.....	20
2.1.5. Detection of hyphae through Cryo Scan Electron Microscopy.....	21
2.1.6. Quantification of wood necrosis, hyphal growth, xylem vessels cross area.....	22
2.1.7. RNA extraction and quantitative real-time PCR.....	23
2.1.8, 9. Stilbene analysis and quantification and lignin measurement.....	25
2.2. The effect of drought on infection development and lignin accumulation.....	26
2.3. Methodology for Invitro studies dissecting the <i>Botryosphaeriaceae</i> - <i>Vitis</i> crosstalk triggering the Apoplexy phase.....	27
2.3.1. Plant cell lines and fungal materials.....	27
2.3.2. Screening effect of different phenylpropanoid derivatives on <i>N. parvum</i> aggressiveness.....	28
2.3.3. Extraction of fungal metabolites, HPLC and HPLC-MS analysis for the toxic fraction.....	29
2.3.4. Dissecting the signaling pathway of Fusicoccin A.....	30
2.3.5. Live imaging of cell cytoskeletons	33
2.3.6. Cytoskeletons manipulation.....	34
2.3.7. Cell death assays	34
2.4. Data Analysis.....	35
3. Results	37
3.1. Chapter 1: Identifying resistant chemotypes of grapevines against Botryosphaeria dieback.....	37

Table of contents

3.1.1 <i>Vitis vinifera</i> spp. <i>sylvestris</i> clustering after phylogenetic analysis based on genome-wide SNPs	37
3.1.2 Susceptibility towards <i>Botryosphaeria dieback</i> differs between stilbene chemotypes.....	37
3.1.3 Wood colonization of <i>Botryosphaeriaceae</i> is significantly impaired in hosts with resveratrol-viniferin chemotype.....	41
3.1.4 Resistance to fungal spread correlates well with the inducibility of <i>Stilbene synthase</i> transcripts.....	43
3.1.5 Resistance to <i>N. parvum</i> spread correlates with accumulation of resveratrol and viniferins.....	46
3.1.6. Susceptible grapevines respond to infection by higher lignin deposition.....	50
3.1.7. Bordered pits act as gateways for hyphal spread.....	51
3.1.8. Effect of drought on infection development and lignin accumulation.....	56
3.2. Chapter 2: Hunting the plant surrender signal switching the <i>Botryosphaeria dieback</i> to the apoplexy phase in grapevines.....	58
3.2.1. Screening fungal behavior towards defense precursors of phenylalanine pathway.....	58
3.2.2. Cellular response to Fusicoccin A.....	64
3.2.3. Mapping stress signaling of Fusicoccin A.....	67
3.2.3.1. Effect of blocking 14-3-3 proteins on the fusicoccin signaling pathway.....	70
3.2.3.2. Blocking RbOH manipulates Fusicoccin A signaling.....	72
3.2.3.3. Effect of microtubules manipulation on Fusicoccin A signaling.....	74
3.2.3.4. Effect of Actin filaments depletion on Fusicoccin A signaling.....	76
3.2.3.5. Overexpression of Metacaspases increased cell death triggered by Fusicoccin.....	78
3.2.3.6. Effect of Salicylic acid and MAPKs on the cell death triggered by Fusicoccin.....	78
4. Discussion.....	81
4.1. Chapter 1; Ancestral grapevines with resistance against <i>Botryosphaeriaceae</i> related Dieback....	82
4.1.1. A minimal experimental system for studying resistance against <i>N. parvum</i>	82
4.1.2. Wood architecture has no role in resistance against <i>Botryosphaeria dieback</i>	83
4.1.3. Resveratrol-viniferin metabolism as a resistance factor against <i>Botryosphaeria dieback</i>	84
4.1.4. Resistance or susceptibility – a matter of channeling phenylpropanoid metabolism?.....	86
4.1.5. Does drought increase fungal development and disease outbreak?.....	89
4.2. Chapter 2: A latent or necrotrophic phase- a matter of chemical communication between <i>N. parvum</i> and the host.....	90
4.2.1. Ferulic acid accumulation as a surrender signal triggering <i>N. parvum</i> to kill the host by fusicoccin A derivative.....	90
4.2.2. 14-3-3 proteins and ROS generation are necessary for Fusicoccin A signaling to drive the apoplexy phase.....	92
4.2.3. Cytoskeletons dynamics modulate Fusicoccin A signaling.....	93
4.2.4. Metacaspases as downstream targets of Fusicoccin A signaling.....	94
4.2.5. Visual model showing molecular events driven by Fusicoccin A signaling for triggering cell death.....	95
5. Concluding remarks and outlook.....	97
6. References.....	99
7. Supplementary.....	118
8. Publications.....	130

Acknowledgment

I sincerely thank *Allah* for all blessings, mercies, and graces given to me for achieving my dreams and my science journey in Germany to get my Ph.D. and overcome all dark moments in my life that made me who I'm.

Also, I'm very grateful to my supervisor, Prof. Dr. Peter Nick, for the ultimate support and kindness, not only in science, giving me a chance to join his lab but also in my life. He was always there to help and guide me either in science or my life issues. During my four years in KIT, he plants the seeds of goodness in the surrounding people and first takes care of human values and morals. He leads his team by heart before science, creating very lovely and scientific teamwork. I'm lucky to perform my Ph.D. and learn molecular cell biology under his supervision.

Furthermore, I would like to give my special thanks to Dr. Vaidurya Pratap Sahi to supervise and teach me a lot regarding histochemistry and plant anatomy and proof-reading the thesis . My gratitude is extended to Dr. Michael Riemann for supervising my molecular biology work during plant stress group meetings and his comments to improve the thesis.

I'm very grateful to the Botanical Garden team of Karlsruhe Institute of Technology for their professional support in growing the required *Vitis* plants for my experiments.

Special thanks to the partners, Eckhard Thines lab (Dr. Jochen Fischer) IBWF, Kaiserslautern, and Philippe Huguene lab, INRAE Institute, Strasbourg, France, and Nano-Imaging lab, University of Basel, Switzerland, for the successful and professional collaboration. I'm very thankful for my professors during my Bachelor's and master's studies who rooted in my soul the passion for plant physiology, especially Prof. Dr. Karim M. Farag, and Prof. Dr.

Acknowledgment

Said M. Gabr. Their recommendation letters as well as the endorsement letter for the DAAD-GERLS program, helped me also get a full Ph.D. scholarship.

My sincere gratitude is extended to Dr. Ahmed Ismail for his ultimate support, guidance, and orientation to prepare a competitive application for the DAAD-GERLS scholarship and to have a smooth and flexible start in the molecular biology world.

During my Ph.D. journey and daily lab-life, my colleagues at Nick lab helped me integrate and taught me a lot about molecular biology basics. Especially Dr. Adnan Kanbar, who helped me during my first days and taught me a lot in Biostatistics and experimental design. He is very social with cultural standards, which made both of us close friends at the family level. I'm very thankful for his daily support to me, in the lab, and to my family during life's ups and downs. Deep thanks to Christian Metzger for his collaborative spirit and for translating my abstract into the German language. Also, I'm very grateful and honored to have such teammates, study circle members, and friends in the lab; Pingyin, Ruipu, Peijie, Karwan, Sarheed, Eman, Christian, Winjing, Nasim, Pallavi, Daniela and Kinfemichael. Also, I got very precious help from students to have my work done and got the honor to be their lab-mentor especially; B.Sc. Judith Sum and M.Sc. Noemi Flubacher.

Last but not least, I dedicate this work to;

- my lovely mother's soul for her kindness, love, and taking care of me during my childhood. It is also dedicated to my dear father for his continuous support, encouragement, compassion, and prayers to finish my Ph.D. and come back to him, and to my sisters for their love and constant encouragement
- To my lovely small world and the goal of my life, "my family," my wife, Shaymaa, for sharing my life ups and downs, and taking care of our sons, "Omar and Elias". I will keep doing my best to provide you the best I can.

Abbreviations

GTDs: Grapevine Trunk Diseases

PAMPs: Pathogen-associated molecular patterns

DAMPs: Damage-Associated molecular patterns

PRRs: Pattern recognition receptors

PTI: PAMPs-triggered immunity

ETI: Effector-triggered immunity

HR: Hypersensitive response

NP: *Neofusicoccum parvum* Bt strain 67

SNPs: Single Nucleotide Polymorphism

Ke(xx): Ketsch genotype (xx)

dpi: days post-infection

Cryo-SEM: Cryo Scan Electron Microscopy

PHE: Phenylalanine

TYR: Tyrosine

CINN: trans-cinnamic acid

COUM: *p*-coumaric acid

CAFF: trans-caffeic acid

FER: trans-ferulic acid

RESV: Resveratrol

VINF: Viniferin

PIC: Piceid

PICEAT: Piceatannol

RZ: reaction zones

GFP: Green fluorescent protein

Abbreviations

Vrup-TuB6: *Vitis rupestris* cells with GFP-tagged β -tubulin (*AtTUB6-GFP*)

FABD2: a fluorescent fimbrin actin-binding domain 2 (*AtFABD2*)

MS medium: Murashige & Skoog medium

2,4-D: 2,4-dichlorophenoxyacetic acid

MYC. extract: mycelium extract

CF. extract: culture filtrate extract

MeCN: methanol acetonitrile

FCA: fusicoccin A

(AO/EB): A mixture of Acridine Orange and Ethidium Bromide dyes

CD: cell death

PM ATPases: Plasma membrane ATPases

ROS: reactive oxygen species

O₂⁻: Superoxide anion

NBT: Nitroblue tetrazolium

DPI: diphenyleneiodonium chloride

MeJA: Methyl jasmonate

SA: salicylic acid

ABT: 1-aminobenzotriazole

MTs: microtubules

AF: Actin filaments

Lat B: Latrunculin B

MAPK: Mitogen-activated protein kinase

PD98059: 2-(2-Amino-3-methoxyphenyl)-4H-1-benzopyran-4-one

PAL: *phenylalanine ammonia-lyase*

STS: *Stilbene synthase*

Abbreviations

ICS: *Isochorismate synthase*

PR: *pathogenesis-related protein*

CAOMT: *Caffeic Acid O-methyltransferase*

CAD: *Cinnamyl Alcohol Dehydrogenase*

SOD: *Superoxide Dismutase*

MC: *Metacaspase*

Zusammenfassung

Zusammenfassung:

Holzfäule und ähnliche Krankheiten bedrohen zunehmend den weltweiten Bestand an Weinbergen. Zwar wurden Weinstockkrankheiten bereits im zwölften Jahrhundert detailreich beschrieben, doch breiten sie sich in den letzten Jahrzehnten infolge des Klimawandels massiv aus und sorgen für erhebliche wirtschaftliche Einbrüche. Nach dem Verbot von Arsen in chemischen Behandlungsmitteln rückten vermehrt nachhaltige Strategien zur Kontrolle von Krankheiten in den Fokus.

Eine nachhaltige und sichere Alternative zu Fungiziden ist die Suche nach resistenten, nahen Verwandten der Kultur-Pflanze, um diese für die Resistenz-Züchtung zu verwenden. Eine Population von Wildreben (*Vitis vinifera* spp. *sylvestris*) hat auf einer Rheininsel überlebt und dort, wohlmöglich, unter natürlichem Selektionsdruck Resistenzen gegen *Botryosphaeria* entwickelt. Um die 89 individuellen Linien von *V. sylvestris* wurden im botanischen Garten des KITs eingelagert und kultiviert. Zusätzlich wurde das Genom der Pflanzen sequenziert und auf Single Nucleotide Polymorphismen (SNPs) gescreent. Repräsentative Linien aus verschiedenen Untergruppen der Population wurden mit Myzelium von *Neofusicoccum parvum* (Bt strain 67) angeimpft, um experimentell *Botryosphaeria*-Sterben zu induzieren. Die Anfälligkeit der verschiedenen Linien gegen *Botryosphaeria* wurde über die Ausbildung von Holznekrosen durch das Pathogen quantifiziert. Des Weiteren wurde die Verbreitung der Hyphen über das Xylem mittels Kryo-Scanning-Elektronenmicroscopie gemessen. Trotz unterschiedlicher Kolonisierungsmuster konnte keine Korrelation zwischen Holzstrukturierung und Infektionserfolg festgestellt werden.

Dennoch konnten anhand der Kolonisierungsmuster resistente und anfällige Genotypen bestimmt werden, die in Folge auf ihre Verteidigungsantworten untersucht worden. Dazu

Zusammenfassung

wurden das Metabolom-Profil und die Strady-State Transcript Level von Verteidigungsgenen untersucht. Eine HPLC-MS Analyse wies bei resistenten Genotypen eine hohe Ansammlung von Stilbenen gegen die Infektion auf, wobei zum Großteil unglykosylierte Viniferin Trimere gefunden wurden. Anfällige Genotypen hingegen wiesen generell weniger Stilbene auf. Diese waren sogar zu einem deutlich größeren Teil glykosylierte Stilbene wie kurzfristig Piceid und längerfristig größere Einlagerungen von Ligninen. Erste Studien deuteten auf ein Modell hin, nach welchem die resistenten Genotypen den Phenylpropanoid-Stoffwechsel schnell in Richtung unglykolysierter Stilbene umleiten. Zudem weisen diese Genotypen einen Chemotypen auf, der resistent gegen Weinstockkrankheiten ist und ebnet damit einen Weg für die Resistenz-Züchtung gegen *Botryosphaeria*-Sterben.

Es wurde des Weiteren erforscht, ob der von *Botryosphaeria* verursachte Apoplexie-Ausbruch in den Weinberg durch spezifische Pflanzensignale ausgelöst wird. Hier konnte ein neues Element in der Kommunikation zwischen Pflanze und Pathogen identifiziert werden; das „Surrender Signal“. Der Pilz wechselt zu einem nekrotrophen Verhaltensmuster, wenn er in der ständigen, auf chemischen Stoffen basierenden Kommunikation mit dem Wirt, ein Ansammeln von trans-Ferulasäure, einem Vorgänger von Lignin, erkennt. Wenn die infizierte Rebe unter Trockenstress gerät, was Klimawandel bedingt zunimmt, bildet die Pflanze erhöhte Mengen Lignin, welche mit steigenden Leveln an trans-Ferulasäure einhergehen. Dies erkennt der Pilz als eine Art Warnsignal, auf welches er durch den Wechsel zu einem sexuellen Lebenszyklus reagiert, infolgedessen der Wirt getötet wird. Dies ermöglicht dem Pilz Fortbestehen durch einen Wirtswechsel. Über eine „bio-activity-guided fractionation“ konnte das Polyketid eines Fusicoccin A Derivats als potenzielles Toxin identifiziert werden, das die Apoplexie in der Weinrebe verursacht.

Zusammenfassung

Nähere Untersuchungen zur Fusicoccin Stresssignalübertragung zeigten, dass das Toxin Plasmamembran ATPasen und die Generation von Superoxiden erheblich aktiviert. Zusätzlich reguliert es die Genexpression von Genen hoch, welche in *Vitis* Zellen den Phenylpropanoid-Stoffwechselweg, Phytohormon Signalwege, und Metakaspasen-abhängigen (*MC2* und *MC5*) regulieren. Fusicoccin beeinflusst zusätzlich die Struktur des Cytoskeletts, in dem es Mikrotubuli-Abbau und Aktin-Bündelung induziert. Verschiedene Faktoren zeigen wichtige Rollen in der Signalübertragung des Fusicoccin-Stresses, wie beispielsweise 14-3-3 Proteine, „Respiratory Burst Oxygen“ Homologe, das Cytoskelett und Metakaspasen (*MC2* und *MC5*).

Abstract

Abstract;

Vineyards worldwide face a severe threat of wood-decaying diseases recently. Although Grapevine Trunk Diseases were described in detail since the 12th century, they accentuated in the last decade, causing serious economic losses due to climate change. Sustainable strategies became an integral approach for constraining the disease outbreak in infected vineyards after banning the chemical control by Arsenates due to their ecotoxic effects

The first strategy to achieve sustainability and a safe alternative to fungicides is to search for resistant wild crop relatives for breeding host resistance. Following this hypothesis, an ancient wild grapes population (*Vitis vinifera* spp. *sylvestris*) survived under natural selection pressure in central Europe, along the Rhine river, were screened against *Botryosphaeria dieback*. Around 89 accessions of *V. sylvestris* population were harbored at the Botanical Garden of Karlsruhe Institute of Technology and genetically mapped based on whole-genome Single Nucleotide Polymorphism (SNPs). Representative accessions (from different subclades of the population) were inoculated with mycelia plugs of *Neofusicoccum parvum* Bt strain 67 as an experimental model causing *Botryosphaeria Dieback*. The susceptibility of the candidate genotypes towards *Botryosphaeria dieback* was measured by their ability to induce wood necrosis, and the hyphal coverage through infected xylem vessels using Cryo Scanning Electron Microscopy. While there were different colonization patterns among the tested genotypes, there was no correlation between wood architecture and infection success.

Nevertheless, the variable colonization patterns brought up resistant and susceptible genotypes, which were mapped for their defense responses using the steady-state transcripts of defense genes and metabolomics profiles. HPLC-MS analysis showed that resistant genotypes have a robust stilbenes accumulation against infection, which was significantly channeled towards non-glycosylated viniferin trimers. On the other hand, the susceptible lines accumulated less

Abstract

stilbenes with a substantially higher proportion of glycosylated stilbenes, in the form of piceid, in the short-term and higher lignin deposition in the long-term. The first study came with a model showing that the resistant genotypes allocate rapidly and specifically phenylpropanoid metabolism towards the non-glycosylated stilbenes. Besides, it pinpoints a resistant chemotype against grapevine trunk diseases and paves a way to resistance breeding against grapevine *Botryosphaeria* Dieback.

Further research was performed to identify whether the apoplexy outbreak, driven by *Botryosphaeriaceae* fungi in vineyards, is triggered by specific plant signals. This study arrived to a new level of plant-pathogen crosstalk, the so-called “plant surrender signal”. The fungus switches to the necrotrophic behavior based on chemical communication with the host when it accumulates a lignin precursor, trans-ferulic acid, as the targeted plant surrender signal. While infected grapevines synthesize more lignin under drought stress, which is commonly accentuated under current climate change, the fungus perceives trans-ferulic acid as an alert signal to kill the faint host and turn for sexual cycle searching for new hosts. After Bioactivity guided fractionation for the fungal metabolites, the polyketide “Fusicoccin A derivative” was identified as the potential toxin driving the apoplexy outbreak in grapevines.

Dissecting stress signaling of Fusicoccin showed that it strongly activated both plasma membrane ATPases and superoxide generation. In addition, it upregulated genes regulating the phenylpropanoid pathway, phytohormones signaling, and cell death signaling such as *Metacaspases* (*MC2* and *MC5*) in *Vitis* cells. Fusicoccin also changed cytoskeletons integrity, causing microtubules depletion and actin bundling. Many molecular players showed a crucial role in regulating Fusicoccin stress signaling, such as 14-3-3 proteins, Respiratory burst oxygen Homolog, cytoskeletons, and *Metacaspases* (*MC2* and *MC5*).

1. Introduction

1.1. Worldwide consequences of Grapevine Trunk Diseases

Grapevine trunk diseases (GTDs) became a severe worldwide threat for viticulture in the last decade. There are different forms of GTDs like *Botryosphaeria dieback* (Black Dead Arm), *Eutypa dieback*, and Esca syndrome. Such GTDs forms are driven by a wide range of causal agents, more than Forty different fungal strains colonizing grapevine wood (Bertsch et al., 2013). Among the GTDs forms, *Botryosphaeria Dieback* has increasingly caused severe economic damage not only in vineyards but also in the woody forests (Guan et al., 2016; Slippers & Wingfield, 2007). The pathogenicity of the *Botryosphaeriaceae* family has been strongly triggered by climate change to reach the current geographic spread in all woody plants (for review, see Coakley et al., 1999; Slippers & Wingfield, 2007). The classical approach of plant protection is to control potential pathogens using toxic chemicals. In the context of Grapevine Trunk Disease, this was achieved in the past by using arsenite, which is legally banned in Europe on reasonable grounds by the European Commission (2009). This classical strategy not only leaves harmful ecotoxic traces but also couldn't control pathogens that do not meet the Koch postulates since they are also present in healthy grapevines that are free of symptoms (Loeffler F. 1884).

To avoid the spread of Grapevine Trunk Disease, especially that conventional fungicides fail to control such diseases (Wagschal et al., 2008), most vineyards growers even root out the symptomatic infected plants. Alternatively, they use severe pruning to rejuvenate the trunk, but it needs 3-5 years to reach the productive stage again. So, no wonder that the different forms of GTDs, such as *Botryosphaeria dieback*, *Eutypa dieback*, and Esca syndrome, account for severe economic damage worldwide. For instance, in Europe, about 13% of French vineyards

were infected with financial losses ranging to more than 1140 million \$ per year (Fontaine et al., 2016). In old vineyards in Central and Southern Italy, even up to 60% - 80% were damaged by GTDs (Romanazzi et al., 2009). In California alone, the economic damage due to GTDs reached up to 256 Million \$ per year (Siebert, 2001), and similarly, drastic effects were found in infected vineyards of Australia (Sosnowski et al., 2008).

1.2. Botryosphaeria dieback lifestyle; a silent killer

The Botryosphaeria diseases of Grapevine are very complex syndromes that are poorly understood since the infection symptoms seem to depend more on the sanitary situation of the vineyards as clearly shown in **(Fig. 2)**. *Botryosphaeriaceae* species are classified as endophytes (Slippers & Wingfield, 2007), colonizing the perennial wood through pruning wounds, and subsequently living during a latent phase without any visible symptoms over the years (Djoukeng et al., 2009; Guan et al., 2016). By mysterious conditions that are poorly understood, probably when the host experiences severe stress conditions due to current global warming, the hitherto harmless endophyte convert to an active necrotrophic lifestyle, also known as the apoplexy phase **(Fig. 2)**, culminating in rapid killing of the host (van Niekerk et al., 2006; Slippers & Wingfield, 2007; Guan et al., 2016). The foliar symptoms, diagnostic for infected grapevines, only appear during this pathogenic phase, when the fungi already are committed to extremely aggressive pathogenicity, leading to the death of the colonized plant within few days (Bertsch et al., 2013). Also, the pathogenicity of different forms of GTDs was found more aggressive under drought stress (as a consequence of global warming) either in case of Esca syndrome (Lima et al., 2017) or Botryosphaeria dieback (Galarneau et al., 2019). Further epidemiological data indicate that drought and heat stress, resulting from global climate change, are linked with the higher incidence of this destructive behavior, the apoplexy phase, of Botryosphaeria dieback (Paolinelli-alfonso et al., 2016; Songy et al., 2019).

Also, accumulations of aromatic amino acids like phenylalanine and tyrosine were more pronounced in Esca-infected plants under drought stress (Lima et al., 2017). Also, either water stress marker genes (tonoplast intrinsic aquaporin and 9-cis-epoxycarotenoid dioxygenase 2) or phenylpropanoid genes like stilbene synthase and caffeoyl-CoA O-methyltransferase were altogether more active in apoplectic wood comparing to asymptomatic tissues in Esca-infected grapevines (Magnin-robert et al., 2016).

1.3. Virulence and symptoms of *Botryosphaeria* Dieback in grapevines; A Millennium of observations and ancient, (but sustainable) therapies.

The virulence of the *Botryosphaeriaceae* family in infected vineyards is variable. It can range from severe symptoms like in *Neofusicoccum spp*, over moderate forms, like in *Diplodia spp*, till very mild pathogenicity as reported after infection with *Dothiorella spp* (Úrbez-Torres, 2011). Moreover, there seem to be synergistic interactions. For instance, *Phaeoconiella chlamydospora* is by itself only weakly virulent but can evoke severe symptoms if combined with species from the *Botryosphaeriaceae*, such as *Neofusicoccum parvum* (Pierron et al., 2016; Úrbez-Torres et al., 2013). The complexity of *Botryosphaeria* dieback is extended even further that, so far, more than 20 fungal species of *Botryosphaeriaceae* family have been reported to cause pathogenicity leading to economically significant losses in viticulture (Bertsch et al., 2013).

Despite GTDs complexity, these pathogens share common symptoms when they switch to the necrotrophic lifestyle. For instance, the foliar symptoms pattern is similar: Leaves exhibit colored patches that expand later in consequence of interveinal necrosis giving typical leaf stripe characteristics (**Fig. 1b**). Furthermore, the symptoms develop to individual dead buds, extending through the new shoots' tips causing brown-colored lesions. The symptoms move

then towards the internodes bases, and, eventually killing the whole new shoots, culminating in so-called dieback (as noticed in **Fig. 1c**) and reported by Guan et al. (2016), Bertsch et al. (2013), and van Niekerk et al., (2006). As a result, a devastating breakdown happens in the entire infected vine, which turns into a corpse with a complete yield loss, completely dry clusters (**Fig. 1a,c**), so-called Apoplexy outbreak.

Anatomical investigations in the infected wood of grapevines either by *Botryosphaeriaceae* spp, Eutypa dieback or the Esca disease showed that the fungal hyphae colonize the xylem vessels, fibers, and parenchyma rays (Gómez et al., 2016; Pouzoulet et al., 2014). Although *Vitis* wood is endowed with a robust vascular system with wide vessels, GTDs disrupt the water transport by blocking xylem vessels through the formation of tyloses and black gums or by the fungal mycelia itself (Edwards et al., 2007).

On the other hand, symptoms-dependant GTDs were explained not only by secreted fungal phytotoxins which accumulate in the foliar system following the transpiration stream but also as a result of the hydraulic failure as well as loss in the integrity of blocked xylem vessels by tyloses and gels due to infection (Bortolami et al., 2019). In parallel, susceptibility to Esca syndrome in grapevines was correlated with the xylem vessels diameter, where the wider xylem vessels observed in the *Vitis vinifera* cv. Thompson seedless, were linked to its susceptibility (Pouzoulet et al., 2017).

Interestingly, the pathogenicity of GTDs was described in detail in historical resources from the medieval ages, either in Al-Andalus (the Arabic empire in Spain in the 12th century) or later in the 14th century in Bologna, Italy (Mugnai et al., 1999). *Ibn-ALawam*, the Andalusian scientist, described in his book, *Kitab Al-Filaha* (book of Agriculture), that the GTDs symptoms start at the end of July, where the leaves get the red color, then tendrils and shoots

(which carry symptomatic leaves) turn to black with dying stems. Afterwards, the clusters would dry, and the symptomatic vine eventually would be deceased. The viticulturists of the 12th century adopted at that time a sustainable therapy, and meanwhile forgotten, based on cow urine (containing ammonium compounds that are expected to interfere with nitric oxide). Nitric oxide might modulate the expression of *Phenylalanine Ammonia Lyase*, which controls the first step of the phenylpropanoid pathway (the main defense pathway in grapevines) by cleaving the amino group from the phenylalanine amino acid.



Fig. 1. Typical apoplexy outbreak symptoms due to Grapevine Trunk Diseases after the hot summer of 2018 in the grapevines farm of the State Viticulture Institute, Freiburg, Germany. A) a severely damaged vine due to infection between two symptoms-free plants. b) Dieback

development towards a new fruiting shoot base with dried clusters. c) Typical leaf stripe characteristics.

1.4. Plant defense mechanisms against intruders

Plants have a wide range of defense mechanisms against the invaders and come in three forms: avoidance, tolerance, and resistance, as reported by Priyadarshan (2019). The avoidance mechanism carries out always before the interaction with parasites decreasing the chances and the success of infection. In general, the avoidance is more efficient against animal invaders since it's running almost by morphological features like wax, resin, or Thorns. The other two forms appear after the success of microbial contact; when the host is able to survive by pushing back the invader decreasing its growth rate, the defense mechanism is defined as resistance, while the third for, tolerance, means the ability of the host to survive with a little damage despite the stress. Resistance is the most efficient form against pathogens, and it's employed by chemical defense mechanisms against pathogens.

In general, plant immunity is composed of two layers: i. the first layer is A general, basal defense, termed Pathogen Associated Molecular Patterns (PAMP)-triggered immunity, PTI, is activated by generic molecules from microbial surfaces, perceived by pattern recognition receptors (PRRs). By such receptors, the plant cell recognizes the pathogen attack and activates defense genes to stop the infection progress (Stael et al., 2015). Some endogenous plant signals (triggered by plants either under biotic or abiotic stress) could also activate the PTI. Such plant signals are released due to pathogen attack or the abiotic stress termed as Damage-Associated Molecular Patterns (DAMPs) (Hou et al., 2019). The perception of DAMPs / PAMPs takes place in the plasma membrane surface by localized receptors activating a wide range of defense

responses like secreting phytoalexins, which have antimicrobial activity against the intruders and for damage repair (Chuberre et al., 2018).

ii. The second layer of plant immunity is a strain-specific “so-called effector-triggered immunity (ETI)”, is often deployed in response to biotrophic pathogens and usually (but not always) culminates in hypersensitive cell death, where the infected plant cells kill themselves for the sake of the other cells and by this block the spread of the pathogen that otherwise would quell PTI by secreted pathogenic effectors (Jones and Dangl, 2006).

1.4.1. PAMP triggered immunity (PTI) in grapevines

In grapevine, Stilbene phytoalexins is a central element of PTI in grapevines, and can be triggered by pathogens, such as *Plasmopara viticola*, the causative agent of Downy Mildew (Pezet et al., 2004). In Viticulture PTI could be upregulated by a wide spectrum number of generic term elicitors. For Instance, bacterial elicitor (flg22) upregulated the stilbenes biosynthesis strongly and caused an obvious depletion in cytoskeletons either cortical microtubules or actin filaments (Chang et al., 2012; Guan et al., 2020). Also, chitin, the main substance from the fungal cell wall, was classified as PAMP elicitor activating the stilbenes biosynthesis in grapevines, where the fungal chitooligosaccharides are perceived by specific receptors called LysM receptor kinases, *Vvlyk1-1 and Vvlyk1-2*, triggering down stream events of basal defense. (Brulé et al., 2019). Furthermore, DAMPs plant signals like salicylic acid or Methyl jasmonates play a central role in activating the basal defense and triggered *Vitis* cells to synthesize bioactive stilbenes like trans-resveratrol (Belchí-Navarro et al., 2013). Chang et al. (2017) found in a similar manner that the synthesis of bioactive resveratrol and viniferins is accompanied by the accumulation of jasmonates and subsequent jasmonate signaling evident from the activation of *JAZ* genes.

It's worth noting that stilbenes derive from phenylpropanoid metabolism and are found in 72 different plant species from different families. In *Vitis*, the genome-wide analysis revealed that *Stilbene synthases* (*VvSTS*) are organized in a multigenic family with 48 members that respond differentially to UV, wound, or pathogens (Ismail et al., 2012; Parage et al., 2012; Vannozzi et al., 2012).

1.4.2. Plant signals manipulating the PAMP-triggered immunity in grapevines

Many molecular players regulating the signaling of PTI and stilbenes biosynthesis were identified in *Vitis*. For instance, the activity of calcium channels localized on plasma membrane triggered the promotor of *Stilbene Synthase* gene either in the European grapevines (*Vitis vinifera*) or the Chinese wild grapes *Vitis pseudoreticulata* (Jiao et al., 2016). Also, plasma membrane respiratory burst oxygen homolog accumulated high reactive O₂ species (ROS) in response to the bacterial elicitor, flg22 (Chang & Nick, 2012). Likewise, Brulé et al. (2019) found that the fungal elicitors, chitoooligosaccharides, chitin, and chitosan, induced the expression levels of *Respiratory burst Oxygen Homolog* (*RbOHD*) in *Vitis* plants. Furthermore, the Mitogen-activated protein kinases (MAPKs) signaling pathway is necessary to activate the basal defense in grapevines, either by its negative feedback on apoplastic alkalinization activating the phytoalexins genes (Chang & Nick, 2012).

By dissecting the genetic factors triggering stilbenes biosynthesis in Ancient wild grapes (*Vitis vinifera ssp. sylvestris*), which are known for high stilbenes inducibility under different forms of stress, a specific allele of the transcription factor, *myb14*, found to promote stilbene inducibility as a resistant factor against biotic stress (Duan et al., 2016). In the same study, calcium channels, RbOH, MAPK cascades, and jasmonates were implicated altogether as upstream signals for activating the *myb14* promoter. In a similar way to PAMPs signaling,

DAMPs elicitors like xyloglucans or oligogalacturonides activate phytoalexins biosynthesis and callose deposition by activation ROS generation and MAPK cascades activity (Claverie et al., 2018).

Plant cytoskeletons, with their dynamic intracellular networks, play a central role in microbe's perception and manipulating defense signaling. In grapevines, treating *Vitis* cells by oryzalin for depleting microtubules or Taxol for microtubules stabilization enhanced the expression pattern of phytoalexin genes *stilbene synthase* and *resveratrol synthase* in grapevines. A similar pattern was observed while manipulating actin filaments either by depletion with Latrunculin B or by stabilization with Phalloidin (Qiao et al., 2010). In the context of pathogen perception, there was an apparent microtubules depolymerization in *Vitis rupestris* cells towards five min treatment of culture filtrate of the fungal strain *Eutypa lata* E16012 (Guan et al., 2020). Regarding the actin filaments, Henty-Ridilla et al. (2013) reported Microbe-Associated Molecular Patterns (MAMPs) peptide could rapidly change the actin filament organization activating the basal defense signaling.

1.4.3. Effector-triggered immunity (ETI) in grapevines

Effector-triggered immunity is the main key player against biotrophic pathogens when it provokes hypersensitive cell death in the host, killing the biotrophic pathogens by constraining their reproduction (Delaye et al., 2013). In grapevines, hypersensitive cell death enhanced resistance against *Plasmopara viticola*, the causative agent of Downy Mildew (Trouvelot et al., 2008; Boubakri et al., 2012). Besides, Gong et al. (2019) showed that the observed resistance of the American wild grapes, *V. rupestris*, against Downy Mildew is linked with their potential for robust hypersensitive cell death.

1.4.4. Plant signals regulating Effector-triggered immunity (ETI) in grapevines;

Many molecular regulators of hypersensitive cell death were detected in grapevines. Among them, resveratrol, the phytoalexin which is accumulated in response to PAMPs like flg22 or DAMPs like xyloglucans (Chang & Nick, 2012; Claverie et al., 2018), triggers many molecular responses triggering the hypersensitive-related cell death. For instance, Resveratrol boosted the ROS generation and actin bundling earlier before observing high mortality rates in *Vitis* cells (Chang et al., 2011). Similarly, changes in the dynamics and the organization of the actin filaments, whether actin bundling or depolymerization, induce programmed cell death (Smertenko & Franklin-Tong, 2011; Chang et al., 2015; Akaberi et al., 2018). Metacaspases are also involved in regulating different cell death types in plants, where Metacaspase 9 (*AtMC9*) controls the autolysis of xylem elements during developmentally programmed cell death (Bollhöner et al., 2018). Two metacaspases proteins in *Vitis* plants, *MC2* and *MC5*, were addressed for their potential as executors tools regulating hypersensitive cell death (Gong et al., 2019).

1.5. Fungal signals manipulating *Vitis* responses

Concerning the fungal counteraction, *Botryosphaeriaceae spp.* was reported for secreting phytotoxic polyketides activating plant immunity and causing pathogenicity. For instance, *Neofusicoccum parvum* secretes terremutin polyketide, which caused leaf necrosis and triggered the genes regulating the flavonoid biosynthesis pathway (Abou-Mansour et al., 2015). Also, *Neofusicoccum luteum* secreted the very toxic polyketide, neoanthraquinone, which caused robust shriveling in *Vitis* leaves (Pescitelli et al., 2020). There is a widespread synthesis of mellein in the *Botryosphaeriaceae* family; three *Neofusicoccum* species were identified in Australia secreting mellein and its isomer hydrorxymellein. It's worth mentioning that mellein

polyketide was classified as a pathogenicity factor of *Botryosphaeriaceae* related Dieback, since the fungal strains *Neofusicoccum parvum* Bt-67 and *Neofusicoccum parvum* S-116, which represent the aggressive genus *Neofusicoccum*, secreted more mellein than the moderate-aggressive genus *Diplodia* (Ramírez-Suero et al., 2014). In previous work, no defense responses were noticed in response to O-methyl mellein alone. However, it amplified *Vitis* immunity driven by bacterial elicitor, flg22, either in the accumulated transcripts of phytoalexins genes or in manipulating the cytoskeletons responses (Guan et al., 2020).

1.6. Defense mechanisms in the context of Grapevines trunk diseases

For the context of GTDs, PTI is associated with changes of cell wall composition: Cellulose accumulation during the synthesis of secondary cell walls weakens PTI, while deposition of pectin polysaccharides strengthens the resistance of *Arabidopsis thaliana* against *Botrytis cinerea* and *Pseudomonas syringae* (Bethke et al., 2016; Hernandez-Blanco et al., 2007). Along the same line, impaired PTI can be linked with elevated lignification, which might, therefore, act as a backup mechanism to pathogen penetration, similar to the callosic plugs that are characteristic for basal immunity (Bacete et al., 2018).

Due to the endophytic lifestyle of the *Botryosphaeriaceae* (Slippers & Wingfield, 2007), the cell wall represents the main battlefield of *Vitis-Botryosphaeriaceae* crosstalk. For several GTD related fungi, histochemical changes of the cell wall are known: Suberin accumulation, albeit to variable amplitude, have been reported for *Eutypa lata* dieback, but also for Esca in the infected mature grapevine internodes (Rudelle et al., 2005). For lignin, there is conflicting evidence: In case of *Phaeoconiella chlamydospora*, not any lignin response was detected after staining with either Phloroglucinol-HCl or Fuchsin (Lorena et al., 2001). By contrast, the infection with *Eutypa lata* enhanced lignin deposition in the neighborhood of infected xylem

vessels, which was interpreted as a wood reaction against lignin-degrading enzymes secreted by the *E. lata* mycelia (Mutawila et al., 2011; Rudelle et al., 2005). Such enzyme activities (e.g. Mn-dependent peroxidases and laccases) were also detected in three fungal strains causing Botryosphaeria dieback, namely, *Neofusicoccum parvum* Bourgogne S-116, *Neofusicoccum parvum* Bt strain 67, and *Diplodia seriata* 98.1 (Stempien et al., 2017). Therefore, it is a reasonable hypothesis to expect histochemical changes in the host-cell wall in response to *Botryosphaeriaceae* colonization. However, this has not been addressed experimentally so far.

Resveratrol and its oxidised derivatives, the viniferins, have been described as key players of basal defense in *Vitis*, deterring different pathogens as different as the Oomycete *Plasmopara viticola*, causing Downy Mildew, the Ascomycete *Erysiphe necator*, causing Powdery Mildew, and the Oomycete *Botrytis cinerea*, causing Grey Mold (Duan et al., 2015; Jiao et al., 2016; Rasclé et al., 2015; Adrian & Jeandet, 2012). Due to this wide range of targets, the stilbene pathway might also play a role in the defense against Botryosphaeria dieback. In the context of *Botryosphaeriaceae-Vitis* crosstalk, comparative *in-vivo* infection studies in grapevines showed upregulation of *VvSTS* genes (Guan et al., 2016; Spagnolo et al., 2014). Likewise, a proteinaceous extract collected from Botryosphaeria culture filtrates induced resveratrol and viniferins synthesis in cell cultures from *Vitis rupestris* and *V. vinifera* cv. 'Gewürztraminer' (Stempien et al., 2018). Consequently, different metabolism profiles were noticed in *Vitis* plants after infection with *Neofusicoccum parvum*. There was a considerable decrease in the primary metabolites like sugars followed by high secondary metabolites content like stilbenes derivatives (Labois et al., 2020). In addition, fungicides, such as Sodium Arsenite, which showed a successful disease control in infected vineyards, enhanced the antioxidant activity as well as the expression of defense genes like *Stilbene synthase* and *Pathogenesis-related protein 1*. However, the application of Arsenates as a chemical control approach is not suitable against

GTDs not only due to the ecotoxic effects of arsenates but also because the pathogens can live for years in symptoms free host during the latent phase.

1.7. Chemical control; A classical approach to avoid in favor of sustainable viticulture

Biotic stress led to severe economic losses in grapevines, which motivated the viticulturists to overuse chemical control to save the vineyards. In Europe, up to 75% of the fungicides are implemented for vineyards protection (Duan, 2015). Although the chemical control was very efficient and supported the green revolution to face famines in the last century, it led to new races of the pathogens, over time, with resilience against the pesticides. As a result, the chemical control does not show up currently a decrease in the worldwide economic damage driven by fungi in spite of their ecotoxic footprints. Consequently, counting on host resistance by breeding programs represents a sustainable alternative for viticulture. However, host resistance against virulent pathogens relies on plant-pathogen coevolution dynamics, which means resistance breeding is an evolving process (Priyadarshan, 2019). So, the wild crop relatives and landraces (established by natural selection) are targeted recently in the resistance breeding approaches. For instance, the North American and Chinese wild grapes, despite their foxy taste, were attracted by grapevine breeders. Such wild relatives evolved specific ETI against Ascomycete, *Erysiphe necator*, which has a biotrophic lifestyle, triggering the infected plant cells to suicide quickly before the onset of the fungal sexual cycle. Such defense mechanism succeeded in preventing *Erysiphe necator* spread (Gessler et al., 2011; Pap et al., 2016).

1.8. The scope of the studies

The main scope of the studies is to find out smart and sustainable strategies for mitigating disease outbreak in the context of Grapevine trunk disease. To reach this, there should be, at

first, a clear working model (**Fig.1**) or insight for the wood-decaying fungi interaction with grapevines to predict plant resistance factors and disease outbreak stimulators. Thus, this approach was formulated by two leading hypothesis-driven research;

A) Ancestral wild grapes for sustainable viticulture against *Botryosphaeria dieback*

The main idea is to test whether genetic differences related to stilbenes inducibility contribute to genetic differences with resistance against *Botryosphaeria dieback*. To achieve this, both preconditions have to be met: (1) a set of genotypes that contrast with respect to stilbene inducibility. (2) these genotypes should also be genetically closed to reduce the effects of general genetic background.

Both preconditions can be reached by going back to origins and screening wild grapes relatives that survived under natural selection pressure. For this, *Vitis vinifera* spp. *sylvestris* wild grapes, the ancestor of European grapevines, were selected using the germplasm collection cultivated in the Botanical Garden of the Karlsruhe Institute of Technology (KIT). The harbored *sylvestris* population extended by around 100 genotypes representing the entire wild and ancient domesticated grapevines (*Vitis. vinifera* L. spp. *vinifera*) in Germany. Nevertheless, this collection offered noticeable genetic variability, along with other wild grapes populations of *V. vinifera* ssp. *sylvestris*, in Europe, based on SSR markers (Nick, 2014). Around 89 genotypes of *V. sylvestris* population were further triggered by a UV pulse to identify the potential for stilbene inducibility. *V. sylvestris* population varied considerably, leading to the definition of two chemotypes (Duan et al., 2015). i) α -piceid chemotype produced reasonable amounts of stilbenes, and these preferentially having the form of the biologically inactive glycoside. ii) Resveratrol-viniferin chemotype boosted the stilbenes accumulation, which usually came in non-glycosylated forms like cis-resveratrol, *trans*-resveratrol, and its oxidative oligomers, especially the viniferins. Representatives of this resveratrol-viniferin chemotype also exhibited

high resistance to *P. viticola*. A large part of the *sylvestris* population has been fully sequenced (Liang et al., 2019), which allows to define contrasting pairs of genetically close genotypes but differ with respect to stilbene inducibility.

The working hypothesis gives rise to the suggestion that the genotypes belonging to the resveratrol-viniferin chemotype should be significantly more resistant against *Botryosphaeria dieback* as compared to their inactive-stilbene relatives. This implication was investigated using controlled inoculation with *Neofusicoccum parvum* Bt strain 67, one of the most virulent fungal strains causing grapevine trunk diseases (Guan et al., 2016; Stempien et al., 2017). The spread of the fungal colonization was measured to assess the degree of resistance, but also tested cellular and molecular aspects of colonization and host response. The colonization of xylem vessels was investigated by Cryo-SEM, detected, and quantified histochemical changes in the host cell walls. Also, the steady-state transcript levels of genes regulating phenylalanine channeling were quantified; such as *Phenylalanine Ammonium Lyase (PAL)* as the first committed step of the phenylpropanoid pathway, representative members of the *stilbene synthase* family, two key genes regulating lignin biosynthesis; *Caffeic Acid O-methyltransferase (CAOMT)* and *Cinnamyl Alcohol Dehydrogenase (CAD)* as antagonistic channeling to stilbenes metabolites and *VvJAZ1* as a readout for jasmonate signaling. The local responses were scored in the inoculation site. To detect potential systemic responses, probing sites in defined distances above and below the inoculation site were analyzed. The obtained data are consistent with a causal link between stilbene induction and *Botryosphaeria* resistance but also add new facets to our understanding of fungal spread, manipulation of the host by the pathogen, and molecular hallmarks for the successful defense of the host.

B) Hunting the plant surrender signal triggering *Botryosphaeria* dieback outbreak.

The second hypothesis was ventured that the *Botryosphaeriaceae* related apoplexy in grapevines might be linked with conditional changes in the chemical communication between the host (*Vitis* plants) and the intruder (the fungus) as clearly displayed by the working model below (**Fig. 2**). The same aggressive fungal strain, *Neofusicoccum parvum* Bt-67, was chosen for addressing *Botryosphaeriaceae-Vitis* crosstalk. Since disease symptoms outbreak commonly appears during hot summers (**Fig. 1**), common defense signals (from the phenylpropanoid pathway) against drought were tested to see whether they could change the fungal behavior.

Using an invitro cell-based experimental system, the effect of lignin precursors (which are commonly accumulated macromolecules in grapevines under abiotic stress conditions) on the subsequent fungus aggressiveness was investigated. The followed system was appropriate for hunting the plant signal triggering the *Botryosphaeriaceae* necrotrophic lifestyle. Using bioactivity guided fractionation, the adopted fungal mechanisms regulating aggressiveness behavior were discovered. Moreover, the stress signaling of potential polyketides leading apoplexy was addressed in *Vitis* cells using cellular and molecular aspects.

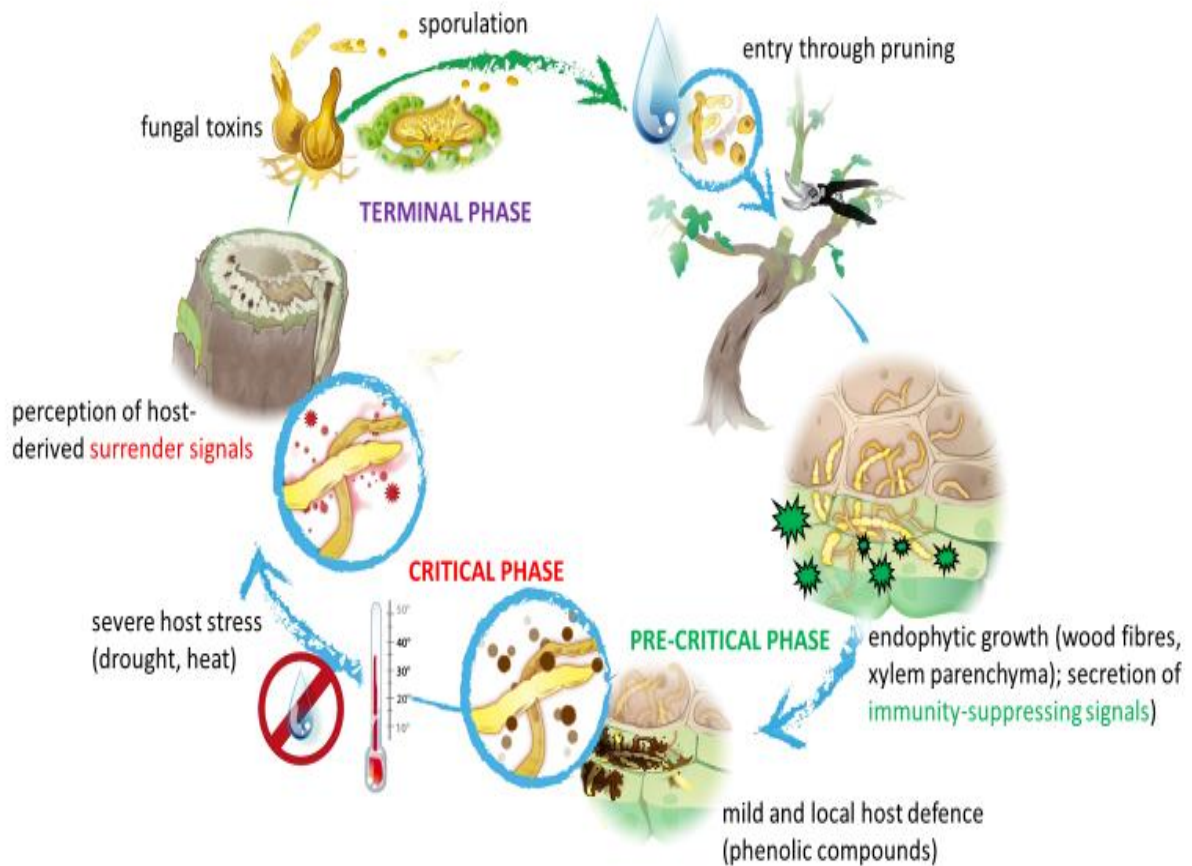


Fig. 2. Working model on host-pathogen interaction during *Vitis-Botryosphaeria* Dieback used to structure the current study. After entry through pruning wounds, the fungus first colonizes wood fibers and xylem parenchyma and is contained by a local and mild defense response of the host (accumulation of phenolic compounds). Host defense is partially quelled by immunity-suppressing signals secreted by the endophyte. This pre-critical phase can last for years, and under favorable conditions, will not impair the productivity nor vigor of the host. However, if the host is shifted under severe stress such as heat or drought, the critical phase can be initiated. Here, the stress-dependent, chronic loss of physiological homeostasis of the host results in molecular changes that can be perceived by the fungus as surrender signals and activate a switch from asymptomatic endophytic growth to necrotrophic phase killing of the host. Therefore, this critical phase is followed by a terminal phase, where the fungus is producing toxins and initiates sporulation and formation of fruiting bodies resulting in the death of the host and the spread of spores that can colonize neighboring vines.

2. Methodology:

2.1. Screening wild grapes population for resistance against *Botryosphaeria dieback*

2.1.1. Phylogenetic analysis based on genome-wide SNPs: Genome-wide analysis based on SNPs has been performed and reconstructed in a phylogenetic tree for 89 *Vitis* genomes representing European *Vitis vinifera* varieties, Asian species, American species, in addition to a collection of ancient wild grapes of *Vitis vinifera* spp. *Sylvestris*, as displayed in **Fig (3)**. Genomic DNA was extracted from leaves of the 89 *Vitis* genotypes for sequencing library construction, then Paired-end sequencing libraries, with 150 bp size, were sequenced following the methodology of previous work (Liang et al., 2019).

Pinot noir genome was used as a reference genome (PN40024), obtained from the Genoscope website (<http://www.genoscope.cns.fr/externe/GenomeBrowser/Vitis/>). The sequencing reads were mapped against the Pinot noir genome by BWA software for mapping Paired-end resequences of the respective accessions. SAMtools software was implemented then for filtering out the unmapped reads (H. Li & Durbin, 2010; H. Li et al., 2009). Duplicated reads were discarded using the Picard package (<http://picard.sourceforge.net/>). The phylogeny was designed based on whole-genome SNPs using SNPhylo software (Paterson et al., 2014) as described in (Liang et al., 2019). The Phylogeny visualization and coloring of the diverged clusters were conducted using iTOL browser (<http://itol.embl.de/>).

2.1.2. Plant material: To address the role of stilbene inducibility, contrasting pairs of an ancestral wild grapes population belonging to *Vitis vinifera* spp. *sylvestris* and collected from Ketsch peninsula in the Rhine valley between Karlsruhe and Mannheim, Germany. This population has been cultivated and propagated in the Botanical Garden of the Karlsruhe Institute of Technology (Duan et al., 2015). The following pairs of *V. sylvestris* accessions

were included in the study because they were genetically close but contrasting with respect to stilbene inducibility: Ke13 (low stilbene activity) and Ke15 (high stilbene activity); Ke28b (low) and Ke28c (high); Ke94 (low) and Ke95 (high), along with Ke30 and Ke33 (both low), and the *vinifera* cultivar Chardonnay, as a model for susceptible grapevines to wood-decaying diseases (Guan et al., 2016) and as a reference for evaluating other tested genotypes. For each genotype, 40 wood cuttings were prepared from mature canes, one year of age during winter pruning 2017 at the Botanical Garden of the Karlsruhe Institute of Technology, and stored at 4° C. Wood-cuttings (having 3 buds) were moved for cultivation in the greenhouse on March 15th 2018, with a photoperiod of 16 h light and 8 h dark at a temperature of 22 °C and 8 °C (day and night, respectively) using small pots containing peat-moss soil and Perlite (1:1), whereby the basal bud was stuck into the soil. After 4 weeks, the rooted wood cuttings got 2 new shoots from the 2 upper buds, and the lower shoot was removed 2 weeks later. After 8 weeks, the foliar system of the plantlets had become vigorous enough to transfer them to bigger pots (15 cm x 15 cm in width, 20 cm in height). The potted plants were equidistantly in a density of 9 plants / m².

2.1.3. Fungal material and inoculation: In the first week of June at a greenhouse temperature rising till 32 - 35° C at midday, each genotype was partitioned into 3 independent experimental sets: 3 unwounded plants as a negative control, 9 wounded plants but not inoculated (served as mock plants), and 9 wounded plants were subjected to the full inoculation treatment with an aggressive fungal strain, *Neofusicoccum parvum* Bt-67, (Guan et al. 2016) kindly provided by Laboratoire Vigne Biotechnologies et Environnement EA-3991 Université de Haute-Alsace, Colmar, France. A small hole (3 mm diameter until reaching the pith area of the wood) was drilled into both mock and infected individuals in the center of the second internode between the second and third bud from which the new shoot emerged (**Fig 3, position B**).

As inoculum, mycelia cultivated for 10 d on Potato Dextrose Agar, PDA, (Sigma-Aldrich, Deisenhofen) were collected by sterilized scalpel from the agar plate and filled into the hole and wrapped tightly with Parafilm. To sterilize the prepared holes of mock plants, they were sprayed with 80% ethanol after drilling the wood and wrapped directly with Parafilm.

2.1.4. Changes of wood anatomy following inoculation

To assess histological changes caused by fungal infection as well as the course of fungal colonization, wood samples were collected from the infection site 2 months after infection. Ke13, Ke15, Ke94, Ke 95, and Chardonnay the infection site and wrapped immediately with parafilm to prevent evaporation. The collected wood samples from Ke13, Ke15, Ke94, Ke 95, and Chardonnay were fixed for 2 days in fixative solution of (4 % w/v Paraformaldehyde, 0.114 % w/v EGTA, 1.512 % w/v PIPES and pH 6.8 using NaOH 1M) (Horn et al., 2012) before washing 3 times for 1 hour by PIPES buffer (1.5 % w/v PIPES with pH 6). The prolonged washing time was required to ensure full equilibration in the lignified specimens. After washing, the samples were dehydrated by passage through an ethanol gradient (ethanol 30% for 1 hr – ethanol 50% for 1 day – ethanol 70% for 6 hrs – ethanol 90% for 1 day – ethanol 100% for 1 hr, followed by a second wash for 1 day). Afterwards, samples were incubated directly in xylol 100% for 2 days, replacing the solvent every 12 hr, and eventually embedded in Paraffin wax (Paraplast, Carl Roth GmbH; Germany) by passage through a gradient of for 1 week xylol: Paraffin (1:1) - , followed by another week of xylol: Paraffin (1:2) for 1 week interval, opening the tubes from the 5th day. The last embedding step was Paraplast 100%. All embedding steps were performed under the fume hood in a drying oven at 56°C. From the embedded specimens, cross sections of 20 µm thickness were made by a microtome (Jung, Heidelberg) and collected in small water droplets, placed on chrome-gelatine-coated slides (0.2

w/v% gelatine with 0.01% CrK (SO₄)₂ · 12(H₂O)), such that after evaporation of the droplets, the sections adhered to the coated slide.

The slides with sections were kept on a hot plate at 40-50°C for 2-3 hours until complete dryness. Before staining, cross sections were rehydrated. Paraffin was removed by washing the cross-sections twice for 5 min in xylol, followed by washing in iso-propanol for 5 min. Afterwards, the sections were rehydrated, passing through an inverse ethanol gradient (100 %; 80%; 50%; 30%; 0%) using intervals of 5 min for each step. The different sections obtained from one specimen were grouped into different sets stained with various dyes: The first set was stained for lignin for 5 minutes in 1% (w/v) Phloroglucinol (Sigma Aldrich, Deisenhofen; Germany) in 18% HCl. In the presence of lignin, this dye yields a red to rose-red color (Soukoup 2014). The second set was stained for pectic polysaccharides for 5 minutes with 0.05% (w/v) Ruthenium Red (Carl Roth GmbH, Germany), which stains pectin pink or pink-red color. To get an overall histochemical impression of the cell wall composition, a third set was stained with 0.1% Toluidine Blue (Sigma Aldrich, Deisenhofen; Germany), giving dark blue color for lignin detection and lighter purple color for pectic polysaccharides. For all dyes, the sections were re-washed with iso-propanol and xylol and embedded in Entellan New (Merck, Darmstadt; Germany) as a rapid mounting medium for microscopy. Images were captured using digital light microscopy (Axioscope and Axio-Cam, Zeiss; Jena).

2.1.5. Detection of hyphae through Cryo Scan Electron Microscopy:

To detect hyphae colonizing grapevine trunks, samples were taken from two genotypes endowed with high stilbene inducibility (Ke15, Ke95), along with Chardonnay as susceptible genotype, and transferred to the Nano-imaging Lab, Basel University, for investigation by Cryo Scan Electron Microscopy (Philips XL30 ESEM) with a Cryo Preparation Unit Gatan Alto

2500. Wood cross sections were cut into specimens with 0.1 cm thickness and fixed by glue, Tissue-Tek® O.C.T (Sakura® Finetek, USA) on a cryo transfer holder, dipped into the cryo unit full of Nitrogen slush for screening directly (due to the lignification, no further measures to preserve tissue integrity were required), and inserted.

2.1.6. Quantification of wood necrosis, hyphal growth, xylem vessels cross area:

To evaluate the susceptibility of the different grapevine accessions, the resulting wood necrosis from the infection was measured one week after the infection using quantitative image analysis in the ImageJ software (<https://imagej.nih.gov/ij/>). The necrotic wood area in a median section of the infected internode of the respective genotype was measured as reported earlier (Guan *et al.*, 2015) with minor modifications. The necrosis area was not represented as an infected cross-area comparing to the infected internode since the length of the infected internodes was variable among the genotypes, such that the obtained value would be misleading. Instead, the necrotic area was calculated relative to the area of 10 cm length of the individual internodes by determining a necrosis score N as

$$N = (N_{\text{inf}} - N_{\text{mock}}) / (N_{\text{total}})$$

where N_{inf} is necrotic area [cm^2] in infected internodes by *N. parvum*, N_{mock} represents necrotic area [cm^2] in internodes subjected to mock inoculation, and N_{total} is total area of 10 cm median section of the respective internode.

Hyphal growth was measured at each infected xylem vessel recognized in the Cryo SEM images, through the entire depth of the specimen (1 mm depth) using Image J. Since the fungal hyphae represent a complex shape, a thresholding strategy was used to select the region of interest to be quantified: After setting the scale, the infected vessel was selected, and isolated

using the clear outside tool. Fungal hyphae and xylem vessels were selected separately, using the thresholding tool, and then the area was measured using the ROI manager tool.

2.1.7. RNA extraction and quantitative real-time PCR.

Steady-state transcript levels for phytoalexins synthesis and jasmonate signaling genes were measured at two time-points after infection with *Neofusicoccum parvum* Bt-67 in Chardonnay and six *sylvestris* accessions (Ke13, Ke15, Ke28b, Ke28c, Ke94, and Ke95). Samples were collected from the infection site as well as from two positions either 4 cm below or above the infection site) as shown in **Fig. 3**, wrapped in aluminum foil, frozen immediately in liquid nitrogen, and stored at -80°C . Wood samples were ground by mortar and pestle in liquid nitrogen. During grinding, the dead cork tissue was floating on the surface of the liquid nitrogen and was removed to reduce the sample content of phenols and tannins. Total RNA was extracted from the ground powder using the Spectrum Plant Total RNA Kits (Sigma Aldrich, Deisenhofen) with a minor modification to the manufacturer's protocol. In the lysis step, samples (120 – 160 mg) were incubated for 10 min at 56°C in 1 ml of lysis solution and then centrifuged for 15 min at 10000 rpm, 4°C to precipitate the abundant starch in the wood parenchyma before transferring the supernatant to the filter column. RNA was purified of genomic DNA by on-column treatment with RNase-free DNase (Qiagen, Hilden; Germany). Samples with low RNA quality were re-purified. 0.1 volume of 3M Sodium acetate was used as a positive charge neutralizing the phosphate backbone of RNA to remove the RNA from water in the presence of 2.5 volume of absolute ethanol that accelerates the electrical attraction between the salt and RNA. The RNA was then precipitated and purified following the method of ethanol precipitation of RNA (Walker & Lorsch, 2013)

For cDNA synthesis, 1 µg of total RNA was incubated first for 5 min with 0,4 µl oligo (dT) primer and 1 µl dNTP, followed by reverse transcription with 0,25 µl M-MuLV (New England Biolabs; Frankfurt am Main, Germany) in the presence of 0,5 µl RNase inhibitor (to protect RNA integrity).

Quantitative real-time PCR was conducted as described in Svyatyna *et al.* (2014) using the Biorad CFX96 PCR System with a C1000 thermal cycler (Bio-Rad, München; Germany). The differences in the expression of phytoalexin synthesis genes were investigated, such as Phenylalanine Ammonia Lyase (*VvPAL*), Resveratrol Synthase (*VvRS/VvSTS47*), and Stilbene Synthase (*VvSTS27*). The STS gene family in *Vitis* is expanded but subdivided into 3 subfamilies with partially different regulatory patterns during biotic or wound stress (Vannozzi *et al.*, 2012). Therefore, in addition to Resveratrol Synthase and *VvSTS27*, more 3 genes, *VvSTS6*, *VvSTS16*, and *VvSTS48*, were selected as the main representatives for each subfamily and investigated.

To probe the status of jasmonate signaling, the expression pattern of *VvJAZI* was observed. Also, the transcripts for caffeic acid O-methyltransferase (*VvCAOMT*) and cinnamyl alcohol dehydrogenase (*VvCAD*) mirrored the activity of the lignin biosynthesis pathway. Two housekeeping genes, Elongation factor (*VvEF-1α*) and Ubiquitin (*VvUBQ*), were chosen to calibrate the transcripts of the other genes since they were found to be constitutively expressed among all samples. The expression pattern of genes of interest was normalized to *Ubiquitin* since steady-state transcript levels *EF-1 α* turned out to fluctuate under the conditions of this experiment, such that it was not suited as a reference gene. The measured C_t values were then used to estimate the steady-state level of the respective transcript using the $2^{-\Delta\Delta C_t}$ method (Livak, K.J., and T.D. Schmittgen. 2001). The final result was expressed as $2^{-\Delta C_t}$ (X), using the

control value of Ke13. The representative primers and conditions for each targeted gene in addition to genes loci are provided in **Supplementary. Table 1**.

2.1.8. Stilbene analysis and quantification:

Wood samples were collected at two different time-points (2 days and three days after infection) and lyophilized for 24 hrs. Wood metabolites were extracted then with 100% methanol (50 μ L / mg wood powder) directly after grinding the samples by a bead mill (TissueLyser II, Qiagen, Courtaboeuf, France). The samples were analyzed using the liquid chromatography-mass spectrometry (LC-MS) platform at INRAE Grand-Est Colmar (France) as described previously (Duan et al., 2015), with the following modifications: chromatographic separations were performed on a Nucleodur C18 HTec column (150 x 2 mm, 1.8 μ m particle size; Macherey-Nagel, Düren, Germany) maintained at 30°C. The eluants consisted of acetonitrile/formic acid (0.1%, v/v) (eluant A) and water/formic acid (0.1%, v/v) (eluant B) at a flow rate of 0.25 mL/min following a gradient: 0 to 4 min, 80 % to 70 % B; 4 to 5 min, 70 % to 50 % B; 5 to 6.5 min, 50% B isocratic, 6.5 to 8.5 min, 0 % B, 8.5 to 10 min, 0% B isocratic. Stilbenes were identified based on the comparison of their retention times and mass spectra with those of the corresponding commercial standards. Putative identification of the resveratrol trimers "viniferin trimers 1 and 2", giving the pseudo molecular ion $[M+H]^+$ with m/z 681.2118, was based on their putative formula (C₄₂H₃₂O₉) and fragment analysis. Data were represented in relation to the control value at day 2 for the accession Ke13.

2.1.9. Lignin measurement

Lignin content was quantified, according to (Barnes and Anderson 2017). After 2 months of infection, wood samples were excised from the center of infected internodes and stored at – 80°C. Samples were ground to a fine homogeneous powder, and 50 mg of the ground samples

were washed with 14 ml of ethanol (80%) for 6 hours in a 75°C water bath, dried and subsequently washed with 14 ml of 100% acetone in a 50°C water bath for 6 hours, before being air-dried under the hood. Afterwards, 10 mg of the dried powder were mixed with 1 ml acetyl bromide/acetic acid (1:3) for 1 hour in a 70°C water bath, and then the mixture was cooled on ice and diluted with 5 ml of acetic acid. Subsequently, for each sample, 300 µl were complemented from a master mix with 400 µl of 1.5 N NaOH, and 300 µl of 0.5 M hydroxylamine hydrochloride, before measuring absorption at 280 nm in a spectrophotometer to calculate lignin content in mg. g⁻¹ dry weight (DW).

2.2. The effect of drought on infection development and lignin accumulation;

Climate change considers the main reason for the drought stress, but it also triggers the disease outbreak in infected vineyards. Infected grapevines were grown under two water regimes to probe whether water deficit is the main motif for the disease development. Wood-cuttings of *V. vinifera* cv, Augster weiß, were planted for 3 months in pots under previously discussed greenhouse conditions. Healthy and homogenous individuals were infected by *N. parvum* Bt-67 mycelia, as explained before, and directly subdivided into 2 experimental sets; i) mock and infected plants were well irrigated in 5 days/week and served as control. ii) mock and infected plants were irrigated only on 1 day/week (20% of the water supply to control plants).

After 30 days post-infection and drought stress, wood necrosis were evaluated under both experimental sets. Also, lignin content was measured spectrophotometrically in the infection site. Further wood samples were collected from the infection site and internode tips (which were 3 cm far either below or above the infection site) as shown in (**Fig. 3**) to evaluate the spread of the fungus through the internodes by detecting the fungal DNA. The genomic DNA was extracted then by the CTAB method (**Supplementary. Method 1**). Quantitative PCR was

conducted to detect the fungal DNA in mock and infected internodes (under control and drought conditions) using 25 ng of DNA template, 1 U *Taq* polymerase (England Biolabs; Frankfurt, Germany), and specific *ITS* primers (BOT), which bind exclusively to *Botryosphaeriaceae* DNA (H. J. Ridgway et al., 2011).

The amount of the fungal DNA was evaluated using a calibration curve, which was calculated based on a dilution series of 1:10 (50:0,5 ng) of transformed plasmid DNA carrying the *Botryosphaeriaceae* marker, BOT. The fungal *ITS* marker, BOT, was transformed into *E. coli* competent cells with pGEM®-T Easy vector by TA cloning (unpublished work by Khattab, Flubacher et al., 2021).

2.3. Methodology for Invitro studies dissecting the *Botryosphaeriaceae-Vitis* crosstalk triggering the Apoplexy phase:

2.3.1. Plant cell lines and fungal materials;

The same fungal strain, *Neofusicoccum parvum* Bt-67 (Stempien et al., 2017) was chosen for the invitro studies. Plant materials in this study were represented by:

- i. Suspension cell lines of grapevines including *Vitis rupestris* cell line expressing a florescent β -tubulin 6 (*AtTUB6-GFP*) described in (Guan *et al.*, 2015) as well as *Vitis vinifera* cv. Chardonnay actin-marker cell line expressing a florescent fimbrin actin-binding domain 2 (*AtFABD2*), in fusion with N-terminal GFP (Guan *et al.*, 2014).
- ii. Tobacco Bright-Yellow2 (BY-2) cell line, *Nicotiana tabacum*, wild type in addition to two transgenic cell lines overexpressing *Vitis rupestris* Metacaspases (BY-2.MC2ox

& *BY-2.MC5ox*) were used to investigate metacaspases response under respective treatment (Gong et al., 2019).

All cell lines were sub-cultured in weekly intervals into Murashige and Skoog (Duchefa, Haarlem, The Netherlands) supplemented with 3% w/v sucrose, 200 mg·L⁻¹ KH₂PO₄, 100 mg·L⁻¹ *myo*-inositol, 1 mg·L⁻¹ thiamine, and 0.2 mg·L⁻¹ 2,4-dichlorophenoxyacetic acid (2,4-D), pH 5.8. The transgenic lines remained under selective pressure by the appropriate antibiotics. Treatments were carried out on the *Vitis* cells while growing in the expansion phase (four days post subculture) and one day post subculture of BY-2 cells.

2.3.2. Screening effect of different phenylpropanoid derivatives on *N. parvum* aggressiveness;

To probe whether the lignin precursors (cinnamic acid, *p*-coumaric acid, caffeic acid, and trans-ferulic acid) can trigger the fungal strain, *N. parvum* to switch to necrotrophic behavior, fungal mycelia were fermented with the 4 different lignin precursors independently with different concentrations (0.5, 1.0, 1.5 mM). Eight plugs, 8 mm diameter, were picked from two weeks old fungal mycelia, grown on Potato dextrose agar media (Sigma-Aldrich, Deisenhofen), and sub-cultured in Erlenmeyer flask (500 ml) with the respective precursor in 250 ml malt extract, 20 g·L⁻¹, and pH 5,3 (Carl Roth GmbH, Karlsruhe, Germany) for further two weeks. Afterwards, the culture filtrate has been sterilized using 0.22 µm PVDF membrane (Carl Roth GmbH, Karlsruhe, Germany) to get rid of the conidia. *Vitis* suspension cells (Vrup-TUB6) were injected then by the sterilized filtrate (35µl. ml⁻¹ suspension cells). Cell death was quantified, as an indicator for phytotoxicity, after 1 day using Evans blue assay 2.5% (w/v) following as described by Gaff and Okong'o-Ogola (1971). Fungal metabolites were extracted

separately either from mycelia or from culture filtrate after 24 hr fermentation with the respective precursor to explore whether the phytotoxic polyketides are kept inside the hyphae or secreted to the culture filtrate. The target lignin precursor has been added after the fungus already consumed whole sugar from the malt media as measured by Diabur 5000 test strips (Roche, Basel, Switzerland).

2.3.3. Extraction of fungal metabolites, HPLC and HPLC-MS analysis for the toxic fraction;

The fungus was cultured in 20L YMG (yeast extract 4.0 g.L⁻¹, malt extract 10 g.L⁻¹, glucose 10 g.L⁻¹, the pH value was adjusted to 5.5 before sterilization) medium in a fermenter (Braun, Melsungen, 120 rpm, 26°C and 3l/min aeration). After 5 days of fermentation (and a glucose level of 5 mmol/L) 0.5 mM trans-ferulic acid was added to the culture. Afterwards, the fermentation was continued until the free glucose was depleted. The culture fluid (18.5 L) was separated from the mycelium by filtration (using a vacuum pump and 595 filter paper, Schleier&Schuell) and extracted with ethyl acetate (12 L). The organic solvent was evaporated to dryness under reduced pressure to give 7.2 g of a crude extract. Aliquots (20 mg mL⁻¹ in MeOH) of 20 µl from those concentrates were analyzed by HPLC (Series 1100, Hewlett–Packard, Waldbronn, Germany; equipped with a LiChrospher RP18 column; 5 µm, 125x4 mm, Merck, Darmstadt, Germany) with a 0.1 % v/v formic acid: MeCN gradient (method: 1 % to 100 % MeCN in 20 min; flow: 1 ml/min) and fractioned into 96-well plates (Greiner Bio-One, Frickenhausen) for bioactivity guided isolation as described by Buckel et al. (2013). Different hydrophobic phases (0, 10, 20, 30, 40, 50, 60, 70, 80, 90, 100% MeCN) were tested for their bioactivity in *Vitis* cell culture system. To identify the synthetic toxic polyketide in response to plant surrender signal, the most toxic phase was re-analyzed by HPLC-MS (Series 1200, Agilent, Waldbronn, Germany) equipped with a UV-DAD and a coupled LC/MSD Trap APCI-

mass spectrometer with positive and negative polarization. Methods were applied described by Buckel et al. (2017). The mass spectrum of the derived molecules and their HPLC-MS analysis were provided in **Supplementary. 2**. For the most toxic fraction, due to *Vitis* cell culture tests, HPLC-MS analysis and coinjection came up with a derivative of Fusicoccin A.

2.3.4. Dissecting the signaling pathway of Fusicoccin A

After identifying that the toxic fraction is a derivative of a known fungal toxin Fusicoccin A (FCA), a chemical product from (Santa Cruz Biotechnology, Heidelberg, Germany) was procured. *Vitis* cells were treated with two concentrations of FCA (6 μM and 12 μM) to identify the toxic concentration in the *Vitis* cell culture system.

2.3.4.1. Inhibiting Respiratory burst Oxygen Homolog (RbOH);

Before FCA treatment, *Vitis* cells were pre-treated for 60 min with 1 μM of Diphenyleneiodonium chloride (DPI) (Sigma-Aldrich, Germany). DPI was pre-diluted in 100 μM DMSO and used as a potential inhibitor binding to NAD(P)H oxidase of the plasma membrane and subsequently blocks reactive oxygen species (ROS) synthesis (Li., Y & Trush, 1998).

2.3.4.2. Blocking FCA receptor, 14-3-3 protein;

Fusicoccin receptors can be blocked using BV02 (Sigma-Alrich, Germany), which inhibits 14-3-3 proteins docking sites ((Stevens et al., 2018). 14-3-3 proteins were blocked in suspension cells of (Vrup-TUB6), by incubating them at first for 60 min with 5 μM of BV02 (diluted in 100 μM DMSO) before adding 6 μM FCA.

2.3.4.3. Extracellular pH measurements

Changes in the extracellular pH were studied in *Vitis rupestris* cells by pH meter (Schott handylab, pH12) as detailed in Qiao *et al.* (2010) and provided by a digital memory recorder displaying the pH at 1-second intervals. Four ml of *Vitis* cells were left on an Orbital shaker for 30 min at first until getting stable pH readouts before adding FCA (6 μ M). To test the effect of blocking FCA receptors (14-3-3 proteins) on ATPases activity, cells were pre-incubated with BV02, 5 μ M, for 45 min, then treated by FCA. Steady-state changes in the pH were calculated as described in Guan *et al.* (2020).

2.3.4.4. Superoxide [O₂⁻] detection

To estimate the intracellular superoxide accumulation in *Vitis* cells, a Nitroblue tetrazolium (NBT) staining assay was performed as described in Steffens & Sauter (2009) and Pietrowska *et al.* (2014) with minor modifications. NBT dye was dissolved in 10 mM phosphate buffer 0.1% (W/V) with pH 7.8, containing 10 nM Sodium azide. *Vitis* suspension cells were filtered from MS medium of the respective treatment at every time point and incubated in the 0.1% NBT in sterilized well plate, kept in darkness, and left on Orbital shaker (150 rpm). After 1 hr incubation, suspension cells were washed by phosphate buffer two times before microscopic observations by light microscopy. Cells accumulating superoxide appeared in purple-blue and were calculated as a percentage of 700-850 counted cells per every biological replicate of the respective time point.

2.3.4.4. Manipulating salicylic acid and mitogen-activated protein kinases (MAPKs) signaling;

Suspension cells (Vrup-TUB6) were pre-treated by 50 μ M of salicylic (Sigma Aldrich, Deisenhofen, Germany) dissolved in 0.2% (V/V) Ethanol for 1 hr before FCA treatment to

dissect whether salicylic acid is involved in FCA stress signaling. Furthermore, 1-aminobenzotriazole, ABT (Sigma Aldrich, Deisenhofen, Germany) was used as an inhibitor for salicylic acid biosynthesis (Leon *et al.*, 1995). *Vitis* cells were incubated with 25 μ M of ABT for 1 hr before FCA treatment. To check whether MAPKs are involved in FCA stress signaling, *Vitis* cells were treated first by 50 μ M MAPKs inhibitor PD98059 (Sigma Aldrich, Germany) as described by Duan *et al.* (2016) before FCA treatment.

2.3.4.5. RNA extraction from (Vrup-TUB6) cells and quantitative real-time PCR

V. rupestris (AtTUB6-GFP) cells were collected, dried using a vacuum pump (Vacuubrand, Wertheim, Germany), and immediately frozen in liquid nitrogen. Samples were ground using Tissue lyzer (Qiagen, Germany). Total RNA was extracted using RNA Purification Kit, Roboklon (Berlin, Germany), and handled by RNase-free DNase column (Qiagen, Hilden, Germany) to get rid of Genomic DNA. Afterwards, 1 μ g of total RNA was used For cDNA synthesis as described before in the presence of RNase inhibitor (to protect RNA integrity).

Steady-state transcripts levels of genes of interest were monitored by quantitative real-time using the CFX PCR System with a C1000 thermal cycler (Bio-Rad, München; Germany) PCR as described in Svyatyna *et al.* (2014). Studied genes in the study included phytoalexins biosynthesis genes (*PAL*, *STS6*, *STS16*, *STS27*, and *STS47*); lignin biosynthesis genes like (*CAOMT* and *CAD*). *Manganese Superoxide Dismutase* genes (*Mn.SOD1*, *Mn.SOD2*), *Copper Superoxide Dismutase* genes (*Cu.SOD1*, *Cu.SOD2*, *Cu.SOD3*) represented the retrograde signaling driven by Fusicoccin A stress. In addition, Further stress-marker genes were examined like *Metacaspases*, *MC2* and *MC5* as markers for regulated cell death (Gong *et al.*, 2019). To investigate phytohormonal signaling, *JAZ* genes; *JAZ1*, *JAZ4*, *JAZ9* were selected for jasmonate signaling, and *Isochorismate Synthase*, *ICS* ; *Pathogenesis-related proteins*,

PR1 and *PR10*, and *NPR1* for salicylic acid signaling and biosynthesis. The Ct values of the respective transcript were subtracted from those of the housekeeping gene, *EF-1 α* , to calculate the steady-state levels using the $2^{-\Delta\Delta C_t}$ method (Livak and Schmittgen, 2001). The final result was expressed as $2^{-\Delta\Delta C_t}$ (X) using the control value at every time point, 1 hr., 3 hrs. and 6 hrs. as reference. The details of primer sequences, gene loci, and PCR conditions for the different target genes are provided in **Suppl. Table S1**

2.3.5. Live imaging of cell cytoskeletons

Vitis cytoskeletons were studied using two GFP marker cell lines. i) a microtubules cell line (Vrup-TuB6) visualizing a β -tubulin 6 from *Arabidopsis thaliana* in fusion with GFP. ii) Chardonnay actin-marker cell line expressing a fluorescent fimbrin actin-binding domain 2 from (*AtFABD2*). Cytoskeletons responses in living individual cells were displayed using spinning disc confocal microscopy provided with AxioObserver Z1 (Zeiss, Jena, Germany), spinning disc device (YOKOGAWA CSU-X1 5000) and 488 nm emission light of Ar-Kr laser as detailed in (Wang & Nick, 2017). Z-confocal stacks were then processed by ZEN software (Zeiss, Oberkochen) and exported as TIFF format.

Actin filaments width as a marker for actin bundling was measured by the ImageJ freeware (<https://imagej.nih.gov/ij/>). Individual cells were selected, transformed to binary images, and adjusted by threshold function to B/W option. Using analyze-particles tool, actin filaments were determined automatically. The background was omitted directly after setting the lower limit to 10 square pixels. Fitting particles by the fit ellipse command displayed the actin filaments dimensions.

The integrity of cortical microtubules was calculated as described in Schwarzerová et al. (2002) and modifications of Guan *et al.* (2020). Four intensity profiles were processed through the

elongation and cross-axis of the living cell with line width of 25 pixels. Subsequent positions were subtracted from each other's to filter out the random noise outside microtubules getting first derivatives. The derivatives were filtered then by ABS function in Excel sheet. The standard deviation of the filtered values was added relative to the maximal intensity value through the respective profile. Twenty-five cells were scored for each treatment representing 5 independent biological replicates.

2.3.6. Cytoskeletons manipulation

To assess the effect of microtubules manipulation on the FCA stress signaling, (Vrup-TUB6) cells were treated either with 10 μM of Taxol (Sigma-Aldrich, Germany), which stabilizes microtubules. For microtubules depletion, (Vrup-TUB6) cells were pre-incubated with 10 μM of oryzalin (Sigma-Aldrich, Germany) for 60 min, followed by FCA treatment.

To probe the effect of actin filaments on manipulating FCA stress signaling, actin filaments were depleted at first in Chardonnay cv. (*AtFABD2*) cells by 2 μM Latrunculin B (Sigma-Aldrich, Deisenhofen, Germany), for 1 hr before FCA treatment. It is worth noting that (Vrup-TUB6) cells were used to study the effect of cytoskeletons manipulation on the regulation of stress-marker genes by FCA signaling.

2.3.7. Cell death assays

Double staining assay was performed by a mixture of dyes (AO/EB); Acridine Orange (100 $\mu\text{g.mL}^{-1}$), which is a membrane-permeable fluorochrome (green signal), and 100 $\mu\text{g.mL}^{-1}$ of the membrane-impermeable fluorochrome Ethidium Bromide (red signal). The staining mixture was diluted in 0.01 M phosphate buffer. *Vitis* cells were mixed gently as 1/1 volume (200 μl cells/200 μl AO/EB) and observed after 2 min using UV filter and digital light

microscopy (Axioscope and Axio-Cam, Zeiss; Jena) to distinguish the different stages of cell death by FCA treatment. The double staining assay characterizes cytological stages of cell death following the protocol of Byczkowska *et al.* (2013). Living cells exclude Ethidium Bromide and appear green. Cells in stage 1 show penetration of Ethidium Bromide into the cytoplasm but still exclude the dye from the karyoplasm giving green-yellow to yellow nuclei. Cells in stage 2 show penetration of Ethidium Bromide into the nucleus giving bright orange nuclei. Dead cells loose the Acridine orange signal due to complete breakdown of the plasma membrane, while Ethidium Bromide remains sequestered at the DNA showing red nuclei.

In addition, Evans blue assay was conducted, which labels dead cells by the blue color due to the plasma membrane damage (Gaff and Okong'o-Ogola 1971). *Vitis* cells were stained with 2.5 % Evans blue (Sigma Aldrich, Germany) for 3 min then washed two times by distilled H₂O as described in (Chang & Nick, 2012). Cell death rates were calculated as a percentage of at least 1000 counted cells / biological replicate of the respective treatment.

2.4. Data Analysis;

The data were analyzed using IBM SPSS statistics 24 software (2017) to conduct one-way ANOVA followed by multiple comparisons of means using the Least Significant Difference approach or Duncan's New Multiple Range test ($P < 0.05$) to probe for significant differences. To verify homoscedasticity, Levene's test was used for the data obtained by RT-qPCR, hyphal coverage, lignin content, wood necrosis, xylem vessels, pith area, cell death assays, superoxide measurements, and cytoskeletons measurements.

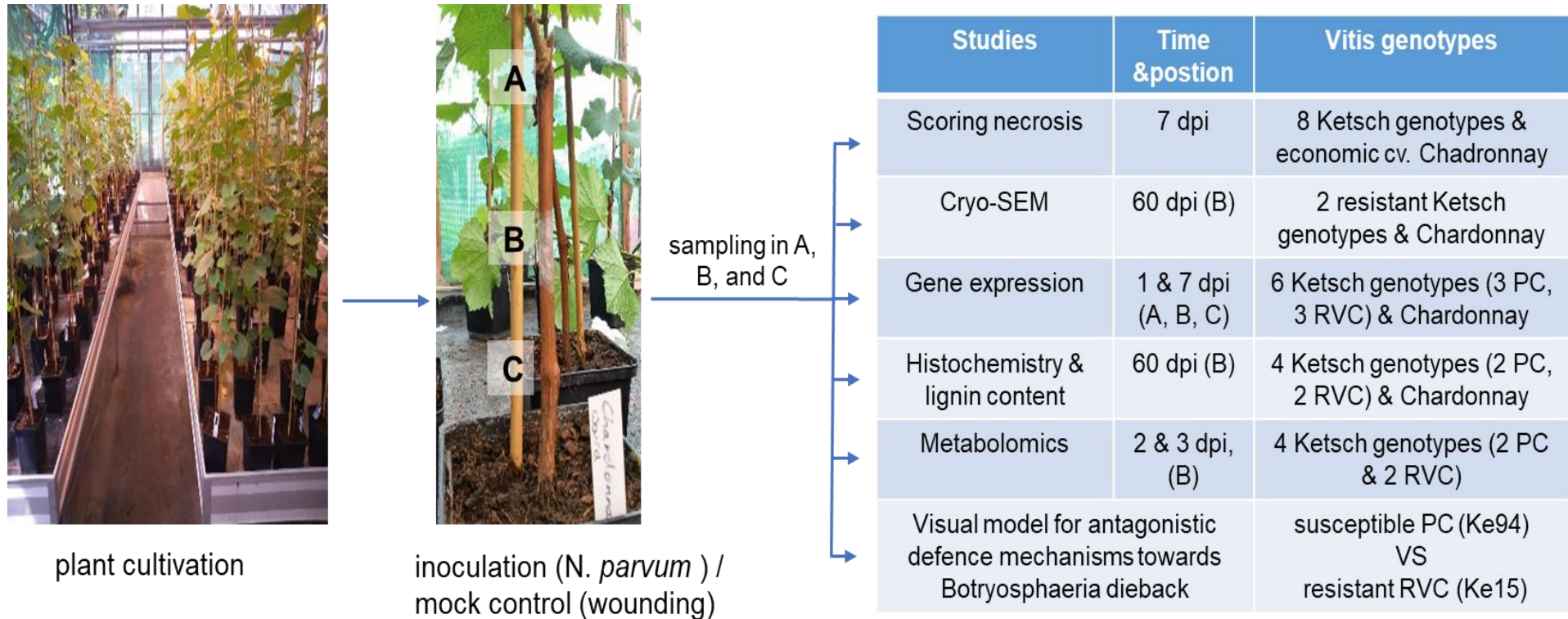


Fig. 3. Experimental design explaining sample position and time points (in days post infection, dpi) for the analysis of gene expression by quantitative real-time PCR, metabolites, scoring necrosis, and the different microscopical investigations. (Published in Khattab et al., *New Phytologist* (2020)).

3. Results

3.1. Chapter 1: Identifying resistant chemotypes of grapevines against *Botryosphaeria dieback*

3.1.1 *Vitis vinifera* spp. *sylvestris* clustering after phylogenetic analysis based on genome-wide SNPs.

A genome-wide phylogeny has been structured based on SNPs from 89 *Vitis* genomes, including European *Vitis vinifera* varieties, American species, Asian species, in addition to an ancient collection of European Wild Grapes (*Vitis vinifera* spp. *sylvestris* (**Fig. 4**). The phylogeny came with 4 main clusters where the *V. sylvestris* accessions, from the last viable population in Germany, appeared altogether into the cluster (I). The *Vitis vinifera* cultivars, as well as 2 species of the American wild grapes, fell into cluster (II). Asian wild grapes constituted cluster (III), while American wild grapes were grouped into cluster (IV). Within cluster (I), up to eight clades could be independently constructed, where the resveratrol-viniferin chemotype was located in one of the clades. In contrast, the α -piceid chemotype was spread over several clades. Therefore, Ke15 and Ke95 were selected as representatives of the resveratrol-viniferin chemotype (along with Ke28c, for which no genome was available, but was from the same chemotype), while the α -piceid chemotype was represented by Ke13, Ke94, Ke30, Ke33, as well as by Ke28b (for which no genome was available, but was from the same chemotype).

3.1.2 Susceptibility towards *Botryosphaeria dieback* differs between stilbene chemotypes

To probe, whether the response towards the infection with *Neofusicoccum parvum* Bt strain 67 depends on genotype, the three genotypes of the resveratrol-viniferin chemotype along with

the six accessions of the α -piceid chemotype (including the *vinifera* variety Chardonnay) were all infected. One week after infection, the bark was peeled from the infected and the mock-treated canes to examine the wood lesions (**Fig. 5a**) to quantify the spread of necrosis as a measure of susceptibility (**Fig. 5b**). The susceptibility was variable since the lowest necrosis was observed in the three resveratrol-viniferin chemotype representatives. By contrast, all genotypes belonging to the α -piceid chemotype (except Ke30, which turned out to be fairly resistant) were obviously more affected by the fungus-induced necrosis. Thus, a resveratrol-viniferin chemotype is a reliable candidate for a significantly reduced susceptibility to *N. parvum* Bt 67, while an α -piceid chemotype, in the majority of cases, correlates with elevated susceptibility (albeit not necessarily as the case of Ke30 demonstrate

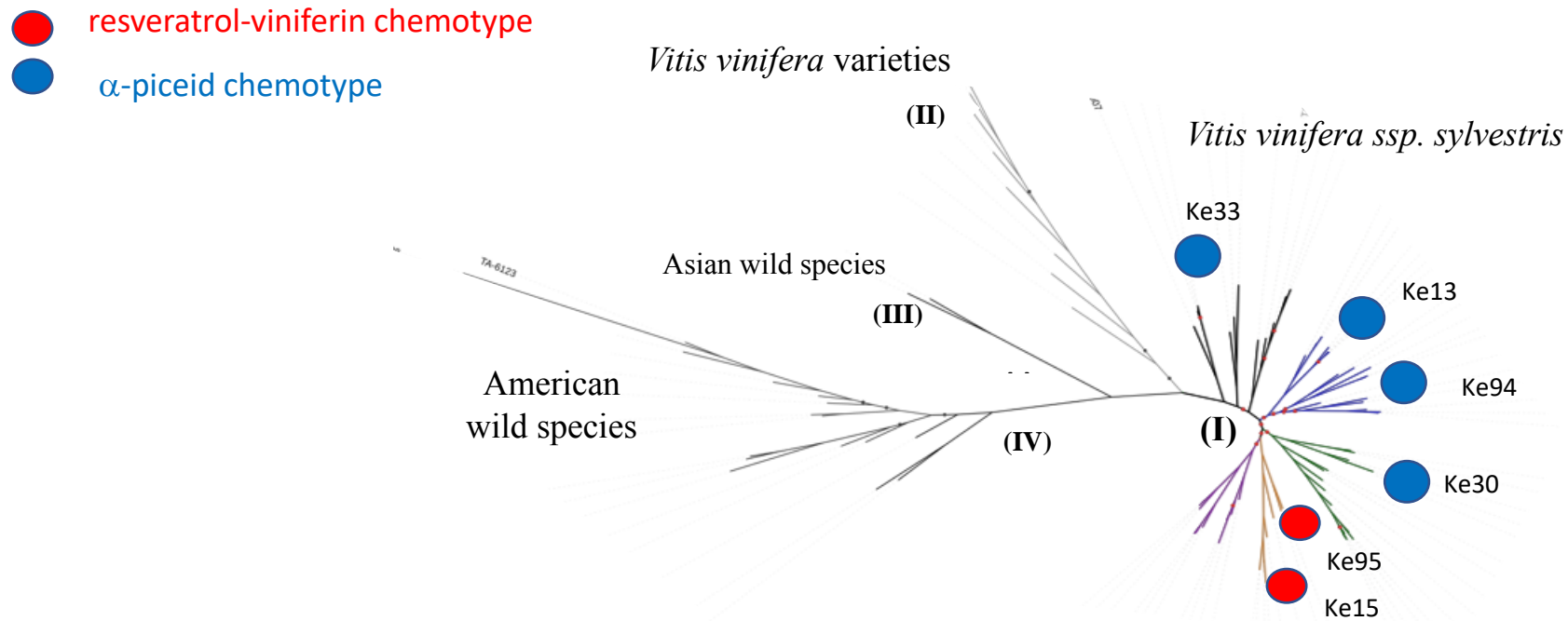


Fig. 4. Position of the genotypes investigated in this study in a phylogenetic tree constructed from genome-wide SNPs for 89 accessions of cultivated *Vitis vinifera* and wild species from Europe, Asia and America. Cluster (I) represents the wild *spp. sylvestris* genotypes from Ketsch, Germany, separated into different clades labeled by colors. Clusters (II) comprises *Vitis vinifera* varieties, Cluster (III) Asian wild *Vitis* species, and cluster (IV) American wild *Vitis* species. Red circles indicate the resveratrol-viniferin chemotype, blue circles indicate the α-piceid chemotype. Published data in Khattab et al., New Phytologist (2020).

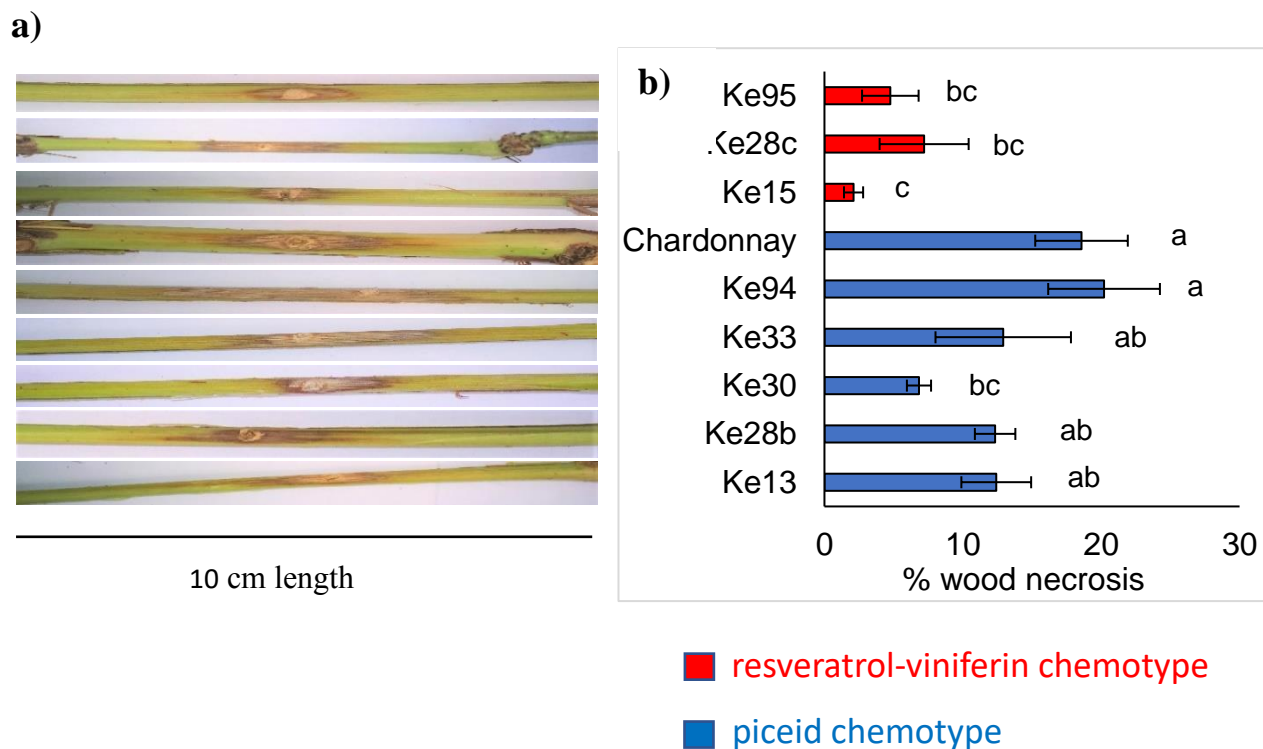


Fig. 5. Susceptibility of *sylvestris* genotypes from different stilbene chemotypes, and the *vinifera* variety Chardonnay to *Neofusicoccum parvum* strain Bt 67. Susceptibility was quantified as proportion of necrotic cross area corrected for the area of wound-damaged area over the cross section of a 10 cm internode segment. a) Representative images of each infected genotype is shown in the left-hand panel, b) corresponding means and standard errors from 3 individuals per genotype are given in the right-hand panel. Different letters after the bars indicate statistical differences among infected genotypes on the level of $P < 0.05$. Published data in Khattab et al., New Phytologist (2020).

3.1.3 Wood colonization of *Botryosphaeriaceae* is significantly impaired in hosts with the resveratrol-viniferin chemotype

To find out the reasons behind the reduced necrosis in infected genotypes belonging to the resveratrol-viniferin chemotype, cross-sections were collected two months after either mock treatment or infection (**Fig. 6**). Infected xylem vessels of Ke15, and Ke95, as representatives of the resveratrol-viniferin chemotype, were compared to *Vitis vinifera* cv. Chardonnay (as representative of the α -piceid chemotype) by Cryo Scanning Electron Microscopy. There were no symptoms or indications for fungal growth in the cross-sections from mock internodes, confirming that the wood was healthy and free from uncontrolled infection (**Fig. 6; a1-a3**). In infected plants, irrespectively of the genotype, the *N. parvum* hyphae were localized in xylem vessels and quite far from the phloem, as well as pith parenchymatic regions. The mycelia growth rates were more plentiful in the xylem vessels from Chardonnay cv. plants as compared to the vessels of Ke15 and Ke95 (**Fig. 6; b1-b3, c1-c3**). This qualitative impression was confirmed by quantifying hyphal coverage across the xylem vessel cross-area (**Fig. 6d**). Here, Ke15 showed the lowest values that were just about 20% of those seen in Chardonnay, and also for the somewhat less resistant Ke95 the coverage was around 40% of those found in Chardonnay. These differences were highly significant and predictable since both genotypes, Ke15 and Ke95, also showed the lowest inducibility of wood necrosis one week after infection (**Fig. 5**), with Ke15 being superior in resistance over Ke95, exactly mirroring the values obtained for hyphal coverage two months later. This supports that wood necrosis (on the outer surface of the xylem and underneath the phloem) one week after infection can be a reliable indicator for detecting the susceptibility of a genotype.

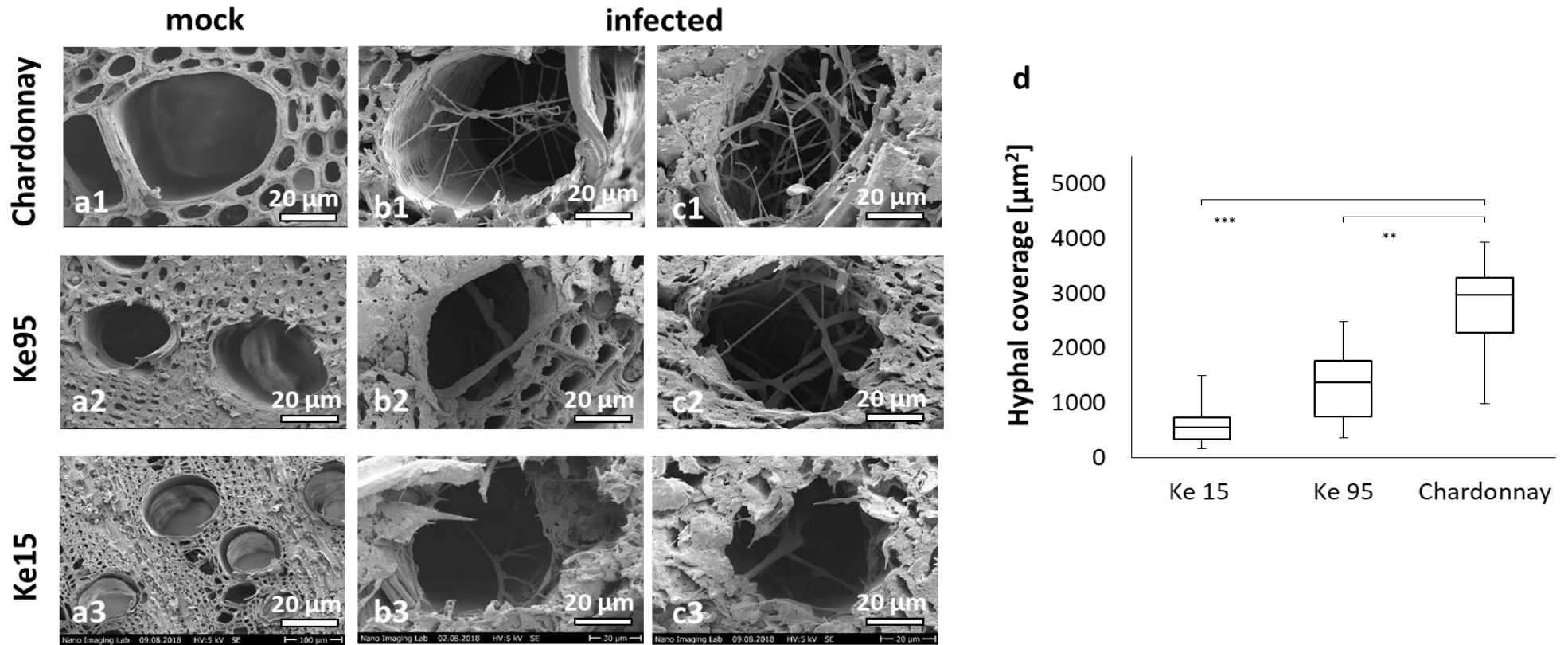


Fig. 6. Colonization of xylem vessels in the variety Chardonnay compared to the *V. sylvestris* genotypes Ke15 and Ke95 (belonging to the resveratrol-viniferin chemotype). (a-c) representative CryoSEM images from mock-treated (a) and infected (b, c) internodes, 2 months after the respective treatment. Infection was conducted with *Neofusicoccum parvum* Bt strain 67. (d) Quantification of hyphal growth. Whisker and box plots showing median and interquartile range of hyphae growth area per infected xylem vessel (1 mm depth) of 3 biological replicates. Asterisks represent the significant differences among means of hyphae growth area through the infected xylem vessels. ** $P < 0.01$; *** $P < 0.001$. Published data in Khattab et al., New Phytologist (2020).

3.1.4 Resistance to fungal spread correlates well with the inducibility of *Stilbene synthase* transcripts.

Steady-state transcript levels of genes regulating phytoalexins biosynthesis were studied to determine a potential defense response to infection with *N. parvum*. These included *VvPAL* as the first committed step of the phenylpropanoid pathway, *VvSTS6*, *VvSTS16*, *VvSTS27*, *VvSTS47*, as representative members of the different stilbene synthase clades (Parage et al. 2012), and *VvJAZ1*, reporting the status of basal defense. These transcripts were measured in four lines of the α -piceid chemotype (*sylvestris* Ke13, Ke28b, Ke94, and the *vinifera* cultivar Chardonnay) and three lines of the resveratrol-viniferin chemotype (*sylvestris* Ke15, Ke28c, and Ke95). Mock controls, where the hole for inoculation was drilled without adding the pathogen probed for the effect of wounding (**Fig. 3. site B**). During preparatory experiments, the durability of the defense reaction had been tested by measuring expression at different time points (**Fig. 7**). Likewise, potential systemic responses had been explored by testing the reaction of sites above or below the inoculation site. Based on this preparatory study, the focus was on the local response at day 1 after infection.

The steady-state transcripts levels of genes of interest showed a consistent upregulation due to infection at that was more abundant than the upregulation seen for wounding alone at mock plants (**Fig. 7**). Nevertheless, the expression pattern was variable depending on the respective transcript, and also on the genotype. The highest abundance for all studied transcripts was observed for Ke94. However, it has to be noticed that, for *JAZ1* and *STS47*, already the ground levels were strongly elevated for Ke94 (**Fig. 7**), such that the induction in response to infection was also prominent. Leaving out Ke94, the induction was consistently and significantly more pronounced in the resveratrol-viniferin genotypes Ke28c and Ke95, as compared to the α -piceid genotypes Ke13, Ke28b, and Chardonnay (**Fig. 7a**). The resveratrol-viniferin genotype

Ke15 followed a different pattern: In response to infection, the steady-state levels were lower than in the other two tested resveratrol-viniferin genotypes and more in the range seen for the α -piceid genotypes. However, the resting levels in control plants were significantly lower in Ke15 than in the other genotypes (**Fig. 7b**). To get insight into a potential link between the accumulated transcripts of *Stilbene Synthase* with jasmonate signaling, the response of *STS6*, *STS16*, and *STS47* to methyl jasmonate was addressed in a *V. rupestris* cell culture (**Suppl. Fig. S1**) as approximation approach to the situation in the wood itself since it is hard conduct this experiment in the internodes with the necessary precision.

To explore exemplarily, to what extent this gene induction persisted over time, the expression was scored one week after infection. The induction had generally dissipated, depending on the measured transcript. Compared to the other genotypes, the expression in Ke94 seemed to be the most persistent for *PAL*, *STS27*, and *STS47*, which contrasts with the high susceptibility observed in the necrosis score (**Fig. 5**). In contrast, among the resveratrol-viniferin chemotypes, only Ke28c still showed elevated expression after one week. Thus, the resistance against *N. parvum* is not correlated with the elevated persistence of phytoalexin gene expression at the infection site.

In a different approach, the potential systemic spread of the defense response was studied at day 1 after infection (**Fig. 7 a, c**). In the most heavily colonized accession, Ke94, all genes of interest regulating the phenylpropanoid pathway (*PAL*, *STS27*, and *STS47*), as well as for *JAZ1*, were significantly upregulated, either 4 cm to the base or to the tip of the infection site. This was not observed for the phenylpropanoid pathway genes in the other genotypes, irrespective of whether they were easily colonized or not. However, for *JAZ1*, also two of the resistant genotypes, Ke28c and Ke95, showed a significant upregulation at 4 cm towards the tip of the infection site, but not to the base. Regarding Ke94, there was a considerable directionality

because *JAZ1* was upregulated more than an order of magnitude stronger apical from the infection site as compared to the response of the internode base. Such asymmetries were not seen for the two tested *Stilbene Synthases*, but also *PAL* was activated in Ke94 depending on direction. Here, the gradient was inverse, with induction being around twofold more pronounced at the base as compared to the tip. By following how far this systemic response in the susceptible genotype, Ke94, one week after infection, it was noticed that the induction of *PAL* and the two tested stilbene synthases *STS27* and *STS47* had generally eased off, but significantly less in the site apically from the infection site. Also the transcript levels of *JAZ1* were higher in the apical probing site, albeit the difference between infection and wounding control was, with the exception of Ke13, not significant.

In brief, the expression of genes regulating phytoalexin biosynthesis is still almost limited to the infection site. Only in the piceid chemotype, Ke94, where colonization was robustly progressing, the distant position (especially the one apically from the infection site) showed induction of these genes. Therefore, this systemic response cannot be a readout for resistance but rather seems to be a readout for susceptibility and might represent a local response to the rapidly spreading fungus. In the genotypes that were able to restrain colonization, rapid and consistent activation of phytoalexin genes was observed at the infection site. This activation remained transient and was not seen if the response was checked six days later. Also, no systemic response was observed. The situation for *JAZ1* is somewhat different. Here, even in the resistant genotypes, a significant induction was observed apically from the infection site.

3.1.5 Resistance to *N. parvum* spread correlates with the accumulation of resveratrol and viniferins.

To test whether the differential induction of *Stilbene Synthases* at 1 dpi was followed by accumulation of the respective metabolites, wood samples were collected at 2 and 3 dpi in the center of inoculated internodes for a set of four *sylvestris* varying susceptibility (Ke13 and Ke94 as representative of the α -piceid chemotype; Ke15 and Ke95 as representatives of the resveratrol-viniferin chemotype). About Fourteen stilbene derivatives, as well as their precursors phenylalanine, tyrosine and *p*-coumaric acid, were evaluated by HPLC-MS analysis. To compare the abundance of a particular metabolite between genotypes, treatments and time points, the readouts were normalized to the value found in non-wounded plants of Ke13 at day 2 (**Fig. 8a, b**). For all tested genotypes, already wound treatment alone was able to induce *p*-coumaric acid, *trans*- and *cis*-resveratrol, as well as their derivatives piceatannol, δ -viniferin, and the viniferin trimers 1 and 2 (**Fig. 8a; Suppl. Fig. S2**). In the infected plants, again, for all genotypes, piceatannol and *cis* ϵ -viniferin were produced beyond the levels seen for mock plants. Also, infection accentuated the synthesis of *trans*- and *cis*-resveratrol, in addition to α -viniferin. This was prominent already at 2 dpi, while these compounds accumulated in a slow manner for wounding alone (**Suppl. Fig. S2**).

There were significant changes in the amplitude and time course of these metabolomics accumulations on the background of this qualitative pattern. Generally, the genotypes representing the resveratrol-viniferin chemotype accumulated stilbenes robustly and more intensively as compared to the genotypes belonging to the α -piceid chemotype, which was true for both, wounding alone and infection (**Fig. 8**). For instance, both genotypes, Ke15 and Ke95, synthesized more *trans*- and *cis*-resveratrol than any genotype belonging to the α -piceid chemotype at 2 dpi already for wounding alone. Regarding infection, Ke15 produced the

highest levels of the stilbene precursors tyrosine and *p*-coumaric acid, along with the non-glycosylated stilbenes monomers already at 2 dpi. For instance, *trans*-resveratrol was accumulated to 41 fold, and *cis*-resveratrol even 82 fold in Ke15, while the two α -piceid chemotypes produced 27-28 fold of *trans*-resveratrol, and only about 1.17-2.76 fold of *cis*-resveratrol (after normalization to untreated Ke13 plants). For resveratrol oligomers, such as stilbene dimers and trimers, were seen only in Ke15 after two days post-infection and followed by a decrease on the third day. Also, a similar pattern was seen in *trans*- ϵ -viniferin accumulation, which accumulated specifically for infection. In contrast, *cis*- and *trans*- δ -viniferins were enhanced at 3 dpi in this genotype. Nevertheless, Ke15 was ranked first in the induction of the stilbene trimer α -viniferin, as well as of the viniferin trimers 1 and 2 against infection. Especially, viniferin trimer 2 increased from 6.4 fold to 12.7 fold at 3 dpi in Ke15, while it remained at 4.7 fold for the infected α -piceid chemotypes for the same time point. Also for Ke95, infection triggered the induction of both *trans*- (41 fold) and *cis*- (31 fold) resveratrol already at 2 dpi, followed later by elevated levels of the viniferins trimers 1 and 2, comparing to α -piceid chemotypes (**Fig. 8a, b; Suppl. Fig. S2**). This robust accumulation in stilbene aglycons of the genotypes, belonging to the resveratrol-viniferin chemotype, was accompanied by an obvious reduction in α -piceid as expected from the preferential channeling of resveratrol towards viniferin derivatives.

Results

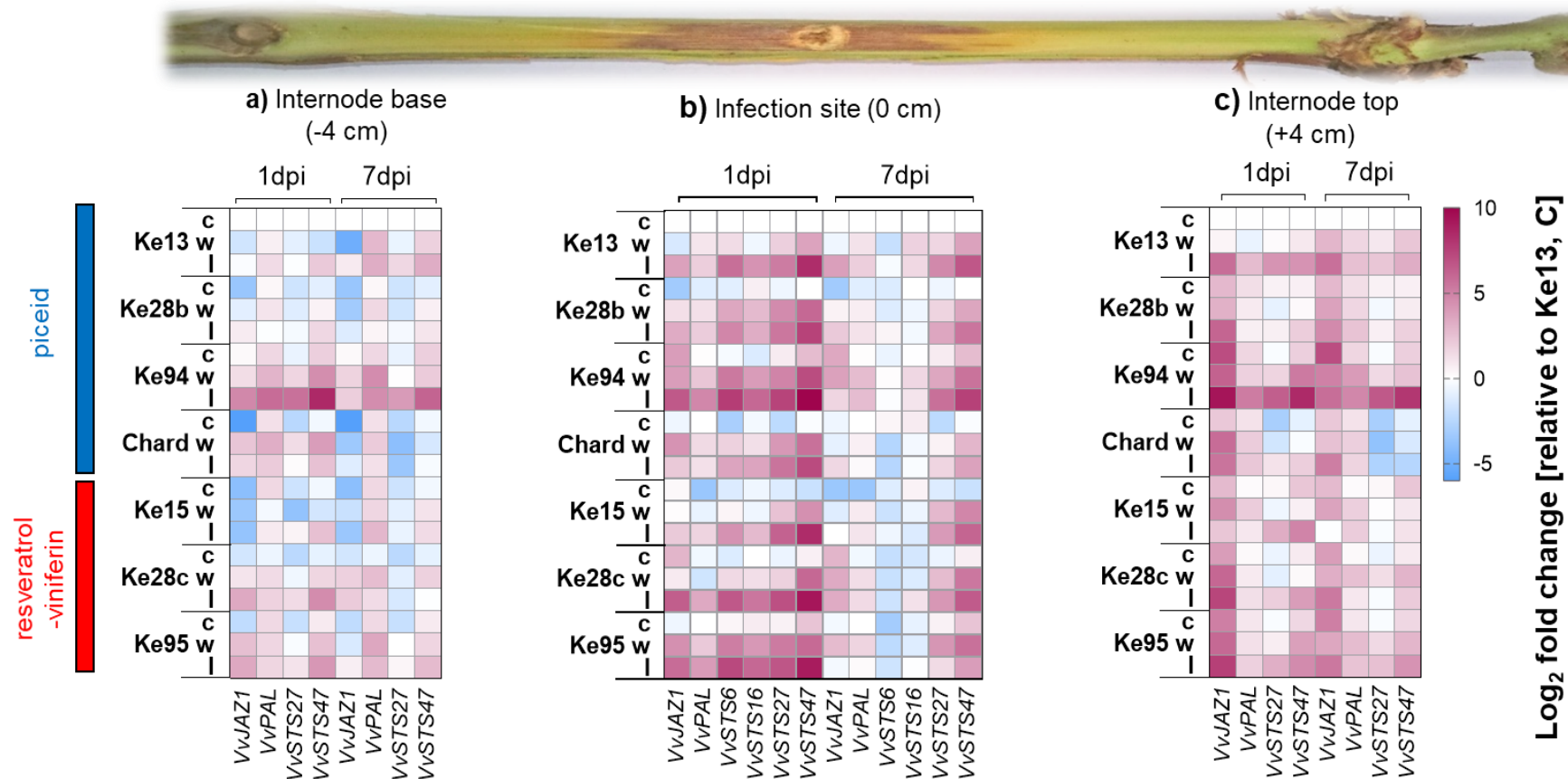


Fig. 7. Heat maps show the Log₂ fold changes in steady-state transcripts levels of defence-related genes (*VvJAZ1*, *VvPAL*, *VvSTS6*, *VvSTS27*, *VvSTS47*, *VvSTS16*) in genotypes belonging to the piceid (Ke13, Ke28b, Ke94, Chardonnay), and the resveratrol-viniferin (Ke15, Ke28c, Ke95) chemotypes by RT-qPCR after 1 day (1d) and 1 week (1w) infection. For each genotype, transcript levels for control (unwounded), mock (wounded) and infected plants were analyzed at 3 positions; internode base **(a)**, infection site **(b)** and internode top **(c)**. Color code presents Log₂ fold changes in transcripts levels which normalised first relative to expression levels in control plants of the piceid chemotype (Ke13). Data represent mean values for 3 biological replicates per each genotype and time point. Published data in Khattab et al., *New Phytologist* (2020).

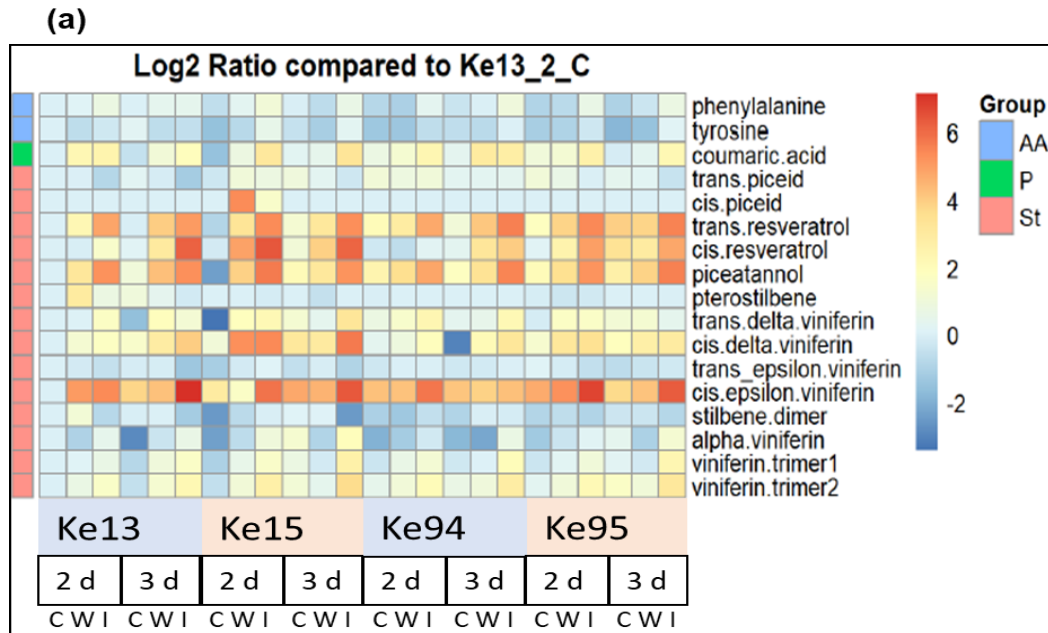
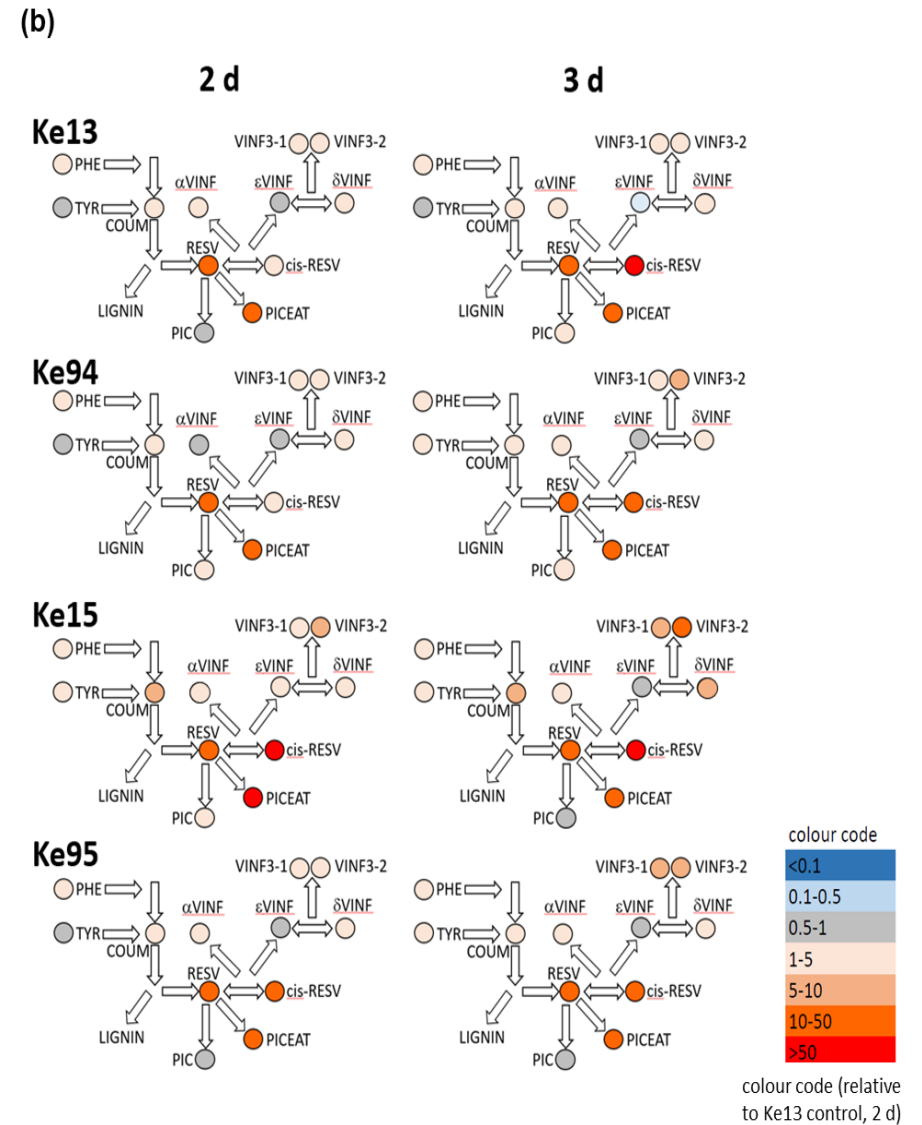


Fig. 8. Heat map of metabolite abundance in response to infection with *Neofusicoccum parvum* Bt strain 67 at the infection site in four *sylvestris* accessions measured 2 and 3 dpi. **(a)** Log₂ ratios of mean metabolite abundance in untreated controls (C), wounded, non-infected (W) and infected (I) plants as compared to the control of Ke13 at day 2. Metabolites are grouped into amino acids (AA), phenylalanine derivatives (P), and stilbenes (St). **(b)** at 2 and 3 dpi after normalisation to the control of Ke13 at day 2. Colour code represent fold changes. Data represent mean values of 3 or 4 biological replicates for each genotype and time point. Statistical analysis was performed using Tukey's test, with p-value ≤ 0.05. Published data in Khattab et al., New Phytologist (2020).



3.1.6. Susceptible grapevines respond to infection by higher lignin deposition

The lignin synthesis pathway competes with stilbene synthesis for the same precursors deriving from phenylalanine. To study the effect of *N. parvum* infection on the partitioning between these competing pathways, the expression pattern of two key genes regulating lignin biosynthesis (*VvCAOMT*, *VvCAD*) was tested one day, or one week after infection, respectively. Wood samples were collected from the inoculation site of Chardonnay and the *sylvestris* genotypes used for the metabolite analysis, i.e. Ke13, Ke15, Ke94, and Ke95 (**Fig 8. A, B**). Like the defense genes, transcripts levels of *VvCAOMT* and *VvCAD* in the different genotypes were normalised to Ke13 control plants. With exception of Ke94, there were no considerable changes in the accumulated transcripts of *VvCAOMT*. In Ke94, the expression pattern of transcript was strongly upregulated in infected plants, as compared to the wound alone or any other infected genotypes on the first day after infection, and still elevated 1 week later. By contrast, at this time point, *VvCAOMT* transcripts in mock plants increased to a level exceeding that upregulated by infection. For *VvCAD*, none of the genotypes tested at 1 dpi showed any significant induction in response to infection, nor to the mock treatment. However, after 1 week, *VvCAD* was upregulated in infected Ke94, to a lesser extent in wounded plants. This was not seen by infection in the other genotypes. Interestingly, wounded plants of Ke95 showed a significant induction as well, which was not seen in the infected wood.

Variations in lignin accumulation over 2 months of infection were measured spectrophotometrically after extraction (**Fig. 9b**), and qualitatively by histochemical staining of cross sections (**Fig. 9c, d**). In the cross sections, lignin was stained by either 1% Phloroglucinol-HCl, or 0.1% Toluidine Blue 0.1 %. Compared to the mock-treated plants, the histochemical label for both lignin assays increased in infected plants (**Suppl. Fig. S3**).

Likewise, Ruthenium Red, staining for pectic polysaccharides, displayed an increased signal in the stained reaction zones of infected sections (**Suppl. Fig. S3**).

On the other hand, the color intensity was variable between the stained RZ among infected genotypes (**Fig 8. C, D**). Especially, the RZ of infected Ke94 was more intensively stained with both, Phloroglucinol-HCl and Toluidine Blue, as compared to any of the other genotypes. Likewise, the other piceid chemotypes (Ke13 and Chardonnay) showed intensified Phloroglucinol-HCl and Toluidine Blue signals around the infected xylem vessels of their RZs. In contrast, the two tested accessions belonging to the resveratrol-viniferin chemotype exhibited a lighter staining signal. Especially infected Ke15 did not show any obvious increase in lignin accumulation, neither by Phloroglucinol-HCl nor by Toluidine Blue staining. To test these qualitative findings, lignin was extracted from the inoculation site and quantified spectrophotometrically (**Fig. 9b**). Hence, the three tested α -piceid genotypes all showed more lignin content by infection over the wound treatment, with the highest levels found in Ke94. This pattern was not seen in the genotypes of the resveratrol-viniferin chemotype, for Ke15, even the reverse response was seen, i.e. lignin deposition was less upon relative to wounding alone. Consequently, the qualitative pattern observed in the histochemistry (**Fig. 9c, d**) is confirmed by the spectrophotometrical quantification of extracted lignin (**Fig. 9b**).

3.1.7. Bordered pits act as gateways for hyphal spread

Cryo-SEM imaging conducted with infected wood from the susceptible variety Chardonnay revealed details of the colonization process (**Fig 10**). For instance, bordered pits perforating the later xylem vessels walls (**Fig. 10a**) seem to be used as spatial cues for the orientation of hyphal growth during early colonization process (**Fig 8b**). After full attachment to the touching wall,

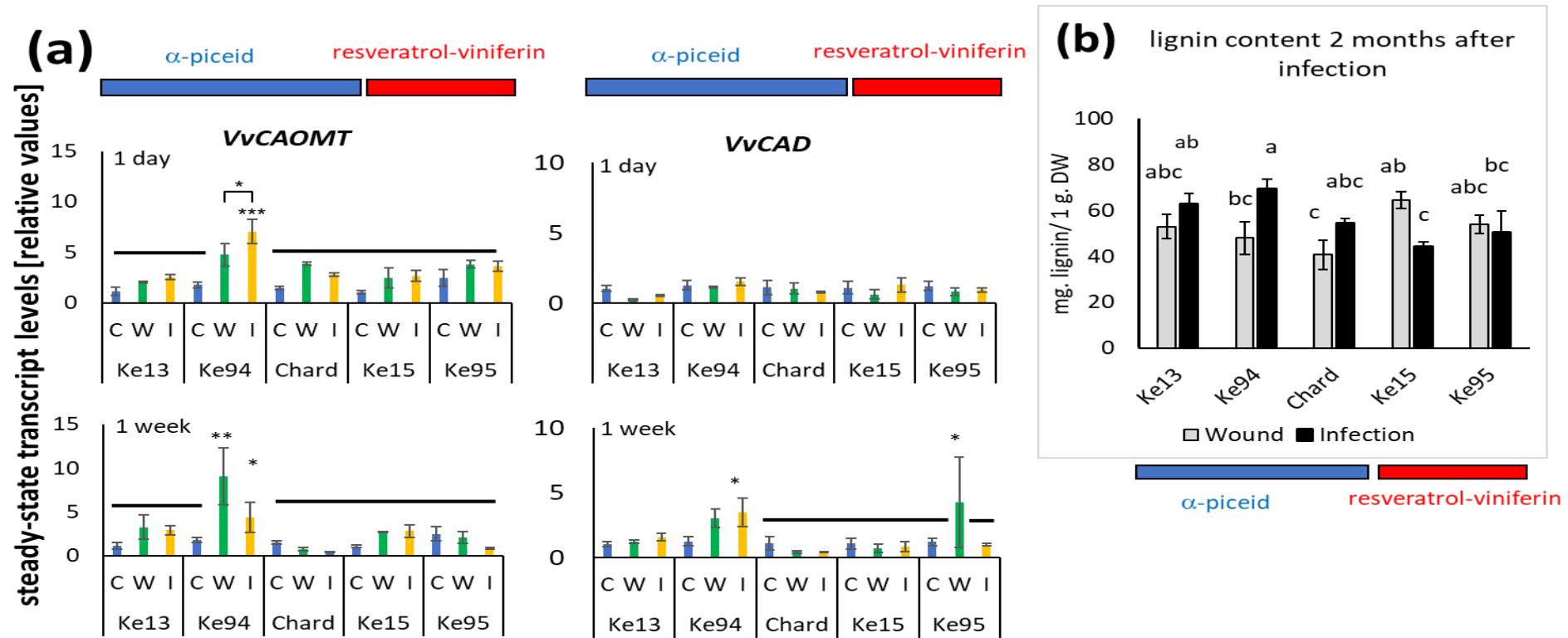


Fig. 9. Genotypic differences in lignin metabolism in response to *Neofusicoccum parvum* Bt strain 67. **(a)** Steady-state transcripts levels of the two lignin-biosynthesis genes *VvCAOMT* and *VvCAD*, 1 day and 1 week after infection, normalised to the levels in Ke13 control plants. Asterisks indicate differences between infected (I), and mock treatment (wounding only, W) over the untreated controls (C) with $P < 0.05$ (*), $P < 0.01$ (**), and $P < 0.001$ (***), respectively based on a LSD test. **(b)** Lignin content at 2 months after infection at the infection site at wounded and infected canes. Different letters specify the statistical significances among the genotypes in lignin content. Error bars indicate to SE and three biological replicates were counted for each assay related to biosynthesis and the content of lignin. Published data in Khattab et al., New Phytologist (2020).

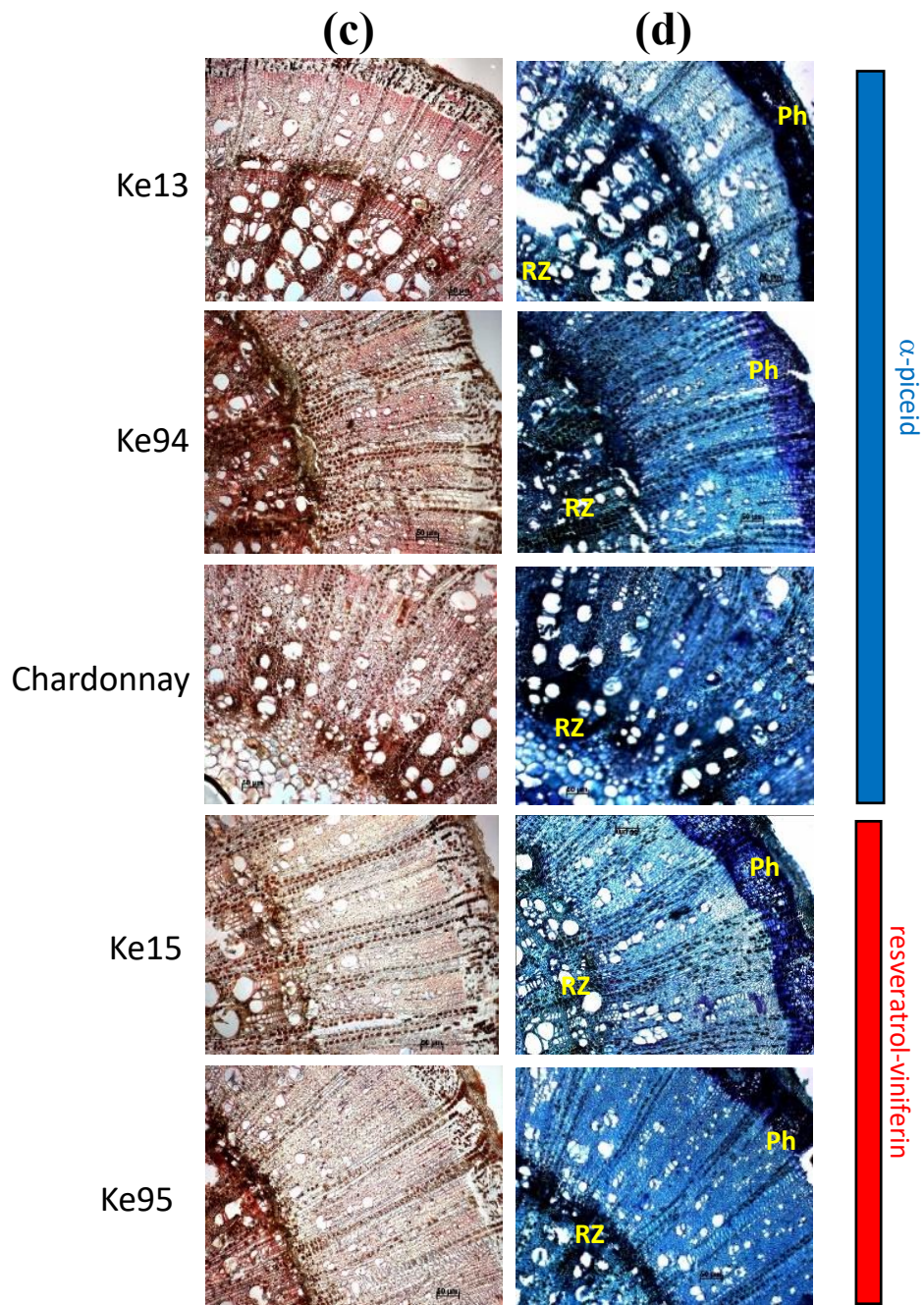


Fig. 9c, d. Histochemical staining of cross sections taken from the infection site 2 months after infection with Phloroglucinol-HCl staining lignin in light red or rose (c), and Toluidine Blue staining lignin in blue, and pectic polysaccharides in purple (d). RZ Reaction Zone of plant-fungal interaction, Ph Phloem. Size bar 100 μ m. Published data in Khattab et al., New Phytologist (2020).

new Hyphae reach out towards the direction of the bordered pits of the opposite wall, making a mycelium network with a geometric growth pattern (**Fig. 10c**). Afterwards, the new hyphae penetrate through the bordered pits from infected vessels in the radial direction into the neighbour para-tracheal parenchymatic cells, thereby increasing the horizontal fungal spread (**Figs. 10d, e**). During later stages, the mycelium cannot only completely block the xylem vessels (**Fig. 10f**), but also colonize cracks in the *Vitis* wood for further spread (**Fig. 10g**).

Since the high susceptibility of certain grapevines varieties was explained by a higher vessel diameter (Pouzoulet et al., 2014; Pouzoulet et al., 2017), the mean cross areas from 50 individual xylem vessels, below the infection site directly, were determined for the different genotypes (**Fig. 10h**) to probe for a potential correlation with necrosis area. The cross- area of xylem vessels were significantly smaller in the *sylvestris* genotypes as compared to Chardonnay. By contrast, the resistant genotypes Ke15 and Ke95 displayed similar vessels to those of the susceptible genotypes, Ke13. However, the smallest vessel cross area was observed in the most susceptible genotype, Ke94. A similar pattern was seen for the stem cross area (**Suppl. Fig. S4. b**). The *sylvestris* accessions were significantly thinner than Chardonnay, but did not show significant differences among themselves. In contrast, the relative coverage of pith area was elevated in the susceptible genotypes Chardonnay and Ke94 as compared to the resistant genotypes Ke15 and Ke95 (**Suppl. Fig. S4, a**). On the other hand, the smallest proportion of pith parenchyma was measured for the susceptible genotype Ke13. Overall, there was no correlation between genotypic differences of wood anatomy and infection success.

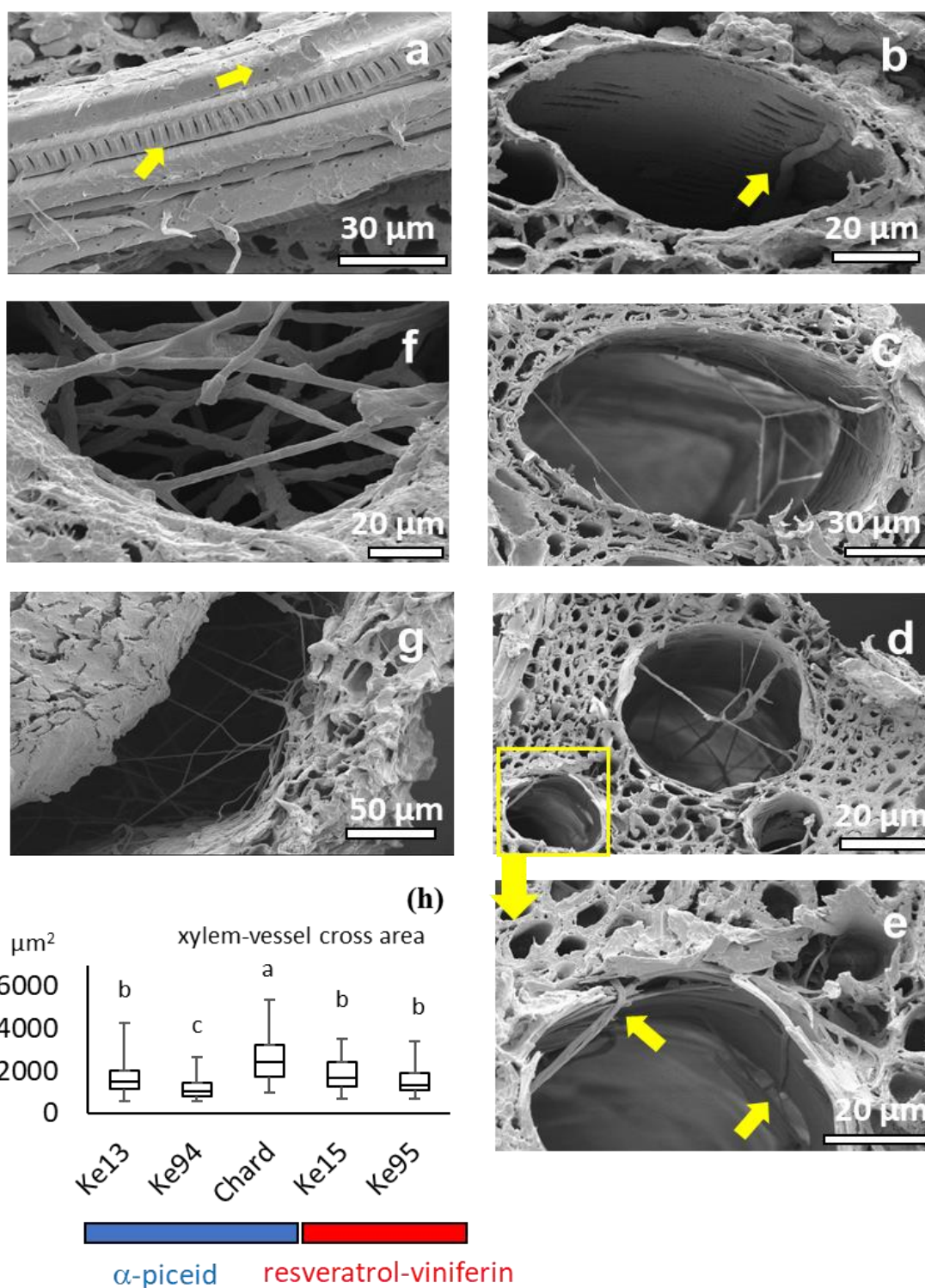


Fig. 10. Cryo-SEM images reveal cellular details of colonization of *Neofusicoccum parvum* Bt strain 67 in infected Chardonnay xylem vessels. **(a)** longitudinal section of xylem vessel displaying the bordered pits. **(b)** A fungal hypha probing the xylem bordered pits during an initial stage of growth. **(c-e)** *Neofusicoccum parvum* hyphae grow in a geometrical pattern utilizing the bordered pits for horizontal growth or colonization of neighbouring vessels (yellow arrows). **(f, g)** Fungal mycelia blocking the xylem vessels and spreading through

wound cracks during late infection. **(h)** Whisker and box plots displaying the median and interquartile range of xylem-vessel cross areas of *Vitis vinifera* ‘Chardonnay’, and four *sylvestris* accessions belonging to different chemotypes (Ke13, Ke94, Ke15, Ke95). Data represent medians from 50 individual vessels from 3 biological replicates per genotype and statistically differentiated using Duncan’s test. Published data in Khattab et al., New Phytologist (2020).

3.1.8. Effect of drought on infection development and lignin accumulation

Since disease outbreak in infected vineyards is triggered by climate change, infected plants of Augster weiß cv. were grown under drought stress, which has accelerated recently due to climate change. In general, plants under drought stress didn’t show equivalent growth rates to well-irrigated ones since the necrotic leaves appeared under drought stress and elevated by infection (**Fig. 11a**). Also, grapevine susceptibility was increased under one-month drought stress where infection made the internodes more symptomatic and caused larger wood necrosis up to 2 folds as compared to infection under optimal water supply (**Fig. 11b**).

To identify whether the increase in symptomatic wood under drought stress is related to fungal development, the genomic DNA was extracted to evaluate the amount of fungal DNA using a specific *ITS* marker (*BOT*) for *Botryosphaeriaceae* DNA detection. The drought stress for one month increased the number of fungal DNA copies at infected internodes, especially at the middle, where fungal DNA copies were more than two folds under drought comparing to optimal water regime.

Regarding lignin accumulation, lignin content was measured at the inoculation site after one-month of both infection and drought stress. Infection alone increased the lignin content significantly under the optimal water regime. Furthermore, drought stress had a more substantial effect on lignin deposition in infected plants. Drought stress enhanced the lignin

deposition in infected plants than those infected but well-irrigated as compared to the healthy mock plants.

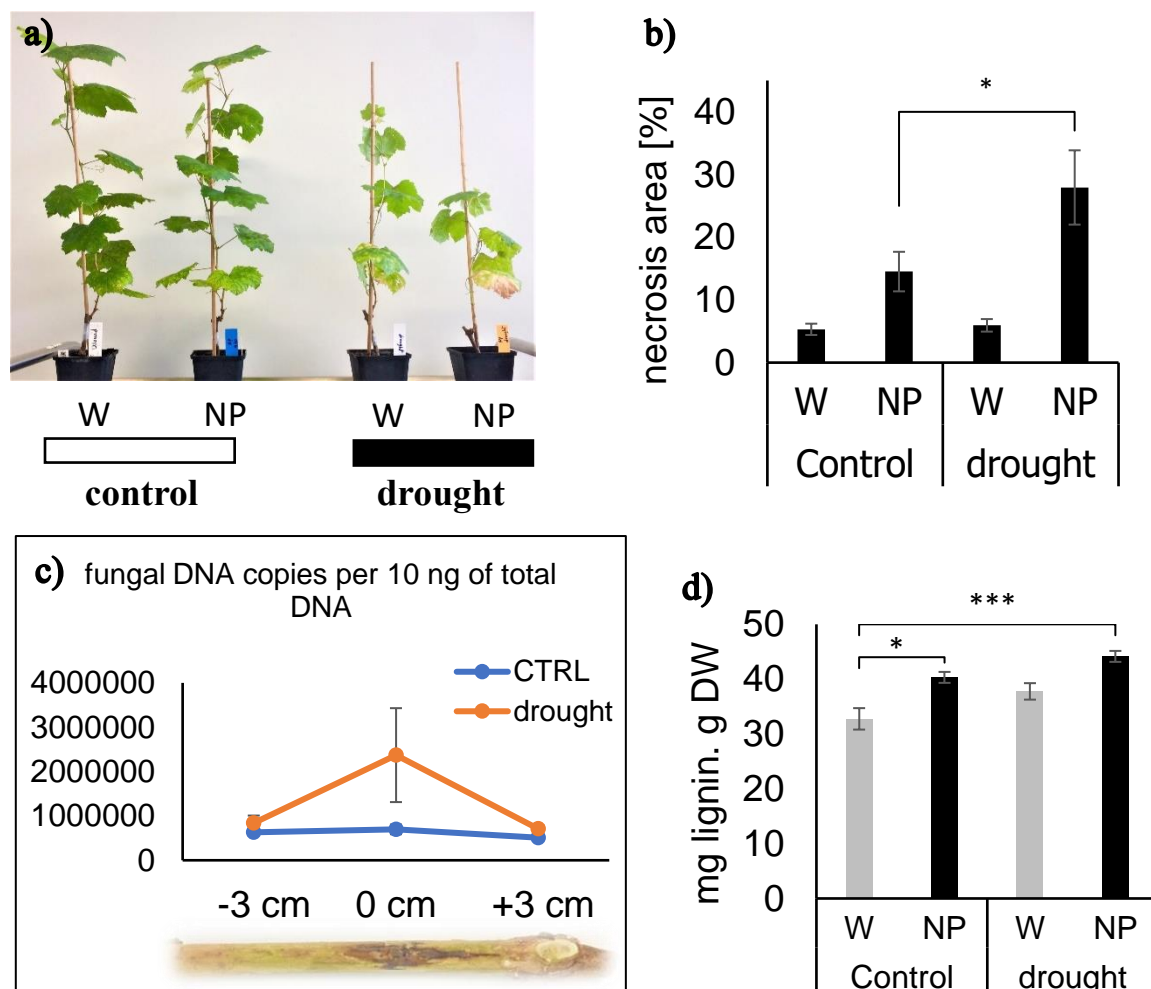


Fig. 11. Effect of drought stress on the *in-planta* growth rates of the fungal strain, *Neofusicoccum parvum* Bt-67, and lignin accumulation in grapevine plants (Augster weiß cultivar) cultivated under greenhouse conditions. a) Potted grapevines under two experimental sets, either control conditions (plants with optimal water regime) or drought stress (20% of optimal water regime). b) The average of wood necrosis area in wounded (W) and infected plants with *Neofusicoccum parvum* Bt-67 (NP) after one-month infection. c) the accumulated fungal DNA copies in one-month infected internodes either under control or drought. d) Lignin content after one-month infection at the inoculation site at wounded and infected canes. Error bars indicate SE, and three biological replicates were counted for each treatment. Asterisks refer to the statistical differences among different treatments using the LSD test. * $P < 0.05$ ** $P < 0.01$; *** $P < 0.001$.

3.2. Hunting the plant surrender signal switching the *Botryosphaeria dieback* to the apoplexy phase in grapevines;

3.2.1. Screening fungal behavior towards defense precursors of the phenylalanine pathway;

For investigating whether a chemical communication with the host triggers the apoplectic breakdown in infected grapevines, fungal mycelia of *Neofusicoccum parvum* were fermented with different lignin precursors (**Fig. 12**), especially that elevated lignin content was more linked with vine susceptibility and fungal development (**Fig. 9; Fig. 11**). The phytotoxicity of *N. parvum* was then screened using *V. rupestris* suspension cells (**Fig. 13a**). Cinnamic acid supplement to the fungal medium significantly reduced the mortality rates of *Vitis* cells driven by culture filtrate of *N. parvum*. Similarly, both *p*-coumaric acid and caffeic acid supplements alleviated the toxic effect of the fungal culture filtrate reaching the normal mortality levels of the control, regardless of the screened precursor's concentration (0.5, 1.0, or 1.5 mM) (**Suppl. Fig. S5**). On the other hand, fermenting the mycelia with ferulic acid boosted the toxicity of the culture filtrate, increasing the mortality levels from 32 % to 55% (**Fig. 13b**), especially with the low concentration of 0.5 mM ferulic acid. Also, the fungal mycelia strongly switched to the sexual cycle, releasing spores on the PDA medium due to ferulic acid supplement. The antagonistic fungal behavior to ferulic acid (unlike other isomers such as coumaric acid) was further analyzed. Here, the effect of the fungal metabolites secreted to the culture filtrate was separated from the metabolites of the mycelia. Mycelium extract of *N. parvum* alone or fermented with phenylpropanoid isomers (*p*-coumaric acid and ferulic acid for only 24 hrs) led to similar mortality rates (**Fig. 13c**). However, after coumaric acid supplement for 24 hours, culture filtrate extracts were less toxic than *N. parvum* alone or mycelium extract. In addition,

the culture filtrate after ferulic acid supplement for 24 hrs showed higher death rates in *Vitis* cells than the culture filtrate of *N. parvum* alone or its mycelium extract (**Fig. 13c**).

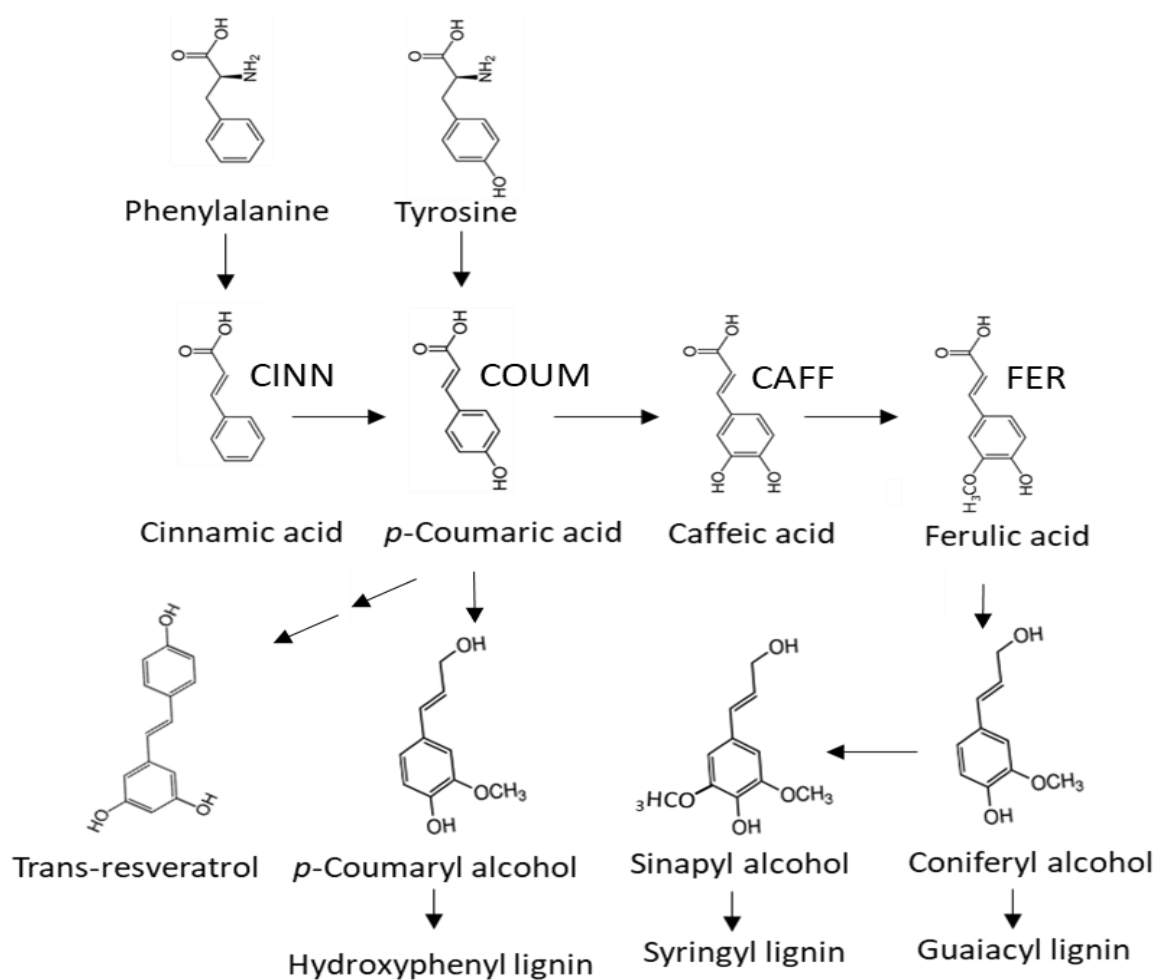


Fig. 12. Monolignol pathway showing the positions of cinnamic acid (CINN), *p*-coumaric acid (COUM), caffeic acid (CAFF), and ferulic acid (FER)

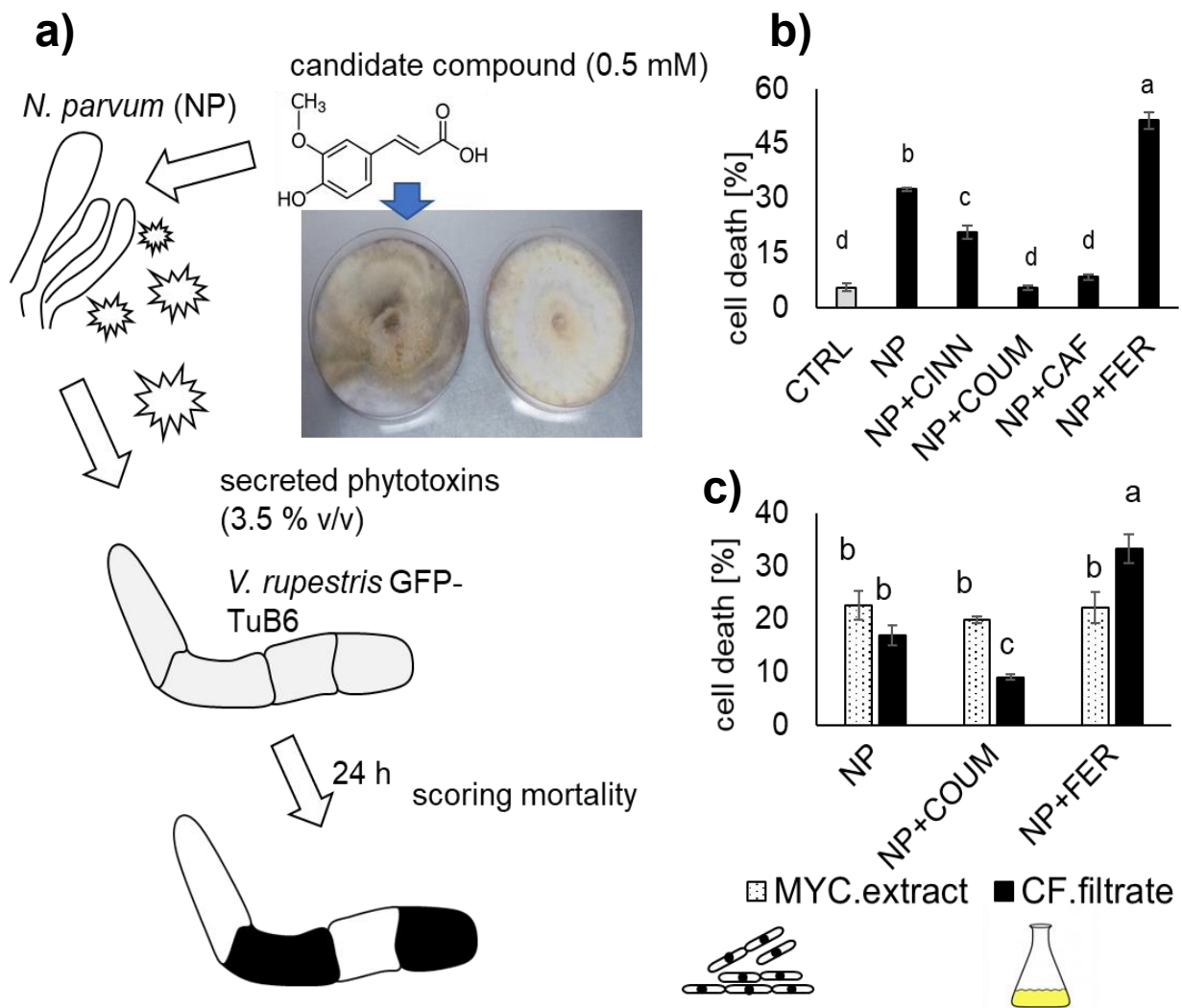


Fig. 13. Screening effect of monolignols precursors on the *Neofusicoccum parvum* behavior. **b)** Experimental design to screen for the surrender signal. Candidate monolignols are fed to *N. parvum* (NP) and the culture filtrate collected after 2 weeks is added to *V. rupestris* GFP-TuB6 as recipient to screen for phytotoxicity **(c)** Mortality of the recipient cells scored in response to culture filtrate from *N. parvum* after feeding the fungal donor with different monolignols as compared to culture filtrate from mock-treated cells (NP), or without any filtrate (CTRL). **(d)** Mortality of the recipient cells in response to fungal metabolites extracted from mycelia (MYC) or recovered from the culture filtrates (CF) after fermentation for 24 hr with *p*-coumaric acid or ferulic acid to probe for potential differences in the secretability of the phytotoxins. Data represent means and SE from three independent biological experiments. Different letters represent statistical differences based on Duncan's test with significant levels $P < 0.05$.

The toxicity of the fungal metabolites was investigated by separating the fungal metabolites based on the hydrophobicity and bioactivity guided fractionation. The fungal metabolites from culture filtrate showed different metabolite profiles by HPLC UV/VIS detectors at different hydrophobic phases. Here, specific fractions only appeared after the ferulic acid supplement enhanced by increasing the hydrophobicity of the solid phase extraction by acetonitrile (MeCN) as shown in (**Fig. 13; Suppl. Fig. 6**). For instance, the peak area of vanillic acid-like compound (orange labeled) increased until 75% MeCN solvent, and Mellein-like compound showed a similar pattern until 50% MeCN solvent. In comparison, the unknown fraction (red labeled at retention time 4,79 min) increased consistently with increasing the hydrophobicity of the extraction phase. By testing the toxicity of the fungal metabolites by different extraction phases on the *Vitis* cells, mortality assays showed that the metabolites of ferulic acid-challenged fungus (NP+FER) became more toxic than metabolites of the fungus alone.

Nevertheless, the fungal metabolites of (NP+FER) were more toxic while increasing the hydrophobic phase of the solvent concentration (MeCN) during the extraction process, showing a very strong correlation ($R= 0,99$) between the metabolites of (NP+FER) under different concentrations of MeCN and cell mortality (**Fig. 15a**). There was a noticed fraction (the red labeled fraction, at retention time 4,79 min (**Fig. 14**) growing by the amplifying hydrophobicity of the extraction phase for metabolites of (NP+FER). Plotting its peak area with the increased cell death presented a high correlation between such fraction and the increased mortality rates in the *Vitis* cells ($R=0,9$) (**Fig. 15b**).

Consequently, the most hydrophobic phase was selected for further LC-MS analysis to purify the bioactive polyketide. Afterwards, the most bioactive polyketide increasing death rate in *Vitis* cells was found in the fractions B1 and B2 (**Fig. 15c**). The structure analysis identified the bioactive polyketide as a derivative of Fusicoccin A (**Fig. 15d**).

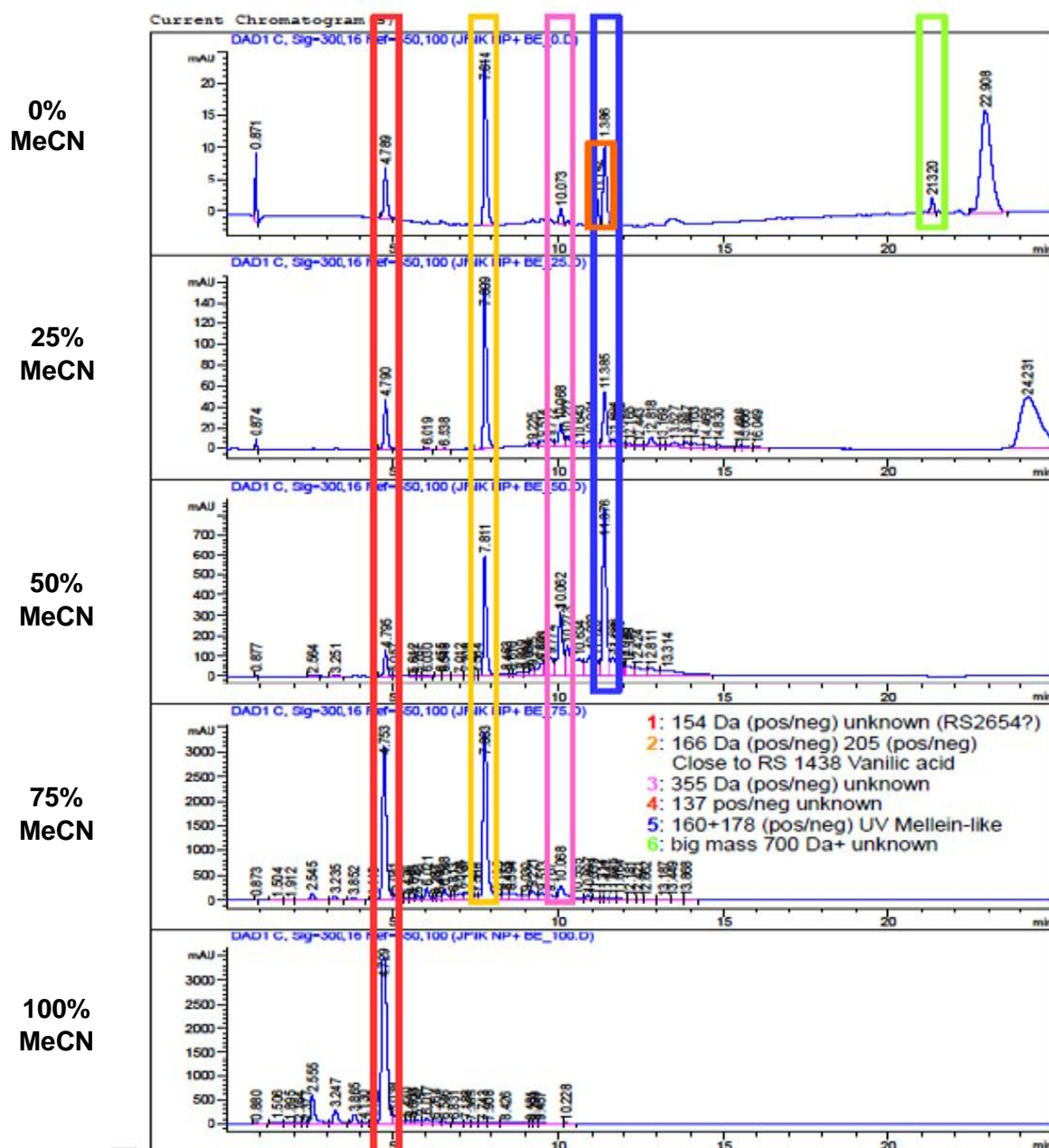


Fig. 14. Identifying the fungal toxin released in response to fermentation with lignin precursor, ferulic acid, for 24 hr. a) HPLC UV readouts for the fungal metabolites secreted by *Neofusicoccum parvum* Bt-67 in response to fermentation with 0,5 mM ferulic acid and extracted using a solid phase extraction by a gradient of acetonitrile, MeCN (0%:25%:50%:75%:100%).

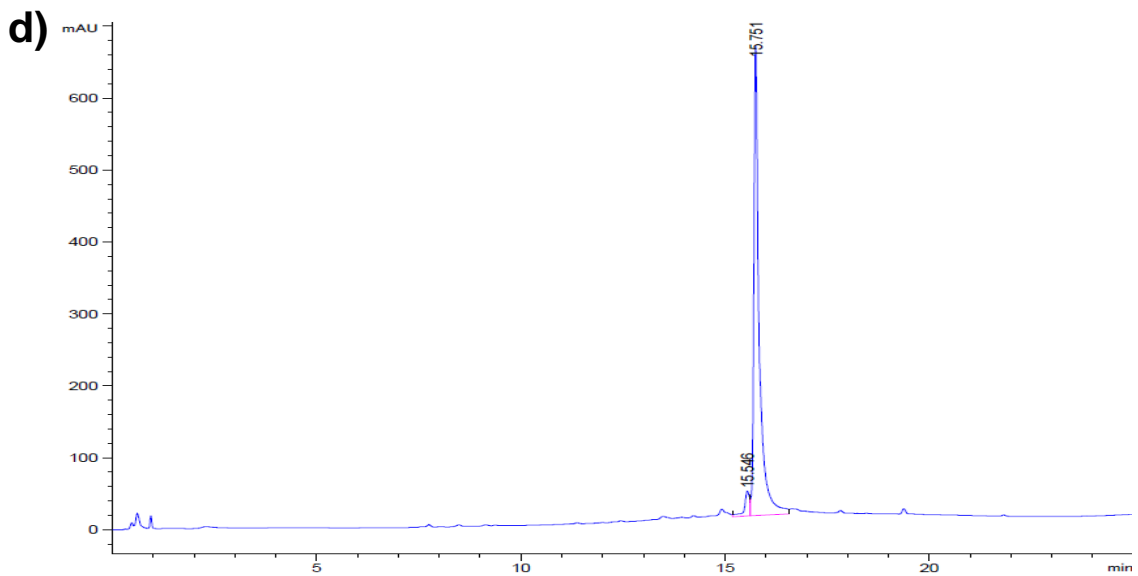
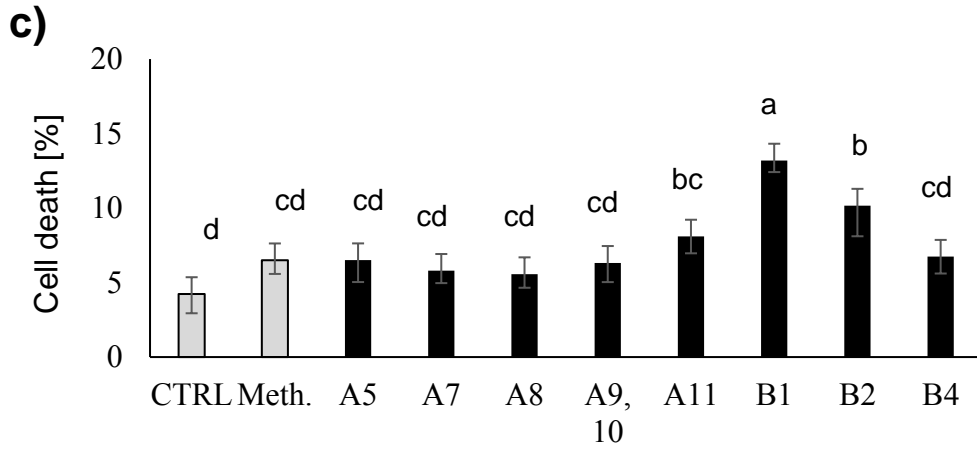
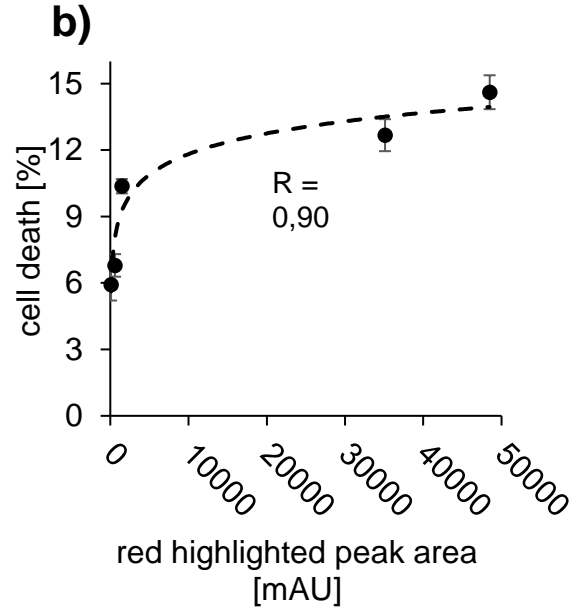
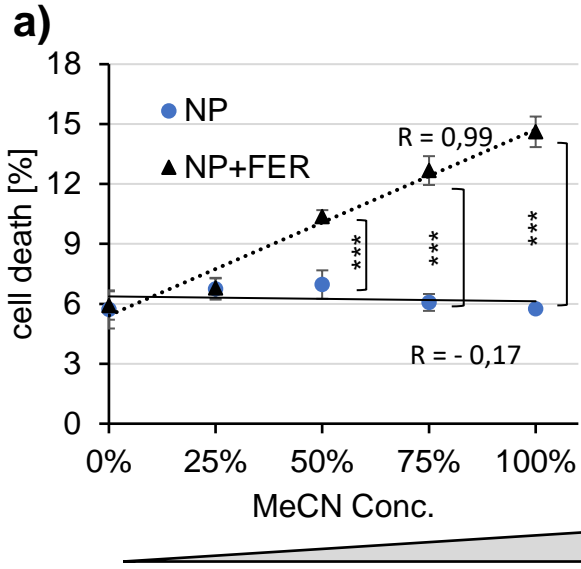


Fig. 15. Bioactivity guided fractionation for the fungal metabolites. a) Mortality of *Vitis rupestris* GFP-TuB6 suspension cells in response to 24 hr treatment of the fungal culture filtrates (20 µg/ml *Vitis* cells) extracted by different concentrations of acetonitrile (MeCN). c) The correlation between the cell death percentage and the peak area of the red labeled fraction extracted by a gradient of MeCN (0%:25%:50%:75%:100%). d) Mortality of *V. rupestris* GFP-TuB6 cells in response to fractions purified from secreted culture filtrates (hydrophobic phase, MeCN 100%) of *N. parvum* treated with ferulic acid (10 µg fraction per 750 µL *Vitis* cell suspension) scored after 24 h. Bars represent means and SE from three independent experimental series. Different letters represent statistical differences based on the least significant difference, LSD, test with significant levels $P < 0.05$. e) Compound isolated from fractions B1 and B2 by LC-MS analysis and identified as a derivative of Fusicoccin A.

3.2.2. Cellular response to Fusicoccin A

To probe the FCA effect on the cell mortality, *Vitis rupestris*, AtTUB6-GFP, were treated with two different concentrations, 6 and 12 µM of Fusicoccin A (**Fig. 16a**). The cytological characterization of cell death stages due to FCA treatment was studied at 2 time points, 3 hrs and 6 hrs, using double staining assay (AO/EB), which classifies dying cells to 3 stages as described in the methodology. The higher concentration of FCA (12 µM) was faster in killing *Vitis* cells. The living cells (green-colored) decreased significantly to 39 % after just 3 hrs. In parallel, the dying cells at the first step with a partial loss in plasma membrane integrity (green-yellow; yellow-colored cells) increased to 20 % as well as dead cells (red-colored cells) to 36 %. However, the low concentration of FCA, 6 µM, needed 2 time-folds, 6 hrs, to cause similar mortality rates

driven by 12 µM FCA for 3 hrs treatment. Also, the fatal effect of 12 µM FCA was elevated by time, after 6 hrs, increasing the percentage of dying cells at the early stage to 47%, dead

cells to 46 % (complete cell membrane breakdown) and, as a consequence, healthy cells were drastically decreased to only 4%.

In addition, double staining assay showed that FCA-challenging cells were characterized with cytological hallmarks of autolytic cell death. For instance, chromatin condensation appeared earlier in the 1st stage of cell death (**Fig. 16c**), followed by the formation of lytic vacuoles in the cytoplasm of dying cells (**Fig. 16d, e**). However, some cells were completely stained by Ethidium Bromide, showing red-stained nuclei without noticing the common cytoplasmic signals observed in (**Fig. 16c, d, e**). Such type of cell death was classified as accidental cell death (**Fig. 16f**)

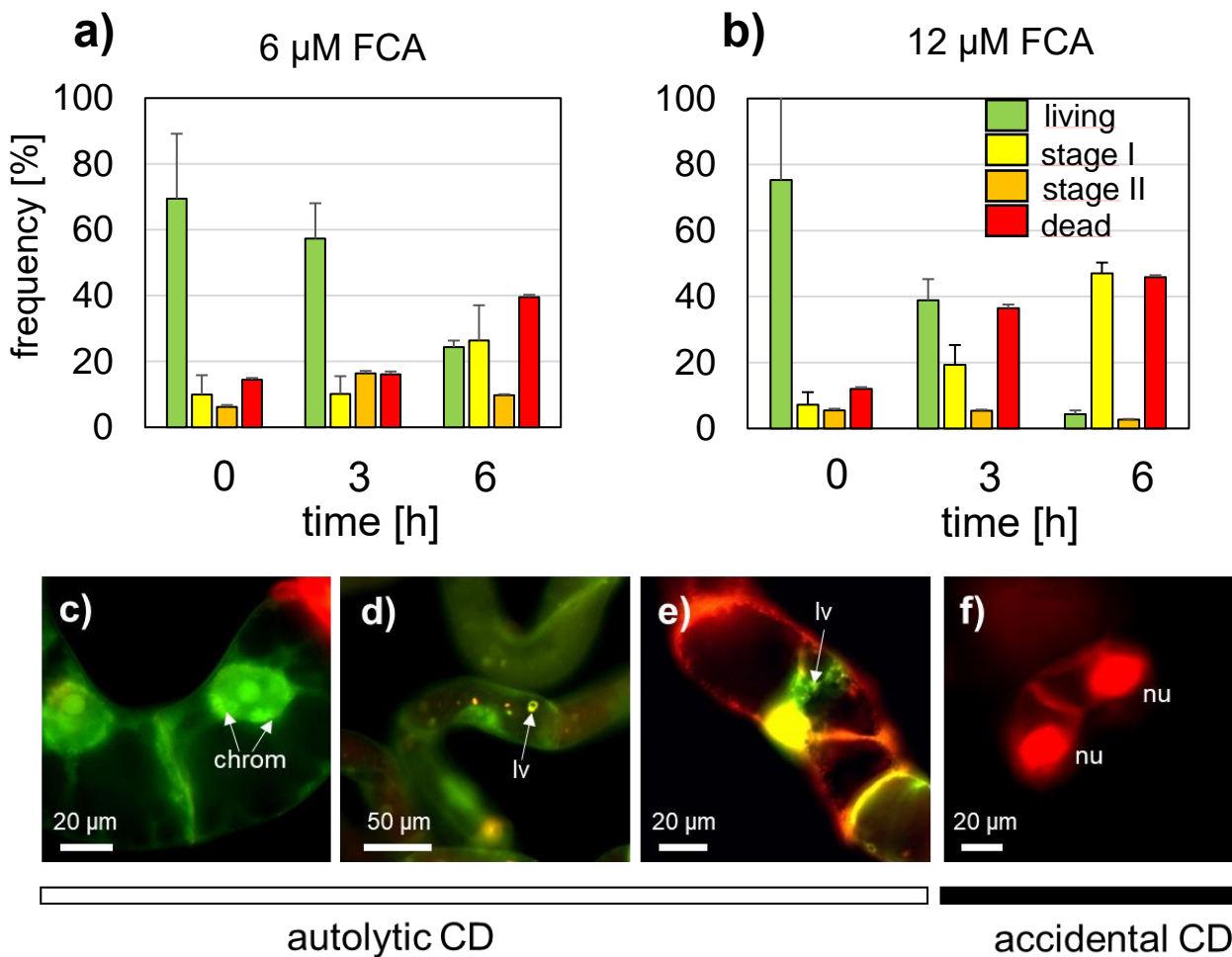


Fig. 16. Cytological characterization of cell death in *Vitis* cells in response to Fusicoccin A. The cell death response was classified based on double staining with the membrane-permeable fluorochrome Acridine Orange (green signal) and the membrane-impermeable fluorochrome Ethidium Bromide (red signal). Living cells exclude Ethidium Bromide and appear green, cells in stage 1 show penetration of Ethidium Bromide into the cytoplasm but still exclude the dye from the karyoplasm, cells in stage 2 show penetration of Ethidium Bromide into the nucleus, dead cells lose the Acridine Orange signal due to complete breakdown of the plasma membrane, while Ethidium Bromide remains sequestered at the DNA. Time course of these stages in response to 6 μ M (a) and 12 μ M (b) Fusicoccin A. Frequency distribution represents 300-400 individual cells collected from three independent experimental series. (c-e) cytological hallmarks of autolytic cell death induced by Fusicoccin A, such as chromatin condensation in interphase nuclei (c, chromatin), or appearance of lytic vacuoles (lv) in the cytoplasm (d, e). For comparison, a dead cell void of cytoplasmic signals, but nuclei (nu) labeled by Ethidium Bromide is shown (f). A predominance of this latter cell type would be an indicator of accidental cell death.

3.2.3. Mapping stress signaling of Fusicoccin A

A low concentration of FCA, 6 μ M, was selected for mapping its stress signaling. Early stress signaling of 6 μ M FCA led to a robust and fast activity of plasma membrane (PM) ATPases, which pumped the protons acidifying the extracellular pH. The differences in PM ATPases activity due to FCA was estimated by steady-state changes in the pH readouts (Δ pH), which dropped fast to -0,1 units after 5 min in a consistent manner till -0,3 units through the first 90 min of FCA treatment (**Fig. 17**).

To measure RbOH activity, Nitroblue tetrazolium staining assay (0,1%) was performed to visualize cells accumulating superoxide anion, O₂⁻, in purple-blue color as reported in Steffens & Sauter (2009) and Pietrowska *et al.* (2014). Effect of FCA on RbOH activity in *Vitis* cells appeared quickly after 10 min, where *Vitis* cells started to accumulate superoxide getting significant purple-blue color. The percentage of cells accumulating superoxide increased dramatically and culminated after 60 min FCA treatment. Afterwards, the superoxide regeneration came slightly down in FCA-challenging cells but with highly significant levels as compared to the FCA-free cells at all observed time points (**Fig. 18**).

To get insight into Fusicoccin A signaling pathway, steady-state transcripts levels of potential stress-marker genes were studied after FCA treatment (**Fig. 19**). Transcripts levels of *Superoxide Dismutase* genes (*Mn.SOD1*, *Mn.SOD2*, *Cu.SOD1*, *Cu.SOD2*, *Cu.SOD3*) were monitored as markers for retrograde signaling at different time intervals, 1, 3 and 6 hrs. Only two genes (*Mn.SOD1* and *Cu.SOD2*) showed induction by FCA treatment at all time points. This was not seen in the other *SOD* genes, especially *Mn.SOD2* and *Cu.SOD3* (**Fig. 19a**). Also, *Cu.SOD1* only showed up more transcripts after 3 hrs of FCA treatment. Likewise, FCA upregulated Metacaspases genes, MC2 and MC5, (as markers for regulated cell death (Gong *et al.*, 2019)) in different patterns. FCA led to amplifying the transcripts levels of MC2

progressively from 3.1 folds after 1 hr to 5.2 folds after 3 hrs. In contrast, the highest abundance of *MC5* transcripts was noticed only after 1 hr treatment and reversed afterwards gradually.

Transcripts of genes regulating the phenylpropanoid pathway were studied after 1 hr of FCA treatment as a potential defense response (**Fig. 19b**). The induction of *PAL* was more striking than any other genes regulating the phenylpropanoid channeling. Lignin biosynthesis genes, *CAOMT* and *CAD*, didn't show significant induction, while stilbenes biosynthesis genes accumulated significant transcripts levels, especially *STS27* and *STS47*.

In addition, FCA-challenged cells accumulated more transcripts of *JAZ* genes (*JAZ1* and *JAZ9*), respectively, as markers for activated jasmonate signaling and basal defense. To probe salicylic acid-dependant pathway regulation by FCA, transcripts of the key player gene *NPRI* were upregulated significantly more than resting levels. In parallel, pathogenesis-related proteins, *PR1* and *PR10*, were upregulated to 6 and 1,6 induction folds, respectively (**Fig. 19c**).

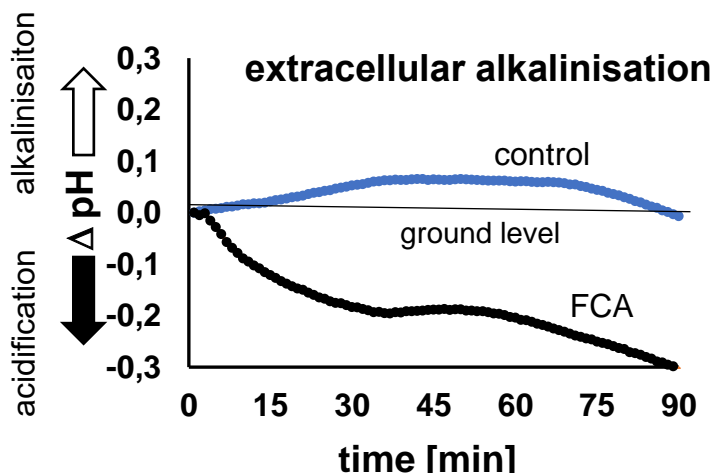


Fig. 17. Rapid responses of *V. rupestris* GFP-TuB6 cells to Fusicoccin A, which activates plasma-membrane ATPases by Fusicoccin A (6 μ M) as detected by acidification of the extracellular medium.

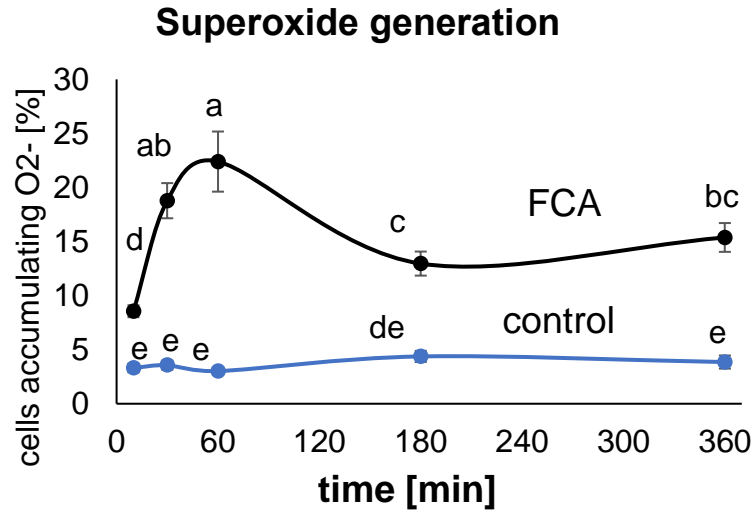


Fig. 18. Superoxide anion detection in *V. rupestris* GFP-TuB6 cells by 0.1% Nitroblue tetrazolium (NBT) staining. Every time point represent the average of 600-700 stained cells at three different experimental sets.)

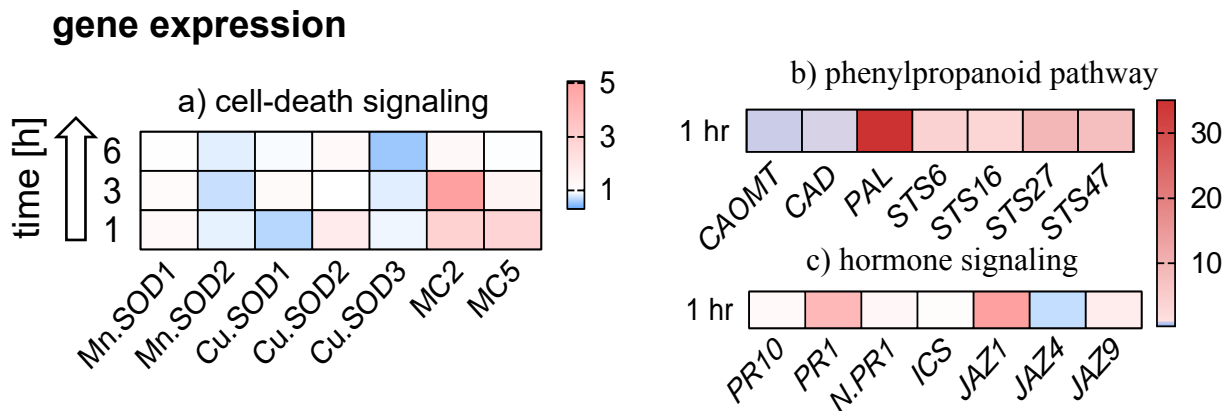


Fig. 19. Modulation of steady-state transcript levels of stress-marker genes measured by qPCR in response to Fusococcin A (6 μ M). a) steady-state levels for transcripts involved in cell-death signaling such as mitochondrial (*MnSOD*) and plastidic (*CuSOD*) superoxide dismutase genes, as well as defense-related metacaspases (*MC2*, *MC5*) over 1hr, 3hrs, and 6 hrs. b) The transcripts of the phenylpropanoid pathway initiating from \square henylalanine ammonia-lyase (*PAL*), exemplarily probing monolignol synthesis (*CAOMT*, *CAD*) and stilbene synthesis (*STS6*, *STS16*, *STS27*, *STS47*). C) Transcripts of phytohormonal signaling genes (*JAZ1*, *JAZ2*, *JAZ9* for jasmonates; *PR1*, *ICS* for salicylic acid). Color code represents the significant fold changes of 3 biological replicates normalized to the control of the respective time-point. Different letters represent statistical differences based on Duncan's test with significant levels $P < 0.05$.

3.2.3.1. Effect of blocking 14-3-3 proteins on the fusicoicin signaling pathway

To test whether blocking FCA receptors (14-3-3 proteins) could inhibit its signaling, many molecular and cellular events were investigated in *Vitis* cells that were pre-treated first by 14-3-3 inhibitor, BV02 (Stevens *et al.*, 2018). Regarding extracellular pH, BV02 decreased the pH acidification driven by FCA treatment since it reduced the available FCA receptors, 14-3-3 proteins, which minimized the downstream PM ATPases activity (**Fig. 20a**). Further changes were observed on the transcripts levels of stress-marker genes in pre-treated cells by BV02 against FCA (**Fig. 20b**). *Stilbene synthase* genes (STS27 and STS47) expression pattern was strongly elevated in FCA-challenged cells. On the other hand, BV02 reduced the observed induction of *PAL* and *PRI* regulated by FCA with statistical differences of ($P < 0.001$). Similarly, Metacaspases genes regulating cell death signaling (*MC2* and *MC5*) in FCA challenged cells were statistically downregulated ($P < 0.05$ and $P < 0.001$ respectively) in 14-3-3 blocked cells.

The consequences of blocking 14-3-3 proteins not only changed PM ATPases activity and stress-marker genes against FCA but also reduced mortality rates strongly by about 50% (**Fig. 20c**). For instance, the mortality ratio decreased from 30% (FCA alone) to 16 % after 6 hrs in the 14-3-3 blocked cells (BV02 + FCA). Here, it's worth noting that, cell death assay, Evans blue, showed that the double treatment of BV02 and FCA couldn't significantly enhance mortality rates as compared to 14-3-3 blocked cells since BV02 treatment led to significant mortality levels up to 20% in *Vitis* cells.

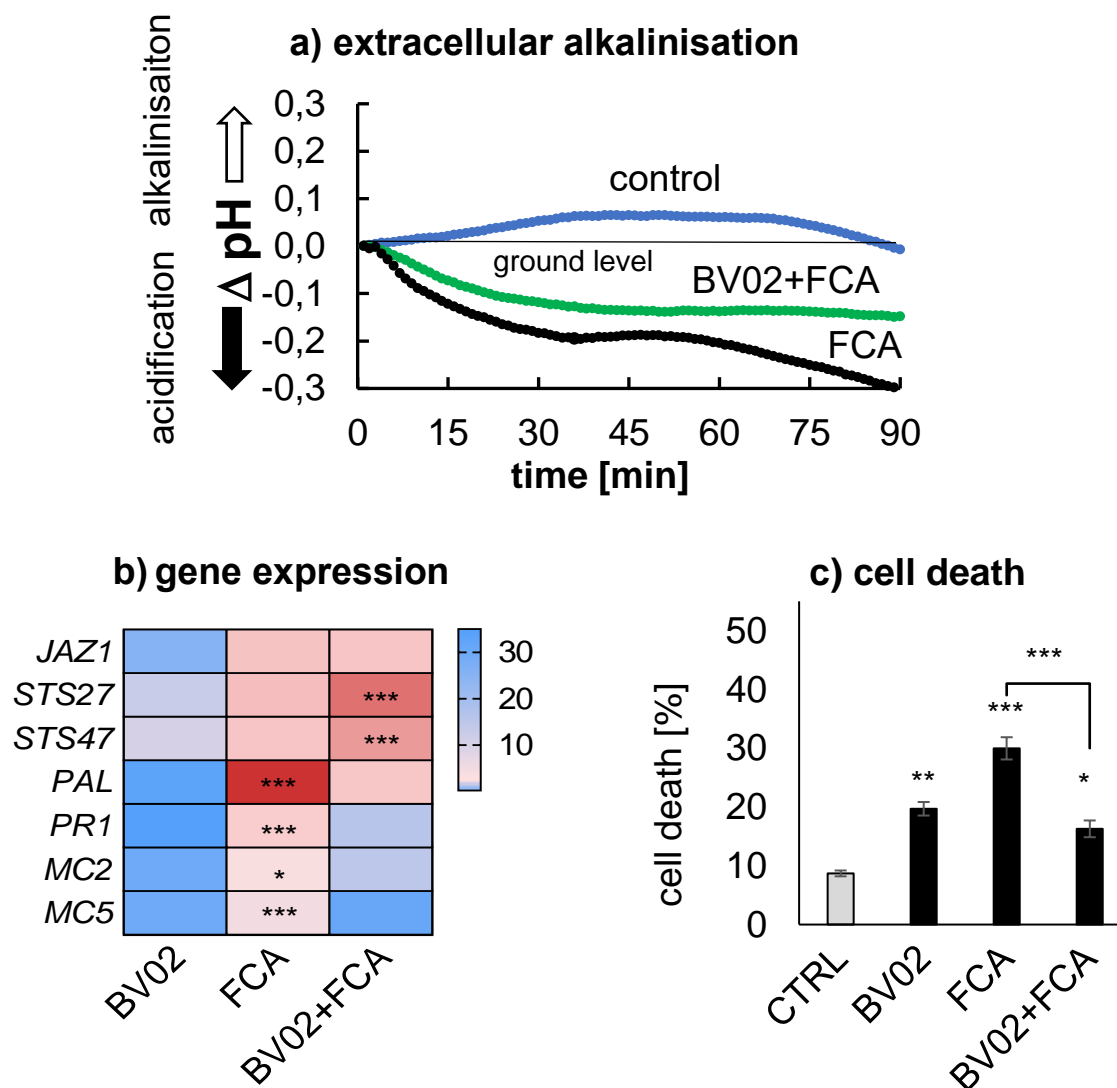


Fig. 20. Role of 14-3-3 proteins for the cellular responses to Fusicoccin A. a) effect on extracellular acidification in response to 6 μM Fusicoccin A (FCA) as a readout for plasma-membrane localized proton ATPases and after pre-treatment with 5 μM of the 14-3-3 inhibitor BV02 for 30 min. Effect of the 14-3-3 inhibitor BV02 on specific defense-related transcripts (b), and mortality (c). BV02 was given in 5 μM 60 min before adding FCA. Transcripts were scored after 1 h, mortality after 6 h. Color code represents means normalized to the control from 3 biological replicates, and asterisks indicate a significant difference between Fusicoccin A alone versus the combination with the respective inhibitor. Bars represent means and SE from 3 biological replicates. Asterisks indicate statistical differences by LSD test at significance level with $P < 0.05$ (*), $P < 0.01$ (**), and $P < 0.001$ (***)

3.2.3.2. Blocking RbOH manipulates Fusicoccin A signaling

To probe whether ROS are involved in the stress signaling of FCA, RbOH was blocked by DPI before FCA treatment. DPI treatment led to changes in molecular and cellular stress responses regulated by FCA alone. DPI-treated cells showed similar Superoxide regeneration to control cells. However, DPI strictly reduced the Superoxide regeneration in FCA-challenging cells as visualized by NBT staining, since DPI pre-treatment reduced the ratio of O₂⁻ accumulating cells due to 1 hr FCA stress from 22% to 10% (**Fig. 21a**).

DPI treatment altered the FCA effect on steady-state transcripts levels of stress-marker genes significantly (**Fig. 21b**). DPI alone was able to induce basal defense genes (*JAZ1*, *STS27*, and *STS47*). Moreover, it increased their transcripts in response to FCA stress. Although DPI alone triggered PAL expression, the accumulated transcripts by double treatment of DPI plus FCA declined until 50% of the induced transcripts by FCA alone. Similarly, RbOH-blocked cells responded to FCA stress with less transcripts of *PR1* and *MC5* with significant levels $P < 0.001$ and $P < 0.01$, respectively. Afterwards, to test whether the DPI inhibitor could reduce cell death triggered by FCA, Evans blue staining showed that inhibiting RbOH before FCA treatment reduced the triggered mortality by FCA as compared to the sole treatment of FCA (**Fig. 21c**). Nevertheless, FCA treatment after blocking RbOH couldn't induce mortality rates higher than DPI treatment alone.

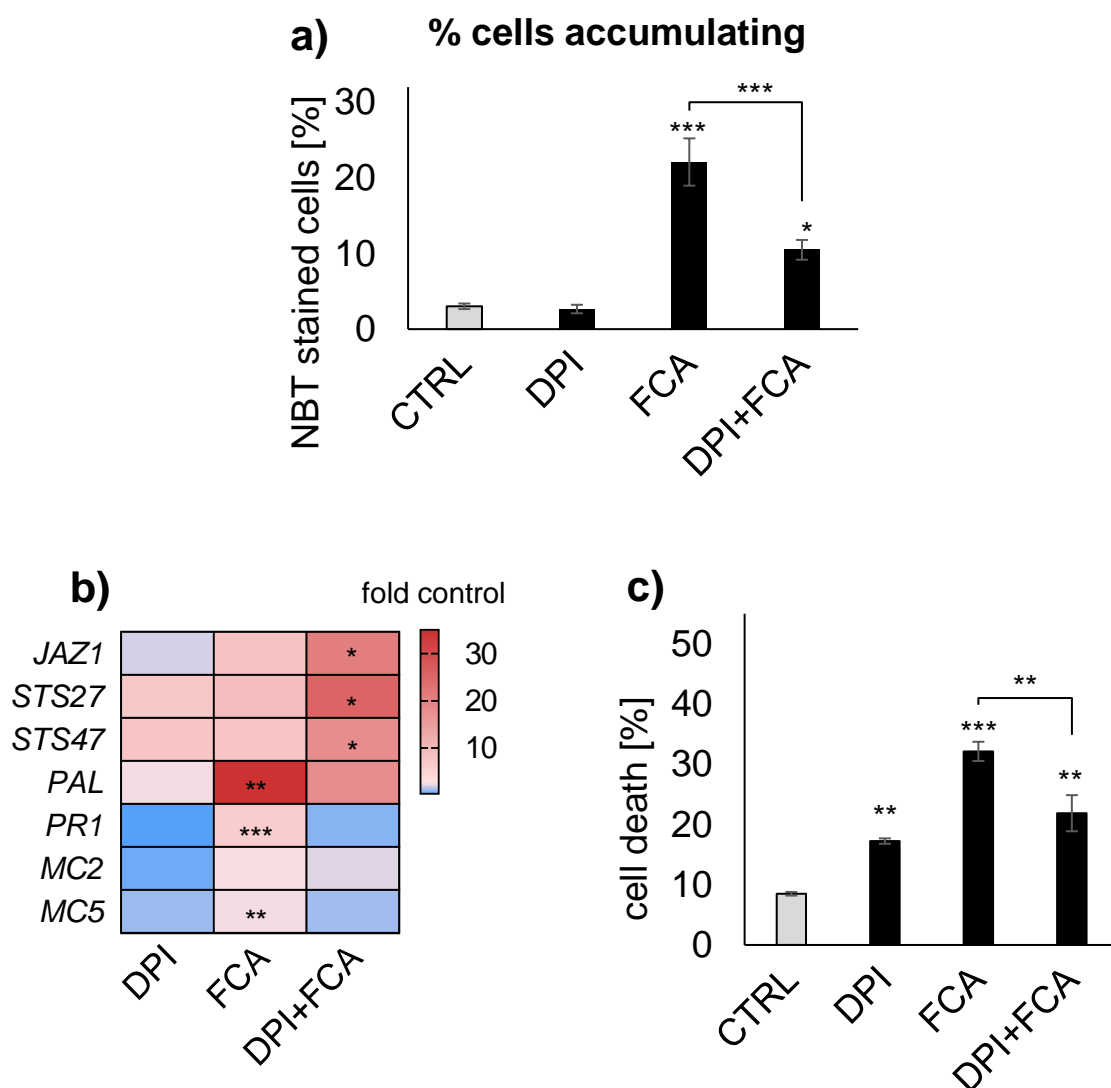


Fig. 21. Effect of Respiratory burst oxygen Homolog on the cellular responses to Fusicoccin A. a) Detection of cells accumulating intracellular superoxide O_2^- triggered by Fusicoccin A in case of blocking the respiratory burst oxidase homologue by 1 μ M diphenylene iodonium, DPI. b) Dissecting effect of the DPI pre-treatment on defense-related transcripts and mortality (c) induced by 6 μ M Fusicoccin A. DPI in 1 μ M, was given 60 min prior to adding FCA. Transcripts were scored after 1 h, mortality after 6 h. Color code represents means normalised to the control from 3 biological replicates, and asterisks indicate significant difference between Fusicoccin A alone versus the combination with the respective inhibitor. Bars represent means and SE from 3 biological replicates. Asterisks indicate statistical differences by LSD test at significance level with $P < 0.05$ (*), $P < 0.01$ (**), and $P < 0.001$ (***)

3.2.3.3. Effect of microtubules manipulation on Fusicoccin A signaling.

For studying the effect of FCA on microtubules integrity, *Vitis rupestris* cells with GFP-tagged β -tubulin (*AtTUB6*-GFP) were incubated with FCA treatment. After 30 min, FCA caused strong depolymerization in the cortical microtubules compared to the control cells (**Fig. 22a,d,g**). Microtubules were stabilized first for 1 hr by 10 μ M taxol before FCA incubation. The pre-treatment of taxol increased the microtubules network integrity even more than control cells (**Fig. 22a,b,g**). It also reduced the microtubules depolymerization driven by FCA treatment (**Fig. 22d,e,g**). Regarding the effect of stabilizing microtubules on the expression of stress-marker genes, taxol alone upregulated *Stilbene Synthase* genes *STS27* and *STS47* (**Fig. 22h**). Also, stabilizing microtubules changed the regulation of stress marker genes in response to FCA stress. For instance, *Vitis* cells accumulated significantly more transcripts of genes regulating phytoalexins biosynthesis, *PAL*, *STS27*, and *STS47*. By contrast, less transcripts of metacaspases genes, *MC2* and *MC5*, in addition to *PR.1*, were seen when the cells were pre-treated 1 hr earlier by taxol before FCA treatment. Although taxol treatment enhanced microtubules integrity and modulated the gene expression, it couldn't decrease cell death in *Vitis* cells by FCA treatment (**Fig. 22i**).

To test whether microtubules depletion can eliminate the effect of FCA, *Vitis* cells were pre-incubated with 10 μ M oryzalin, which strongly depolymerized the microtubules after 30 min (**Fig. 22c**). Combining oryzalin and FCA led to similar damage in microtubules structure seen by oryzalin alone (**Fig. 22f, g**). Furthermore, there was no added advantage of depleting microtubules 1 hr earlier, before FCA treatment, since it couldn't halt FCA's effect on the cell death rates measured by Evans blue assay. However, the overexpression of β -tubulin *V. rupestris* cells decreased the susceptibility in the long term and showed less mortality than the wild type (**Suppl. Fig. 7**)

Results

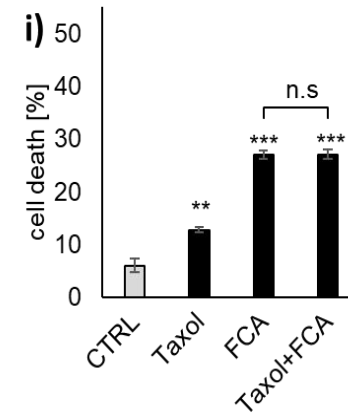
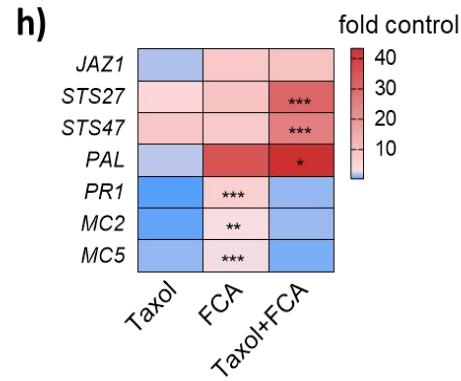
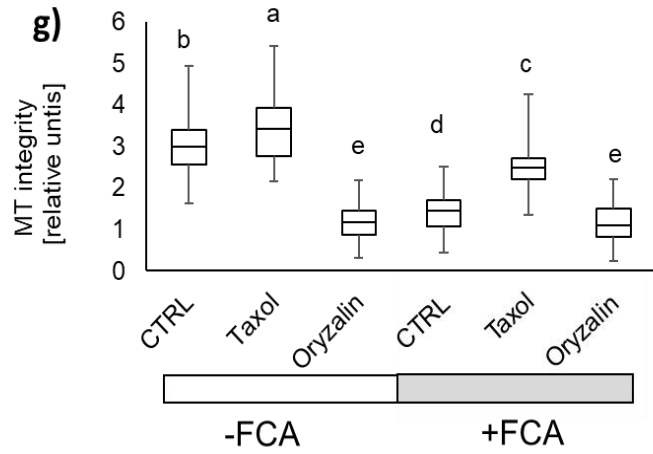
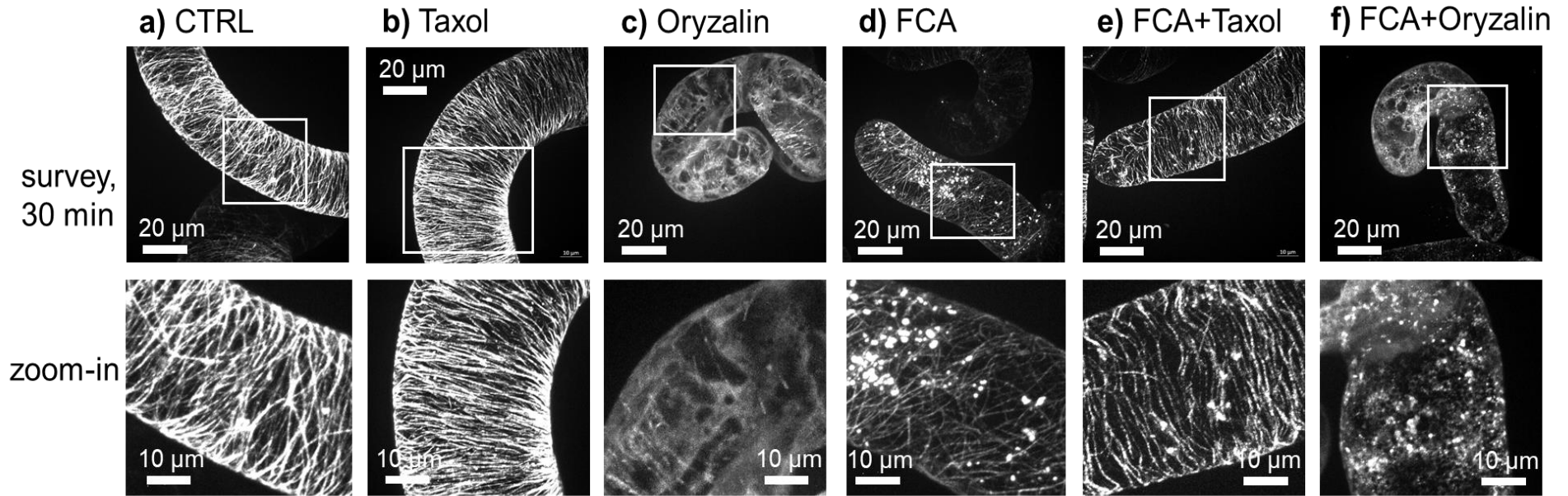


Fig. 22. Microtubular response to Fusicoccin A, and role of microtubules for the cellular responses to Fusicoccin A. Representative *V. rupestris* GFP-TuB6 cells after 30 min of treatment with microtubule-modulating compounds either in the absence (**a-c**) or in the presence of FCA (**d-f**). Solvent controls (**a, d**) 0.1% DMSO, 10 μ M taxol (**b, e**), or 10 μ M Oryzalin (**c, f**) are shown. **g**) quantification of microtubule integrity for the treatments shown representatively in (**a-f**). Data represent medians, inter-quartiles, and extreme values for measurements from at least 30 individual cells. **h**) heat map of steady-state transcripts levels of stress-marker genes 1 h after addition of 6 μ M FCA either alone or in combination with 10 μ M taxol. **i**) Mortality scored at 6 h after the addition of either 6 μ M FCA, 10 μ M Taxol, or a combination of both compounds. Data represent mean and standard errors from three independent biological experiments comprising 1500 individual cells. Different letters represent statistical differences based on Duncan's test with significant levels $P < 0.05$.

3.2.3.4. Effect of Actin filaments depletion on Fusicoccin A signaling.

Since actin filaments are implicated in programmed cell death signaling (for review, see Smertenko & Franklin-Tong, 2011; Chang et al., 2015), Chardonnay actin-marker cell line (*AtFABD2-GFB*) was used to visualize the actin filaments responses to FCA. There were changes observed in the actin structure in response to FCA treatment after 90 min exhibiting a very dynamic actin bundling (**Fig. 23a,c**). The actin bundling was statistically confirmed by measuring the actin bundle width, which was significantly thicker in FCA-challenging cells than control cells with P -value < 0.001 (**Fig. 23e**).

To probe whether actin bundling is necessary as an upstream of cell death signaling triggered by FCA, actin strands were depleted at first for 1 hr by 2 μ M Latrunculin B before incubating cells with FCA (**Fig. 23b**). The observed bundling in Chardonnay cells by FCA stress alone was not seen after depleting the actin filaments by Latrunculin B (**Fig. 23d, e**). Furthermore, actin depletion by latrunculin B led to a noticeable decrease in the mortality rates driven by FCA (**Fig. 23g**). To check whether actin depletion could modulate the effect of FCA on the stress marker genes, qPCR readouts showed that the pretreatment of latrunculin B enhanced

the upregulation of basal defense genes, *JAZ1*, *STS27*, and *STS47* in FCA-challenging cells. On the other hand, cells with depleted actin strands did not upregulate Metacaspases gene, *MC5*, and showed less transcripts of *PAL* and *PR.1* due to FCA stress (**Fig. 23f**)

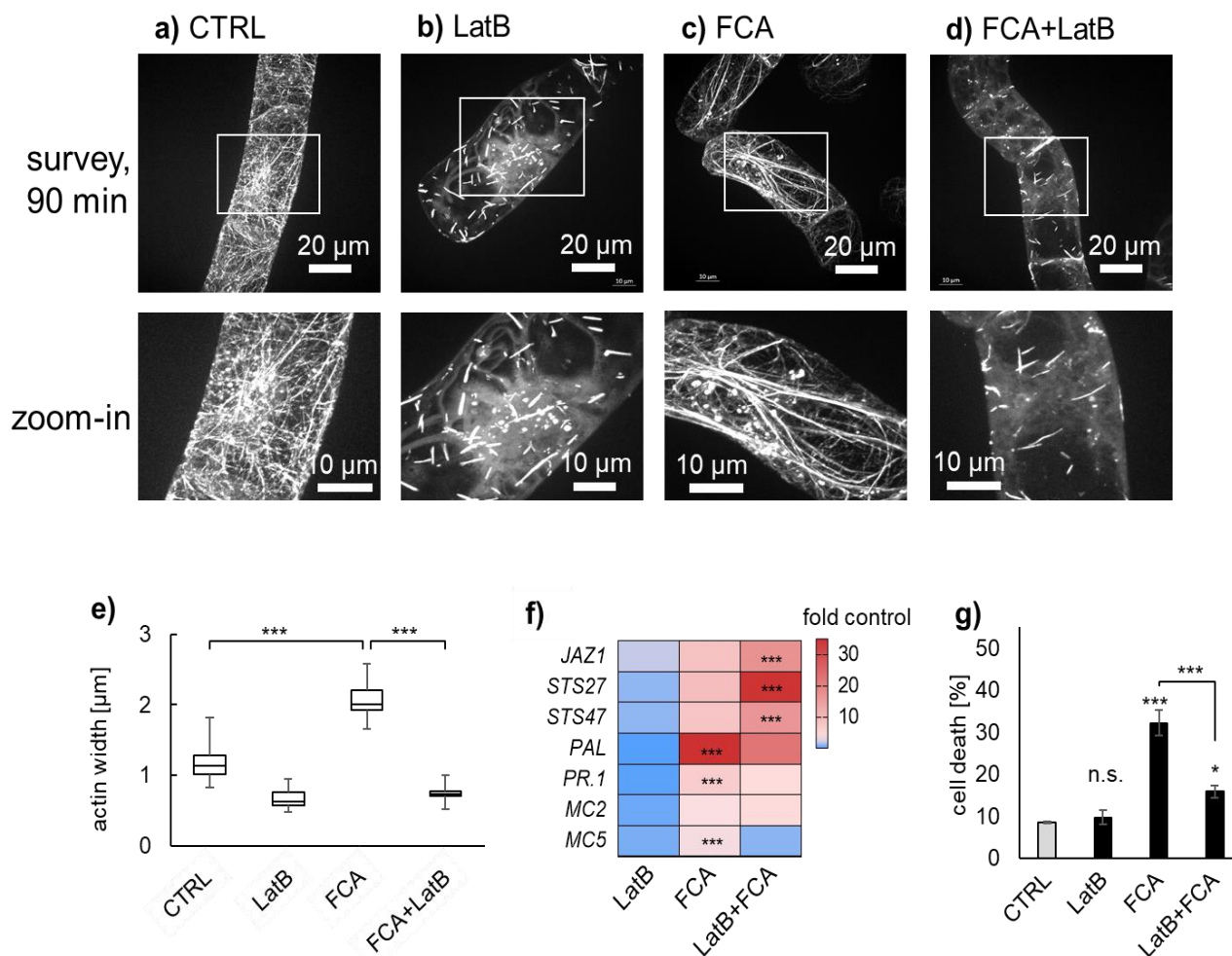


Fig. 23. Actin response to Fusicoccin A, and role of actin for the cellular responses to Fusicoccin A (6 μM). Representative *V. vinifera* cv. Chardonnay FABD2-GFP cells after 90 min of treatment with the actin-eliminating compound Latrunculin B (2 μM) in the absence (**b**) or in presence of FCA (**d**), compared to the solvent control (**a**) 0.1% DMSO, or to Fusicoccin A alone (**c**). **e**) quantification of actin bundling for the treatments shown representatively in (**a-d**). Data represent medians, quartiles, and extreme values for measurements from at least 30 individual cells. **f**) heat map of steady-state transcripts levels of stress-marker genes 1 h after addition of 6 μM FCA either alone or in combination with 2 μM LatB . **i**) Mortality scored at 6 h after addition of either 6 μM FCA, 2 μM FCA, or a combination of both compounds. Data represent mean and standard errors from three independent biological experiments comprising 1500 individual cells. Asterisks indicate statistical differences based on LSD test with significant levels $P < 0.05$ (*), $P < 0.01$ (**), and $P < 0.001$ (***)

3.2.3.5. Overexpression of Metacaspases increased cell death triggered by Fusicoccin

To test whether the metacaspases are involved in the cell death driven by FCA, two BY-2 cell lines overexpressing *V. rupestris* metacaspases, *MC2ox* and *MC5ox*, were treated with FCA and compared to the wild type of BY-2 tobacco cells. The FCA treatment led to variable mortality rates among different cell lines in the respective time points (**Fig. 24a**). The overexpression of *Vitis* metacaspases caused higher mortality levels in BY-2 cells than the wild type, earlier after 3 hr of FCA stress and in a consistent manner till 24 hrs. Comparing metacaspases lines to each other, The overexpression of *MC2ox* was more sensitive to FCA than *MC5ox* and showed higher mortality rates at the earlier time points (3 and 6 hrs of FCA treatment).

3.2.3.6. Effect of Salicylic acid and MAPKs on the cell death triggered by Fusicoccin.

To test whether salicylic acid can enhance the FCA toxicity, *Vitis* cells were pre-incubated by 50 μ M of salicylic acid (SA) for 1 hr before FCA treatment. While SA couldn't cause significant cell death in *Vitis* cells for 6 hrs, it enhanced the sensitivity of *Vitis* cells towards FCA stress, increasing the mortality levels from 31% to 44% after 6 hrs (**Fig. 24c**). To test whether inhibiting SA signaling could reduce the cell death driven by FCA, *Vitis* cells were pre-treated first by 25 μ M 1-aminobenzotriazole (ABT), a cytochrome 450 inhibitor, and reported as SA inhibitor (Leon *et al.*, 1995). ABT alone has no toxic effect on the *Vitis* cells. Moreover, it partially decreased the cell death induced by FCA and showed an antagonistic effect on salicylic acid on FCA signaling (**Fig. 24c**). On the other hand, manipulating MAPK signaling by a specific inhibitor for MAPK cascades (PD98059) increased the mortality levels in *Vitis* cells but didn't show a significant change in the cell death driven by FCA (**Fig. 24c**).

a) metacaspases

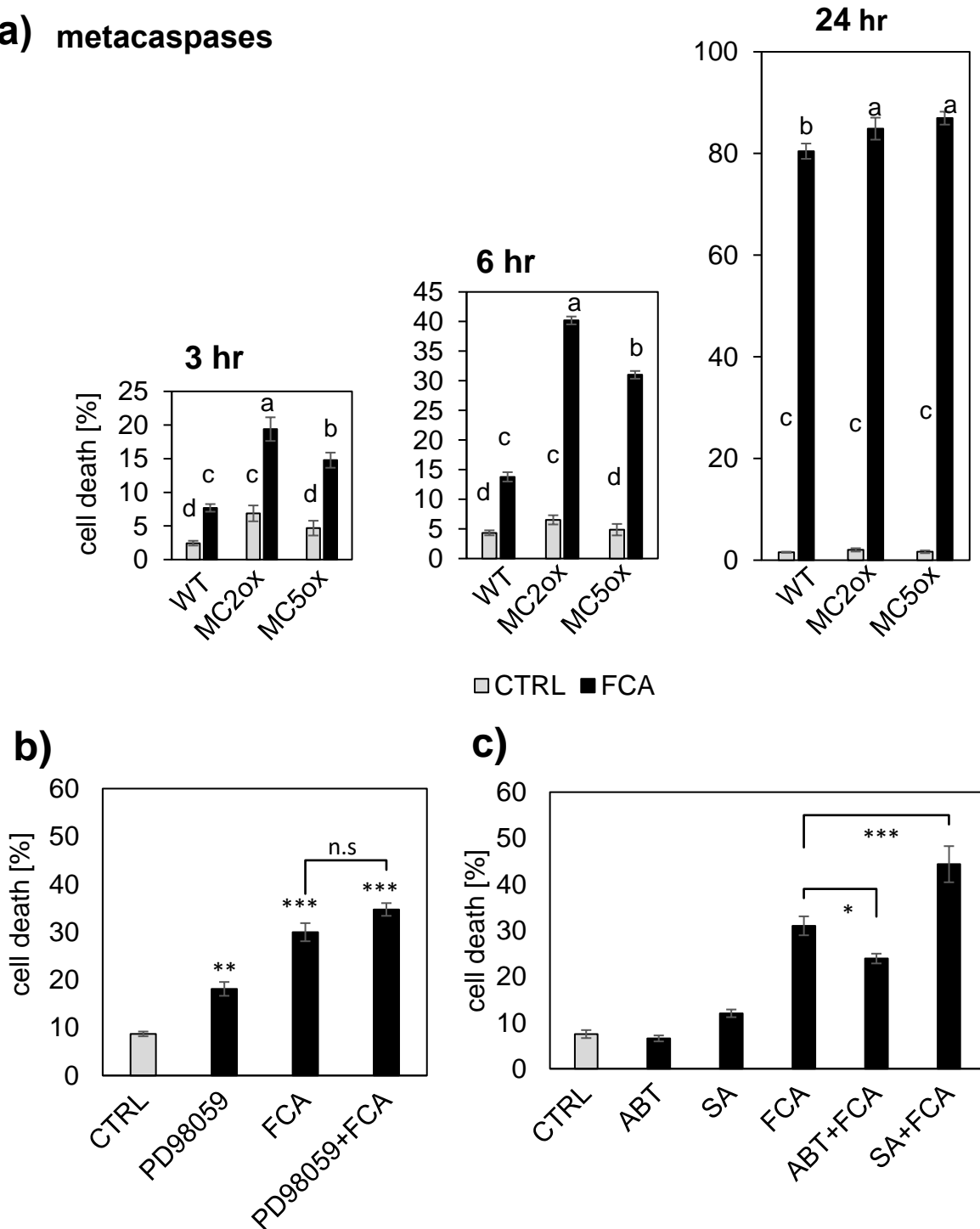


Fig. 24. Probing for molecular components of the FCA response. (a) Role of metacaspases. Time course of cell death in response to 6 μ M Fusicoccin A in non-transformed tobacco BY-2 cells (WT), and in cells overexpressing either metacaspase 2 (*MC2ox*) or metacaspase 5 (*MC5ox*) from *Vitis rupestris*. (b) Role of MAPK signaling. Cell death scored 6 h after the addition of 6 μ M Fusicoccin A to *Vitis* cells (*Vrup-TuB6*) after pretreatment with 50 μ M of the MAPK inhibitor PD98059. (c) Role of Salicylic acid (50 μ M) and its inhibitor, 1-aminobenzotriazole, scored 6 h after adding 6 μ M Fusicoccin A to *V. rupestris* GFP-TuB6 cells

Results

after pre-treatment with 50 μM of the MAPK inhibitor PD98059. (c) Role of Salicylic acid (25 μM), on cell death triggered by Fusicoccin A . Data represent means and SE from 3 biological replicates comprising 1500 individual cells per data point. Different letters represent statistical differences based on Duncan's test with significant levels $P < 0.05$ (a), asterisks indicate statistical differences based on LSD test with significant levels $P < 0.05$ (*), $P < 0.01$ (**), and $P < 0.001$ (***) in b) and c).

4. Discussion

The plant-pathogen dialogue is very complex and mysterious in the context of Grapevine Trunk Disease. Wood-decaying endophytes have an uncommon pathogen lifestyle. After a latent lifestyle for years, they switch into necrotrophic killers, causing the disease outbreak in infected grapevines. In the present work, the chemical communication between grapevines and *Botryosphaeriaceae* was dissected either to search for resistant genotypes with unique chemical identity warding the infection or to identify the apoplexy breakdown regulation by both the host and the intruder.

In chapter 1: Ancient wild grapes accessions of *Vitis vinifera ssp. sylvestris* were infected and screened against *Botryosphaeriaceae* related Dieback. There was a strong correlation between the robust and high accumulation of resveratrol and its non-glycosylated isomers (viniferins) and resistance. In addition, the role of wood architecture as a potential factor for susceptibility will be discussed. A working model will be then implemented to discuss how genetic factors channel phenylpropanoid metabolism between the stilbene and the lignin branch play a crucial role in resistance.

In chapter 2; The apoplexy breakdown in vineyards due to Grapevine Trunk Disease was hypothesized to be triggered more by the host conditions than the fungal development (**Fig. 2**). A cell-based experimental system was established to screen the effect of candidate plant signals derived from phenylalanine pathway on the behavior of *Neofusicoccum parvum* Bt-67. A new level of plant-endophytes interaction was introduced, called plant surrender signal, and recognized by the pathogen as a signal for severe stress, damaging the host. Such signal triggers the pathogen to start the sexual cycle and subsequently kill the host for the sake of its own survival to start a new life cycle in new host plants. Nevertheless, the changes in the fungal metabolites under necrotrophic lifestyle will be discussed along with the polyketide driving

apoplectic behavior using LC-MS analysis and bioactivity guided fractionation. Also, the stress signaling of the candidate polyketide was dissected to identify how it could massively drive the necrotrophic lifestyle and which molecular players are recruited for this behavior.

4.1. Chapter 1; Ancestral grapevines with resistance against *Botryosphaeriaceae* related Dieback.

4.1.1. A minimal experimental system for studying resistance against *N. parvum*

using a novel *in-planta* inoculation assay (**Fig 3**). Whereas long-term symptoms, such as the tiger stripe discoloration in leaves or apoplexy in the entire infected plants that are usually observed after years of colonization, when the fungus switches off its latent phase killing the host in few days (Bertsch et al., 2013) cannot be investigated, this reductionist approach allowed to analyze, for a specific strain of *Botryosphaeria dieback*, *Neofusicoccum parvum* strain Bt-67 to identify *in vivo* genetic, molecular, and cellular factors contributing to resistance at the early phase of infection. In this study, wood necrosis was used as an operational definition for resistance to *Botryosphaeria dieback* in the respective genotype. Also, the correlation of hyphal growth in xylem vessels after 2 months of infection (**Fig. 6d**) with the wood necrosis area measured after 1 week (**Fig. 5**) in infected Ke15, and Ke95 versus infected Chardonnay support the predictive value of our assay to judge the resistance against fungal invasion. The minimal assay results show that there is a significant difference between the genotypes, although they all originate from one population. The genome-wide SNP analysis shows that *V. vinifera ssp. sylvestris* population formed a separate clade within the genus *Vitis*, distinct either from *V. vinifera ssp. vinifera*, or from wild species from America or East Asia. The phylogenetic findings of current study are consistent with the phylogenetic outputs from a worldwide set of 472 accessions (Liang et al., 2019). The last viable population of *V. vinifera ssp. sylvestris* located in Germany still harboured wide genetic diversity, consistent with

previous data, where this population was compared to other European populations of *sylvestris* and autochthonous *vinifera* (Nick, 2014). While the reason for this diversity in a relict population is not clear, it is composed of individuals that show variable susceptibility to *N. parvum*. This difference is linked with a stilbene chemotype determined from metabolic analysis of leaves subjected to UV stress (Duan *et al.*, 2015). Among the tested accessions, the two most resistant genotypes, Ke15 and Ke95, displayed the resveratrol-viniferin chemotype, while the other, more susceptible genotypes, showed the α -piceid chemotype (Duan *et al.*, 2015). Consequently, the adopted reductionist approach not only truly predicts the long-term colonization development in xylem vessels, but also indicates chemotype differences against infection by metabolic analysis.

4.1.2. Wood architecture has no role in resistance against *Botryosphaeria dieback*

Many studies suggested that xylem vessel diameter is a reliable predictor for the fungal spread of the Esca diseases in grapevines, based on a comparison with three commercial *vinifera* varieties (Pouzoulet *et al.*, 2014; Pouzoulet *et al.*, 2017). In the current study, no correlation was seen between xylem vessel geometry and resistance to *Botryosphaeria Dieback* (**Fig. 10h**). While both resistant genotypes Ke15 and Ke95 were hypothesized to have the smallest vessels, failed to do so, Ke94, which ranked as the most susceptible genotype, showed the tiniest xylem vessels. Nevertheless, Ke94 was similar with respect to the wood necrosis to the susceptible *Vitis vinifera* variety Chardonnay (**Fig. 5**), although its vessels had 2 folds the width of Ke94 vessels (**Fig. 10**). This lack of correlation is not crucial since the fungal hyphae do not remain constrained inside the infected xylem vessels but move horizontally from one vessel to another through the bordered pits without the need to potentially degrade the walls of further vessels colonization (**Fig.10**). Since no significant correlation was detected between wood architecture

and fungal spread, the main hypothesis was to look for the chemical defense mechanisms (such as phytoalexin accumulation).

4.1.3. Resveratrol-viniferin metabolism as a resistance factor against *Botryosphaeria dieback*

Both genotypes Ke15 and Ke95 ranked first, respectively, in constraining the wood necrosis (**Fig. 5**) and efficiently reduced hyphal coverage in colonized vessels (**Fig. 6**). Both genotypes belong to the resveratrol-viniferin chemotype (Duan et al., 2015), and produced more of the stilbene aglycons, especially resveratrol and viniferin trimers (**Fig. 8**), which are linked with strong induction of several *stilbene synthase* transcripts (**Fig. 7**). The antimicrobial activity of stilbenes is well established and can act on many levels. For instance, stilbenes inhibit spore release, germination, and the activity of fungal pectolyases and hydrolases (Kumar and Nambisan, 2014; Langcake, 1981). The role of stilbenes as resistance factors has been demonstrated for several diseases infecting *Vitis* such as Downy Mildew of Grapevine, Powdery Mildew of Grapevine, or Grey Mold (Duan et al., 2015; Jiao et al., 2016; Rascle et al., 2015; Adrian and Jeandet, 2012). Also, for *N. parvum*, mycelia growth rates *in vitro* were inhibited by resveratrol or viniferins supplement (Stempien et al., 2017).

The high induction of the stilbene aglycon resveratrol is followed by oligomerization into different viniferin derivatives (Keylor et al., 2015), which supports the observed patterns (**Fig. 8**): In the resistant genotypes Ke15 and Ke95 already, both *cis*- and *trans*-resveratrol were conspicuously elevated over the values seen in the susceptible genotypes Ke13 and Ke94 during first 2 days of infection. This high resveratrol abundance was followed one day later by a higher accumulation of the non-glycosylated stilbenes; δ -viniferin, and viniferin trimers 1 and 2. Consequently, these stilbene oligomers are correlated with the observed resistance against *N. parvum*. This accumulation is specific because some stilbene oligomers, such as *cis*-

ϵ -viniferin is found in either susceptible or resistant genotypes. Although *cis*- ϵ -viniferin was found in sites infected by the causative agent of Downy Mildew of Grapevine, *Plasmopara viticola* (Pezet et al., 2004), this correlation does not indicate bioactivity but might be resulting from the synthesis of other, bioactive, oligomers. Furthermore, *cis*- ϵ -viniferin was classified as a detoxification product emerging from *trans*-resveratrol by laccases secreted by *Botrytis cinerea*, the causative agent of Grey Mold (Breuil et al., 1999). Also, the synthesis of ϵ -viniferin against advanced wood decay, such as red wood rot in the context of the GTDS would classify this stilbene oligomer as a by-product, rather than a bioactive phytoalexin (Amalfitano et al., 2000).

By contrast, the susceptible genotypes Ke13 and Ke94 exhibited significantly less content of viniferins comparing to the resistant lines. Interestingly, both Ke13 and Ke94 accumulated more α -piceid at 3 dpi (**Fig. 8b**), followed by significantly higher lignin deposition 2 months later (**Fig. 9b**). Also, the expression pattern of all defense genes (*STS*, *PAL*, *JAZ1*) was more upregulated in Ke94 than in the other tested genotypes (**Fig. 7**). Thus, this genotype is more responsive to the infection. However, this induction of transcripts does not lead to efficient resistance against the fungal spread. The reason might be that the accumulation of α -piceid, at this genotype, lack bioactivity against the fungus, consistent with the results against the Oomycete pathogen *Plasmopara viticola*, where the α -piceid accumulation could not restrain the infection (Duan et al., 2015; Alonso-Villaverde et al., 2011). Consequently, it is not sufficient to activate *Stilbene synthesis* transcription – in order to stop fungal spread at an early stage. This induction must be integrated into a proper metabolic context, where resveratrol is channeled towards the non-glycosylated viniferins.

4.1.4. Resistance or susceptibility – a matter of channeling phenylpropanoid metabolism?

The current study incorporates different levels of analysis, including (physiology, histology, gene expression, metabolites), which leads to a working model highlighting the differences of susceptibility towards *N. parvum* by differential channeling of phenylpropanoid metabolism (**Fig. 8; Fig. 9**), which exemplarily shows the contrasting allocation of phenylpropanoid pathway between a resistant (Ke15), and a susceptible (Ke94) genotype. Infection activates defense signaling, conveyed by several parallel pathways. For the sake of simplicity, only jasmonate signaling is shown (**Fig. 25. ①, ②**), which plays as upstream signaling for the phenylpropanoid pathway (Tassoni et al., 2005). An implication of this working model could be that activation of jasmonate signaling should increase phytoalexins synthesis transcripts. While this is difficult to be studied in wood, this implication could be investigated in *Vitis rupestris* suspension cells as an approximation approach (**Suppl. Fig. S1**).

The specific and robust activation of *VvSTS27* and *VvSTS47* transcripts (**Fig. 25, ③**) is followed in the resistant model Ke15 by the synthesis of *p*-coumaric acid and tyrosine, and the enhanced accumulation of *trans*- and *cis*-resveratrol (**Fig. 25, ④**), followed by elevated oligomerization to non-glycosylated resveratrol trimers (α -viniferin, viniferin trimer 1 and viniferin trimer 2, **Fig. 25, ⑤**). Whether all of the stilbene aglycons that accumulated abundantly in infected Ke15 (more than any other genotype) have strong potential as phytoalexins, remains to be explained. Some of the stilbene derivatives, either the monomer *cis*-resveratrol or the stilbene dimer δ -viniferin, might act as transient precursors for the viniferin trimers synthesis, which accumulate one day later. On the other hand, the significant accumulation of *STS* transcripts levels does not lead to a corresponding accumulation of resveratrol in the susceptible Ke94 (delayed by one day as compared to Ke15). Furthermore, Ke94 channeled more resveratrol to the glycosylated α -piceid (**Fig. 25, ⑥**), followed by a lower amplitude and a temporal delay in *cis*-

resveratrol accumulation and viniferin trimers. Ke94 also deposited more lignin around the colonized xylem vessels (**Fig. 25, ②**), as shown by histological staining, upregulated transcripts of *VvCAOMT*, *VvCAD*, and quantification of lignin content (**Fig. 9**). This excessive deposition of lignin was also found in all studied accessions belonging to the α -piceid chemotype (Ke13, Ke94, Chardonnay).

While this study showed no evidence that wood architecture could constrain the fungal spread because the fungal hyphae make use of bordered pits for vessel-to-vessel colonization. In addition, the fast and robust channeling of phenylpropanoid pathway towards the stilbene aglycon resveratrol and subsequent oligomerization into viniferins represents a central resistance factor. This channeling seems to be under genetic control because it is found in accessions belonging to the resveratrol-viniferin chemotype. By contrast, accessions of the α -piceid chemotype partition the phenylpropanoid pathway between glycosylated α -piceid and lignin formation. While lignin was proposed as a resistance factor for Downy Mildew (Dai *et al.*, 1995), it does not qualify as such in case of wood-decaying fungi but rather might support further fungal spread. While the robust induction of *Stilbene synthase* transcripts is a prerequisite for phytoalexin synthesis, it is by no means a sufficient condition as shown by the example of Ke94 (in this genotype it might even be a damage-related, because the spread of the fungus is not contained, such that additional cells are confronted with the fungus).

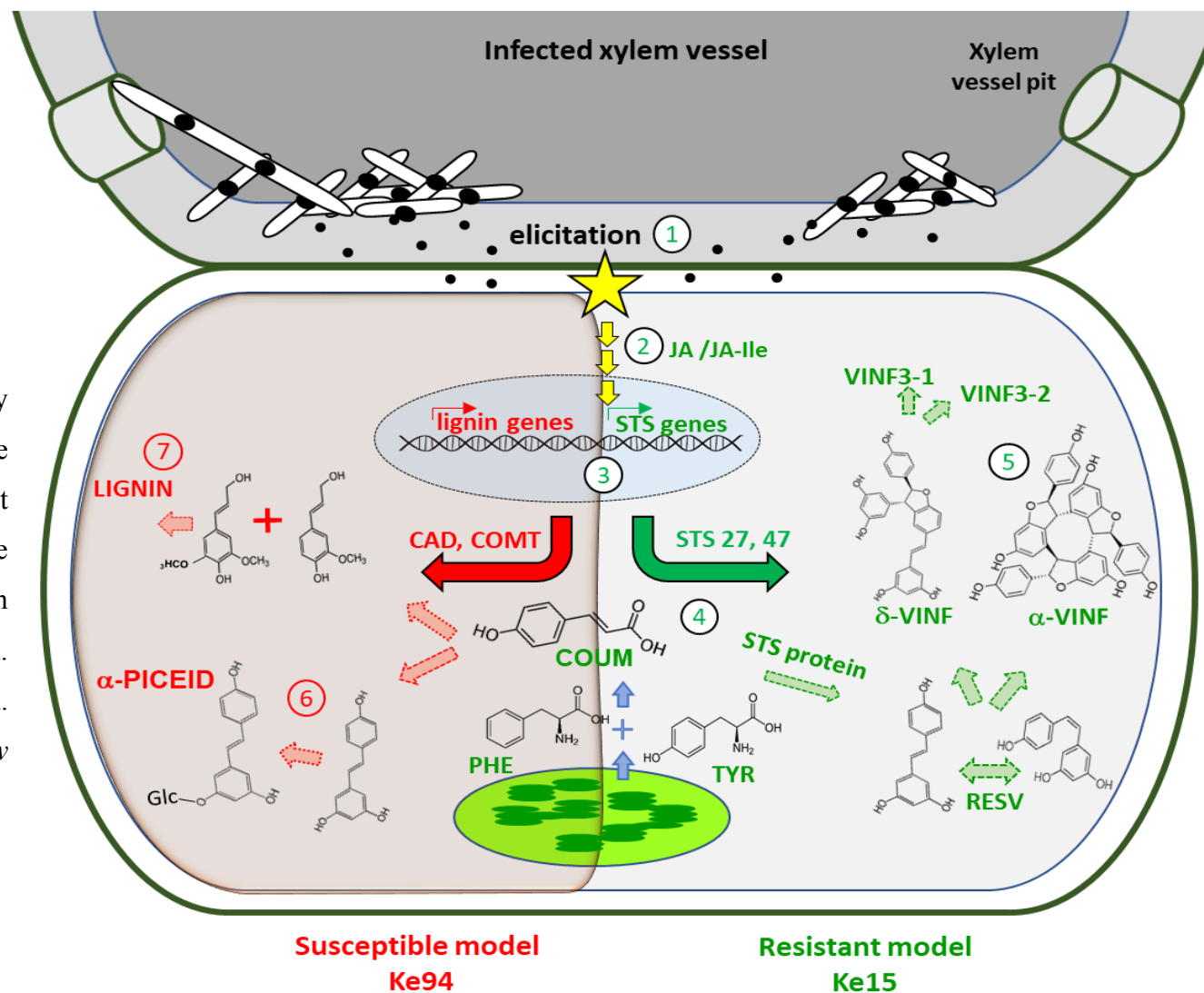


Fig. 25. Visual model representatively illustrating the difference in the response to *N. parvum* in a resistant (Ke15) versus a susceptible genotype (Ke94) through differential allocation of the phenylpropanoid metabolism. For details see the discussion. Published in Khattab et al., *New Phytologist* (2021).

4.1.5. Does drought increase fungal development and disease outbreak?

As observed in susceptible grapevines, infected plants channel the phenylpropanoid pathway towards piceid chemotype (in the short term) and towards lignin deposition in the long-term, which might support the colonization. To check whether the accelerated disease symptoms under climate change might be associated with increased lignin deposition, the infected plants were deprived of 80% of optimal water supply for one month. The fungal growth was then enhanced under drought, as indicated by the elevated fungal DNA copies. Here, the infection progress was accompanied by advanced disease symptoms on the vine physiology, such as 2-fold wood necrosis and impaired plants with necrotic leaves (**Fig. 11**).

Nevertheless, the drought stress led to changes in the cell wall matrix in the infected wood since it significantly increased the lignin deposition. It is worth noting that grapevines actively synthesize lignin (with the hydrophobic nature) under drought stress (Tu et al., 2020) to improve water conductivity in woody tissues reducing their high water permeability due to the accumulation of hydrophilic polysaccharides. Here, the phenylpropanoid partitioning is more allocated towards lignin than resveratrol synthesis, increasing the vine susceptibility. Interestingly, the fungus might perceive the unexpected high lignification, especially if it happened suddenly in long-infected hosts, as an alert signal that the host faces severe stress conditions, and it should search for a new host.

4.2. Chapter 2: A latent or necrotrophic phase- a matter of chemical communication between *N. parvum* and the host

Vitis-Botryosphaeriaceae crosstalk could not be investigated using *In-planta* infection assay since it's hard to separate or control the fungus response to a specific plant signal. Consequently, an experimental cell system was established; the fungal mycelia were *in vitro* fermented with different phenylalanine derivatives acting as lignin precursors. The activity of phenylpropanoid pathway was observed after the *in-planta* infection assay. Since the elevated lignin deposition was linked with the enhanced fungal development either under drought stress or in susceptible genotypes (**Fig. 9; Fig. 11**), lignin precursors were hypothesized to be involved in the *Vitis-Botryosphaeriaceae* crosstalk. The phenylalanine derivatives cinnamic acid and *p*-coumaric acid (hydroxycinnamic acid) succeeded in inhibiting the necrotrophic lifestyle of *N. parvum*. Both phenylalanine derivatives act as precursors for strong phytoalexins and stilbenes (**Fig. ; Suppl. Fig. S2**). Here, the fungus showed a weak aggressive behavior against cinnamic acid and a latent behavior against *p*-coumaric acid. Such action is exhibited in the early infection events when the host powerfully synthesizes these stilbenes precursors, as discussed in Resveratrol-viniferin chemotype (Chapter 1). By contrast, ferulic acid, a lignin precursor and antagonistic to the stilbenes synthesis pathway, triggered the fungus to show an aggressive pattern by segregating phytotoxic compounds. Therefore, ferulic acid accumulation in *Vitis* plants, which might act as an adaptation signal in drought stress context (**Fig. 11**), is perceived by *Neofusicoccum parvum* as an alert signal to kill the host, starting a new life cycle in new plants.

4.2.1. Ferulic acid accumulation as a surrender signal triggering *N. parvum* to kill the host by fusicoccin A derivative

following the concept that the apoplexy breakdown in grapevines driven by *Botryosphaeriaceae* is triggered by hijacked chemical communication, ferulic acid was

identified as “the plant surrender signal” triggering such Apoplexy outbreak (**Fig. 13**). Fermenting *N. parvum* mycelia with ferulic acid triggered the fungus to secrete very toxic polyketide, Fusicoccin A derivative, which boosted the mortality of *Vitis* cells and was classified then as the molecular tool driving the disease outbreak. The progress in cell death stages due to FCA was visualized by double staining assay (**Fig. 16**). Nevertheless, cytological hallmarks of the regulated “autolytic” cell death appeared against FCA, such as chromatin condensation and lytic vacuoles (**Fig. 16**). The presence of autolytic cell death features plus the accidental type was rather seen under the necrotrophic behavior of pathogens (Van Doorn et al., 2011). FCA actuated many molecular cues regulating stress and defense responses. For instance, it activated PM ATPases (**Fig. 17**) as an alert signal manipulated by pathogens in their interaction with plants (Elmore & Coaker, 2011). A similar pattern of PM ATPases activity against FCA was observed in the guard cells of *Vicia faba* (Kinoshita & Shimazaki, 2001). In addition, FCA elicited superoxide O₂⁻ generation in *Vitis* cells, which plays as a central upstream signal manipulating subsequent stress responses in plants against the pathogen attack (Trujillo et al., 2004; Duan et al., 2016).

It's worth noting that FCA changed the expression pattern of genes regulating stress signaling in grapevines. Here, the transcripts of genes regulating programmed cell (PCD) death signaling were significantly increased, especially metacaspases genes (*MC2* and *MC5*) and many members of the *Superoxide Dismutase* gene family (*Mn.SOD1*, *Cu.SOD1* and *Cu.SOD2*). Likewise, the expression pattern of defense genes was strongly elevated; either phenylpropanoid pathway genes (*PAL* and members of *Stilbene Synthase* multigenic family) or phytohormonal signaling genes (*JAZ1*, *JAZ9*, *PR.1*, and *PR.10*). The pattern of FCA signaling on triggering cell death, O₂⁻ accumulation, stress marker genes upregulation (**Fig. 18; Fig. 19**) was similar to other stress conditions activating ROS generation or manipulating cytoskeletons (Qiao et al., 2010; Chang & Nick, 2012). likewise, previous studies confirmed

the provocative effect of FCA on the regulation of *Phenylalanine Ammonia Lyase*, *pathogenesis-related proteins*, and disease symptoms (Frick & Schaller, 2002; Singh & Roberts, 2004)

4.2.2. 14-3-3 proteins and ROS generation are necessary for Fusicoccin A signaling to drive the apoplexy phase

14-3-3 proteins are conserved proteins family, identified as fusicoccin receptors, and take part in a wide range of physiological processes (Olivari et al., 1998). Blocking 14-3-3 proteins by BV02 strongly constrained FCA stress signaling. The triggered stream of proton (H^+) flux due to FCA was less pronounced in the presence of BV02, followed by less accumulated transcripts of cell death signaling genes (*MC2* and *MC5*) as well as defense-related genes *PAL* and *PR.1*. Nevertheless, blocking 14-3-3 proteins reduced the mortality rates driven by FCA (**Fig. 20**), which means 14-3-3 proteins are upstream of cell death signaling triggered by FCA. Previous studies showed that 14-3-3 are involved in events controlling immunity associated programmed cell death like interaction with phosphorylated proteins, MAPK cascades (Oh et al., 2010). In addition, the proteomic analysis showed that 14-3-3 proteins might interact with metacaspases type ii regulating cell death in woody tissues (Bollhöner et al., 2018) and commonly induced by pathogen attack (Watanabe & Lam, 2011).

Since FCA activates either superoxide production or the induction of *SOD* genes, blocking RbOH was tested to see whether it could alleviate the FCA deathly signaling. The role of ROS generation in regulating plant cell death was studied before (for review, see Van Breusegem & Dat (2006)). Blocking the respiratory burst by DPI decreased the superoxide production in FCA-challenging cells but also altered the transcription rates of defense genes. DPI increased the expression of basal defense genes like *JAZ1* and *STS* genes, consistent with the findings observed by Chang et al., (2011). On the other hand, the transcripts of *PAL* and salicylic acid-

inducible gene (*PR.1*) were less pronounced under lower superoxide generation, which came in line with what was reported by Orozco-Cárdenas et al., (2001) and Dat et al., (2003).

Furthermore, DPI inhibited the expression pattern of one of the metacaspases genes (*MC5*), which is classified as a cell death executor gene in grapevines (Gong et al., 2019). Similar results were shown in sycamore cells where DPI reduced the cell death driven by 8 hrs of FCA treatment (Malerba et al., 2008). So, the molecular responses towards blocking RbOH could mitigate FCA toxicity, and it has been supported later by cellular responses such as decreased mortality rates in *Vitis* cells (**Fig. 21**). Consequently, the activity of the RbOH and ROS homeostasis take part in FCA stress signaling for initiating cell death.

4.2.3. Cytoskeletons dynamics modulate Fusicoccin A signaling

FCA could manipulate cytoskeleton organization since it disrupts the microtubular integrity (**Fig. 22**) and provokes the actin bundling (**Fig. 23**) in *Vitis* cells. Cytoskeletons response towards fusicoccin was observed before, where it showed acting depletion rather than bundling in sycamore cells (Malerba et al., 2008). In addition, Burian & Hejnowicz (2011) reported that triggering PM ATPases by FCA could alter the microtubules orientation in the epidermal peels of sunflowers hypocotyl.

To probe whether cytoskeletons dynamics are involved in the driven PCD signaling by FCA, actin filaments were depleted by Latrunculin B, and microtubules were either stabilized by taxol or depleted by oryzalin. Enhancing microtubules polymerization by taxol reduced the effect of FCA on upregulating cell death signaling genes, *MC2* and *MC5* (**Fig. 22h**). Although microtubules remodeling was insufficient alone to halt the triggered PCD (similar results were approached by Škalamera & Heath, (1998)), the overexpression of β -tubulin in *Vitis* cells reduced their susceptibility to FCA (**Fig. 22j**). Depleting actins network was also more specific in inhibiting either the activated PCD by FCA or the accumulated transcripts of *PAL*, *PR.1*,

and the cell death executor *MC5* (**Fig. 23**). In general, manipulating both networks (microtubules and actins) altered the transcripts of cell death signaling genes and the mortality rates. Therefore, cytoskeletons dynamics might play as an upstream signal regulating the activated PCD by FCA. Such results are consistent with the hypothesis that the change in cytoskeletons dynamics is not only a consequence of (PCD), but it takes part also in the molecular events regulating PCD (Smertenko & Franklin-Tong, (2011)). In grapevines, actin bundling was further classified as a deathly cue during the stress signaling of Harpin, the bacterial cell death elicitor (Chang et al., 2015).

4.2.4. Metacaspases as downstream targets of Fusicoccin A signaling

Metacaspases were identified as proteases operating cell death in microorganisms and plants (Tsiatsiani et al., 2011). Not only both metacaspases genes, *MC2* and *MC5* were upregulated in the presence of FCA, but their accumulated transcripts also decreased by manipulating the other involved molecular players in the FCA signaling pathway, such as 14-3-3 proteins, RbOH, microtubules, and actin filaments. Nevertheless, the overexpression of *Vitis rupestris* metacaspases genes *MC2* and *MC5* in BY-2 tobacco cells increased their mortality rates towards FCA, supporting their role as downstream targets for FCA signaling, as executing players for cell death. The metacaspases activity was observed before regulating PCD in the context of plant-pathogen crosstalk against biotrophs like *Plasmopara viticola* in grapevines (Gong et al., 2019) or necrotrophs like *Botrytis cinerea* in tomatoes (Hoeberichts et al., 2003).

4.2.5. Visual model showing molecular events driven by Fusicoccin A signaling for triggering cell death.

A visual model was made to explicit the chemical communication between infected vines and *Botryosphaeriaceae*, triggering the apoplectic breakdown. Using an experimental cell system, we identified a new level in plant-pathogen dialogue, the so-called (plant surrender signal). When the fungus perceives the surrender signal, it commits to switch from a peaceful lifestyle into a necrotrophic behavior and proceeds with the disease outbreak.

In the context of *Botryosphaeria dieback*, the accumulation of ferulic acid, a lignin precursor in the cell wall matrix, acts as the plant surrender signal that emerges *N. parvum*, from a latent endophyte into a necrotrophic lifestyle generating the apoplexy breakdown (**Fig. 26**, ①, ②). It is worth noting that the necrotrophic behavior of *N. parvum* comes with the sexual cycle (**Fig. 13**) to kill the host for releasing the spores outside colonized xylem vessels. Interestingly, under current climate change, the elevated apoplexy breakdown seems to be linked with lignin deposition increase observed under long-term drought stress (**Fig. 11; Fig. 13**).

Using activity-guided fractionation, the fungal polyketide, Fusicoccin A, was discovered to have a high potential as an apoplexy cue boosting mortality in *Vitis* suspension cells, as an indicator for the disease outbreak in vineyards. By dissecting FCA stress signaling, many molecular players were identified to regulate its mode of action for robust mortality rates in *Vitis* cells. For instance, FCA has specific receptors, 14-3-3 proteins (**Fig. 26**, ③), regulating molecular events controlling cell death. After binding to 14-3-3 proteins, it activates PM ATPases in few minutes, consistently decreasing the extracellular pH (**Fig. 26**, ④). The activity of PM ATPases was followed by superoxide generation, which significantly accumulated after 10 min and increased dramatically, reaching the peak after 60 Min (**Fig. 26**, ⑤). Then, cytoskeleton dynamics were disrupted by microtubules depletion after 30 Min (**Fig. 26**, ⑥),

which is associated with the upregulation of defense genes such as phenylpropanoid pathway genes and phytohormones signaling genes after 60 Min, similar to the findings of Guan et al. (2020). Afterwards, a strong actin-bundling came at 90 Min of FCA treatment (**Fig.26, ⑦**) as an upstream molecular player regulating programmed cell death (Smertenko & Franklin-Tong, 2011). In addition, FCA increased the accumulated transcripts of metacaspases genes, *MC2* and *MC5*, regulating cell death (**Fig. 26, ⑧**). Besides, the expression of metacaspases genes significantly decreased by manipulating the molecular players controlling FCA signaling pathway, such as 14-3-3 proteins, RbOH, microtubules, and actin filaments. The role of Metacaspases in FCA stress signaling was then confirmed since the overexpression of *MC2*, and *MC5* genes increased cell mortality against FCA.

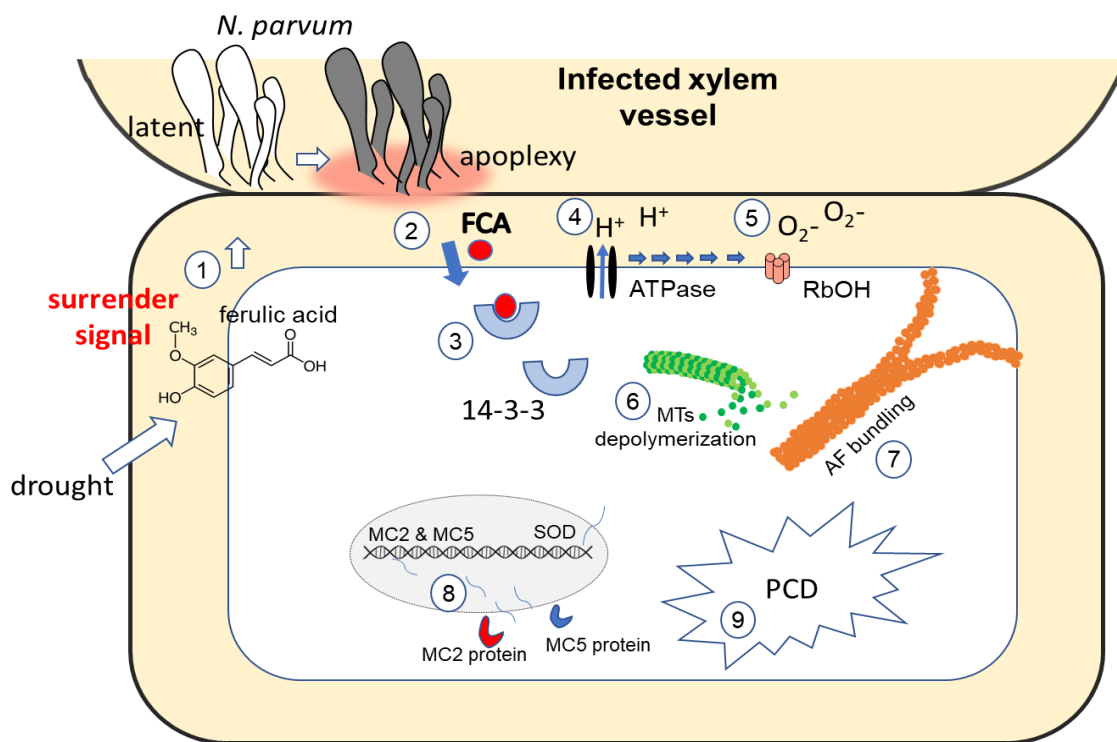


Fig. 26. A Visual model showing the chemical communication driving apoplexy breakdown in *Botryosphaeriaceae-Vitis* interaction, including the stress signaling of the apoplexy cue (Fusicoccin A).

5. Concluding remarks and outlook

The Dissertation outlined many central findings, increasing our knowledge about the Grapevine Trunk Disease complex and how to avoid their economic damage based on smart and sustainable approaches. For instance,

- It showed that the wood architecture has no role in constraining the fungal spread, as previously hypothesized by many studies, but rather facilitating the cross fungal spread through the bordered pits of the xylem vessels.

- For the first time, this study pointed out resistant wild grapes against *Botryosphaeria* dieback with a specific chemical entity (the so-called Resveratrol-viniferin chemotype), constraining colonization effectively. By contrast, the susceptible grapes adopted a weak induction of stilbenes and came as glycosylated isomers “ piceid chemotype” and partitioned the phenylpropanoid pathway towards more lignin accumulation in the long-term.

- This study arrived to a new level of plant-pathogen crosstalk, called Plant surrender signal, which triggers *Botryosphaeriaceae* fungi to emerge from a peaceful endophyte into a necrotrophic killer for the infected vine in a few days. In this context, the capitulation signal or surrender signal comes from the wood matrix, ferulic acid, which acts as a lignin precursor that commonly accentuates under drought stress. The fungus meets lignin increase under drought (climate change) as an external threat that might kill the infected vine, and it is not a valid host anymore. Thus, the fungus switches to the sexual cycle and kills the host by Fusicoccin polyketide to be able to release the spores outside wood vessels.

These outputs pave the way for sustainable applications to control Grapevine Trunk Disease by manipulating the phenylpropanoid pathway in favor of stilbenes synthesis than lignification. To achieve this hypothesis-driven application, two approaches will be followed in the future;

(i) Chemical genetics, targeting key enzymes of the phenylpropanoid pathway (ii) marker-assisted breeding, making use of resistance factors from *Vitis sylvestris*.

Approach (i) Chemical genetics approach is targeted to an immediate strategy to contain disease outbreak to bridge the time until new varieties become available. In this approach, compounds library (van de Wouwer et al., 2016) will be used for modulating the Phenylalanine pathway to avoid the accumulation of lignin precursor (ferulic acid). For instance, the inhibition of many enzymes regulating lignin biosynthesis will be tested to see whether it could halt the disease outbreak, such as *Cinnamate-4-Hydroxylase (C4H)*, *Coumarate Coenzyme A Ligase (4CL)*, and *Caffeic acid O-methyl transferase (CAOMT)*

Approach (ii) marker-assisted breeding; makes use of the fact that most of the *sylvestris* population extended by around 100 genotypes of wild and ancient domesticated autochthonous genotypes from semi-arid regions such as Armenia (the center of origin of domesticated grapevine) and Tunisia were fully sequenced at high quality in collaboration with the Chinese Academy of Sciences. These genomes are currently organized in a searchable database by Nick lab, Botanical Institute, Karlsruhe Institute of Technology, Germany (<http://grapekit.botanik.kit.edu/>). They will be used to apply functional genomics, and different bioinformatics approaches to pinpoint candidate alleles controlling the resveratrol-viniferin chemotype in resistant genotypes.

6. References

- Abou-Mansour, E., Débieux, J. L., Ramírez-Suero, M., Bénard-Gellon, M., Magnin-Robert, M., Spagnolo, A., Chong, J., Farine, S. Betsch, C., L'haridon, F., Serrano, M.,... Larignon, P. (2015).** Phytotoxic metabolites from *Neofusicoccum parvum*, a pathogen of *Botryosphaeria dieback* of grapevine. *Phytochemistry*, 115(1), 207–215. <https://doi.org/10.1016/j.phytochem.2015.01.012>
- Adrian, M., & Jeandet, P. (2012).** Effects of resveratrol on the ultrastructure of *Botrytis cinerea* conidia and biological significance in plant/pathogen interactions. *Fitoterapia*, 83(8), 1345–1350. <https://doi.org/10.1016/j.fitote.2012.04.004>
- Akaberi, S., Wang, H., Claudel, P., Riemann, M., Hause, B., Hugueney, P., & Nick, P. (2018).** Grapevine fatty acid hydroperoxide lyase generates actin-disrupting volatiles and promotes defense-related cell death. *Journal of Experimental Botany*, 69(12), 2883–2896. <https://doi.org/10.1093/jxb/ery133>
- Alonso-Villaverde, V., Voinesco, F., Viret, O., Spring, J. L., & Gindro, K. (2011).** The effectiveness of stilbenes in resistant Vitaceae: Ultrastructural and biochemical events during *Plasmopara viticola* infection process. *Plant Physiology and Biochemistry*, 49(3), 265–274. <https://doi.org/10.1016/j.plaphy.2010.12.010>
- Amalfitano, C., Evidente, A., Surico, G., Tegli, S., Bertelli, E., & Mugnai, L. (2000).** Phenols and stilbene polyphenols in the wood of esca-diseased grapevines. *Phytopathologia Mediterranea*, 39(1), 178–183. https://doi.org/10.14601/Phytopathol_Mediterr-1551
- Bacete, L., Mérida, H., Miedes, E., & Molina, A. (2018).** Plant cell wall-mediated immunity: cell wall changes trigger disease resistance responses. *Plant Journal*, 93(4), 614–636.

<https://doi.org/10.1111/tpj.13807>

- Barnes, W., & Anderson, C. (2017).** Acetyl Bromide Soluble Lignin (ABSL) Assay for Total Lignin Quantification from Plant Biomass. *Bio-Protocol*, 7(5), 1–11. <https://doi.org/10.21769/bioprotoc.2149>
- Belchí-Navarro, S., Almagro, L., Sabater-Jara, A. B., Fernández-Pérez, F., Bru, R., & Pedreño, M. A. (2013).** Induction of trans-resveratrol and extracellular pathogenesis-related proteins in elicited suspension cultured cells of *Vitis vinifera* cv Monastrell. *Journal of Plant Physiology*, 170(3), 258–264. <https://doi.org/10.1016/j.jplph.2012.10.003>
- Bertsch, C., Ramírez-Suero, M., Magnin-Robert, M., Larignon, P., Chong, J., Abou-Mansour, E., ... Fontaine, F. (2013).** Grapevine trunk diseases: Complex and still poorly understood. *Plant Pathology*, 62(2), 243–265. <https://doi.org/10.1111/j.1365-3059.2012.02674.x>
- Bethke, G., Thao, A., Xiong, G., Li, B., Soltis, N. E., Hatsugai, N., ... Glazebrook, J. (2016).** Pectin Biosynthesis Is Critical for Cell Wall Integrity and Immunity in *Arabidopsis thaliana*. *The Plant Cell*, 28(2), 537–556. <https://doi.org/10.1105/tpc.15.00404>
- Bollhöner, B., Jokipii-Lukkari, S., Bygdell, J., Stael, S., Adriasola, M., Muñoz, L., ... Tuominen, H. (2018).** The function of two type II metacaspases in woody tissues of *Populus* trees. *New Phytologist*, 217(4), 1551–1565. <https://doi.org/10.1111/nph.14945>
- Bortolami, G., Gambetta, G. A., Delzon, S., Lamarque, L. J., Pouzoulet, J., Badel, E., ... Jansen, S. (2019).** Exploring the Hydraulic Failure Hypothesis of Esca Leaf Symptom Formation 1 [OPEN]. *Plant Physiology*, 181(November), 1163–1174. <https://doi.org/10.1104/pp.19.00591>

-
- Boubakri, H., Wahab, M. A., Chong, J., Bertsch, C., Mliki, A., & Soustre-Gacougnolle, I. (2012).** Thiamine induced resistance to *Plasmopara viticola* in grapevine and elicited host-defense responses, including HR like-cell death. *Plant Physiology and Biochemistry*, 57, 120–133. <https://doi.org/10.1016/j.plaphy.2012.05.016>
- Breuil, A. C., Jeandet, P., Adrian, M., Chopin, F., Pirio, N., Meunier, P., & Bessis, R. (1999).** Characterization of a pterostilbene dehydrodimer produced by laccase of *Botrytis cinerea*. *Phytopathology*, 89(4), 298–302. <https://doi.org/10.1094/PHYTO.1999.89.4.298>
- Brulé, D., Villano, C., Davies, L. J., Trdá, L., Claverie, J., Héloir, M. C., ... Poinsot, B. (2019).** The grapevine (*Vitis vinifera*) LysM receptor kinases VvLYK1-1 and VvLYK1-2 mediate chitoooligosaccharide-triggered immunity. *Plant Biotechnology Journal*, 17(4), 812–825. <https://doi.org/10.1111/pbi.13017>
- Buckel, I., Molitor, D., Liermann, J. C., Sandjo, L. P., Berkemann-Löhnertz, B., Opatz, T., & Thines, E. (2013).** Phytotoxic dioxolanone-type secondary metabolites from *Guignardia bidwellii*. *Phytochemistry*, 89, 96–103. <https://doi.org/10.1016/j.phytochem.2013.01.004>
- Buckel, I., Andernach, L., Schüffler, A., Piepenbring, M., Opatz, T., & Thines, E. (2017).** Phytotoxic dioxolanones are potential virulence factors in the infection process of *Guignardia bidwellii*. *Scientific Reports*, 7(1), 8926. <https://doi.org/10.1038/s41598-017-09157-6>
- Burian, A., & Hejnowicz, Z. (2011).** Fusicoccin affects cortical microtubule orientation in the isolated epidermis of sunflower hypocotyls. *Plant Biology*, 13(1), 201–208. <https://doi.org/10.1111/j.1438-8677.2010.00339.x>
- Byczkowska, A., Kunikowska, A., & Kaźmierczak, A. (2013).** Determination of ACC-induced cell-programmed death in roots of *Vicia faba* ssp. *minor* seedlings by acridine orange and ethidium bromide staining. *Protoplasma*, 250(1), 121–128.
-

<https://doi.org/10.1007/s00709-012-0383-9>

Chang, X., Heene, E., Qiao, F., & Nick, P. (2011). The phytoalexin resveratrol regulates the initiation of hypersensitive cell death in vitis cell. *PLoS ONE*, 6(10).
<https://doi.org/10.1371/journal.pone.0026405>

Chang, X., & Nick, P. (2012). Defense signaling triggered by Flg22 and Harpin is integrated into a different stilbene output in Vitis cells. *PLoS ONE*, 7(7).
<https://doi.org/10.1371/journal.pone.0040446>

Chang, X., Riemann, M., Liu, Q., & Nick, P. (2015). Actin as deathly switch? How auxin can suppress cell-death related defense. *PLoS ONE*, 10(5), 1–22.
<https://doi.org/10.1371/journal.pone.0125498>

Chang, X., Seo, M., Takebayashi, Y., Kamiya, Y., Riemann, M., & Nick, P. (2017). Jasmonates are induced by the PAMP flg22 but not the cell death-inducing elicitor Harpin in *Vitis rupestris*. *Protoplasma*, 254(1), 271–283. <https://doi.org/10.1007/s00709-016-0941-7>

Chuberre, C., Plancot, B., Driouich, A., Moore, J. P., Bardor, M., Gügi, B., & Vicré, M. (2018). Plant immunity is compartmentalized and specialized in roots. *Frontiers in Plant Science*, 871(November), 1–13. <https://doi.org/10.3389/fpls.2018.01692>

Claverie, J., Balacey, S., Lemaître-Guillier, C., Brulé, D., Chiltz, A., Granet, L., ... Poinssot, B. (2018). The cell wall-derived xyloglucan is a new DAMP triggering plant immunity in *vitis vinifera* and *arabidopsis thaliana*. *Frontiers in Plant Science*, 871(November), 1–14. <https://doi.org/10.3389/fpls.2018.01725>

Coakley SM, Scherm H, Chakraborty S. (1999). Climate change and plant disease

management. *Annual Review of Phytopathology* 37:399–426.

Dai, G. H., Andary, C., Mondolot-Cosson, L., & Boubals, D. (1995). Histochemical studies on the interaction between three species of grapevine, *Vitis vinifera*, *V. rupestris* and *V. rotundifolia* and the downy mildew fungus, *Plasmopara viticola*. *Physiological and Molecular Plant Pathology*, 46(3), 177–188. <https://doi.org/10.1006/pmpp.1995.1014>

Dat, J. F., Pellinen, R., Beeckman, T., Van De Cotte, B., Langebartels, C., Kangasjärvi, J., ... Van Breusegem, F. (2003). Changes in hydrogen peroxide homeostasis trigger an active cell death process in tobacco. *Plant Journal*, 33(4), 621–632. <https://doi.org/10.1046/j.1365-3113X.2003.01655.x>

Delaye, L., García-Guzmán, G., & Heil, M. (2013). Endophytes versus biotrophic and necrotrophic pathogens-are fungal lifestyles evolutionarily stable traits? *Fungal Diversity*, 60(1), 125–135. <https://doi.org/10.1007/s13225-013-0240-y>

Djoukeng, J. D., Polli, S., Larignon, P., & Abou-Mansour, E. (2009). Identification of phytotoxins from *Botryosphaeria obtusa*, a pathogen of black dead arm disease of grapevine. *European Journal of Plant Pathology*, 124(2), 303–308. <https://doi.org/10.1007/s10658-008-9419-6>

Duan, D. (2015). New Genes from an Ancient Plant. PhD Thesis. Karlsruhe Institute of Technology, Germany.

Duan, D., Halter, D., Baltenweck, R., Tisch, C., Tröster, V., Kortekamp, A., ... Nick, P. (2015). Genetic diversity of stilbene metabolism in *Vitis sylvestris*. *Journal of Experimental Botany*, 66(11), 3243–3257. <https://doi.org/10.1093/jxb/erv137>

Duan, D., Fischer, S., Merz, P., Bogs, J., Riemann, M., & Nick, P. (2016). An ancestral allele of grapevine transcription factor MYB14 promotes plant defense. *Journal of*

Experimental Botany, 67(6), 1795–1804. <https://doi.org/10.1093/jxb/erv569>

Edwards J, Pascoe IG, Salib S, (2007). Impairment of grapevine xylem function by *Phaemoniella chlamydospora* infection is due to more than physical blockage of vessels with ‘goo’. *Phytopathologia Mediterranea* 46, 87–90.

Elmore, J. M., & Coaker, G. (2011). The role of the plasma membrane H⁺-ATPase in plant-microbe interactions. *Molecular Plant*, 4(3), 416–427. <https://doi.org/10.1093/mp/ssq083>

European Commission (2009) Regulation (EC) No 552/2009 of 22 June 2009 amending Regulation (EC) No 1907/2006 of the European Parliament and of the Council on the Registration, Evaluation, Authorisation and Restriction of Chemicals (REACH) as regards Annex XVII.

Fontaine, F., Gramaje, D., Armengol, J., Smart, R., Nagy, Z. A., Borgo, M., ... Corio-Costet, M.-F. (2016). Grapevine Trunk Diseases. A review. International Organisation of Vine and Wine (OIV), (December), 25. Retrieved from <http://www.oiv.int/public/medias/4650/trunk-diseases-oiv-2016.pdf>

Frick, U. B., & Schaller, A. (2002). cDNA microarray analysis of fusicoccin-induced changes in gene expression in tomato plants. *Planta*, 216(1), 83–94. <https://doi.org/10.1007/s00425-002-0887-1>

Gaff, D., and O. Okong'o-Ogola. (1971). The use of non-permeating pigments for testing the survival of cells. *Journal of Experimental Botany*. 22:756-758.

Galarneau, E. R. A., Lawrence, D. P., Travadon, R., & Baumgartner, K. (2019). Drought exacerbates botryosphaeria dieback symptoms in grapevines and confounds host-based molecular markers of infection by *neofusicoccum parvum*. *Plant Disease*, 103(7), 1738–1745. <https://doi.org/10.1094/PDIS-09-18-1549-RE>

Gerlach, D., Botanische Mikrotechnik Eine Einführung. 2., überarbeitete und erweiterte Auflage. XII + 311 S., 45 Abb. Georg Thieme Verlag. Stuttgart, 1977, ISBN 3–13–

444902–1. Feddes Repert., 89: 99-100. <https://doi.org/10.1002/jobm.3620270512>

Gómez, P., Báidez, A. G., Ortuño, A., & Del Río, J. A. (2016). Grapevine xylem response to fungi involved in trunk diseases. *Annals of Applied Biology*, 169(1), 116–124. <https://doi.org/10.1111/aab.12285>

Gong, P., Riemann, M., Dong, D., Stoeffler, N., Gross, B., Markel, A., & Nick, P. (2019). Two grapevine metacaspase genes mediate ETI-like cell death in grapevine defense against infection of *Plasmopara viticola*. *Protoplasma*, 256(4), 951–969. <https://doi.org/10.1007/s00709-019-01353-7>

Guan, X., Buchholz, G., & Nick, P. (2014). Actin marker lines in grapevine reveal a gatekeeper function of guard cells. *Journal of Plant Physiology*, 171(13), 1164–1173. <https://doi.org/10.1016/j.jplph.2014.03.019>

Guan, X., Buchholz, G., & Nick, P. (2015). Tubulin marker line of grapevine suspension cells as a tool to follow early stress responses. *Journal of Plant Physiology*, 176, 118–128. <https://doi.org/10.1016/j.jplph.2014.10.023>

Guan, X., Essakhi, S., Laloue, H., Nick, P., Bertsch, C., & Chong, J. (2016). Mining new resources for grape resistance against Botryosphaeriaceae: A focus on *Vitis vinifera* subsp. *sylvestris*. *Plant Pathology*, 65(2), 273–284.

Guan, P., Terigele, Schmidt, F., Riemann, M., Fischer, J., Thines, E., & Nick, P. (2020). Hunting modulators of plant defense: the grapevine trunk disease fungus *Eutypa lata* secretes an amplifier for plant basal immunity. *Journal of Experimental Botany*, (March). <https://doi.org/10.1093/jxb/eraa152>

Hernandez-Blanco, C., Feng, D. X., Hu, J., Sanchez-Vallet, A., Deslandes, L., Llorente, F., ... Molina, A. (2007). Impairment of Cellulose Synthases Required for Arabidopsis Secondary Cell Wall Formation Enhances Disease Resistance. *The Plant Cell Online*, 19(3), 890–903. <https://doi.org/10.1105/tpc.106.048058>

Henty-Ridilla, J. L., Shimono, M., Li, J., Chang, J. H., Day, B., & Staiger, C. J. (2013).

The Plant Actin Cytoskeleton Responds to Signals from Microbe-Associated Molecular Patterns. *PLoS Pathogens*, 9(4). <https://doi.org/10.1371/journal.ppat.1003290>

Hoeberichts, F. A., Ten Have, A., & Woltering, E. J. (2003).

A tomato metacaspase gene is upregulated during programmed cell death in *Botrytis cinerea*-infected leaves. *Planta*, 217(3), 517–522. <https://doi.org/10.1007/s00425-003-1049-9>

Hou, H., Yan, Q., Wang, X., & Xu, H. (2013).

A SBP-Box Gene VpSBP5 from Chinese Wild Vitis Species Responds to *Erysiphe necator* and Defense Signaling Molecules. *Plant Molecular Biology Reporter*, 31(6), 1261–1270. <https://doi.org/10.1007/s11105-013-0591-2>

Hou, S., Liu, Z., Shen, H., & Wu, D. (2019).

Damage-associated molecular pattern-triggered immunity in plants. *Frontiers in Plant Science*, 10(May). <https://doi.org/10.3389/fpls.2019.00646>

Ismail, A., Riemann, M., & Nick, P. (2012).

The jasmonate pathway mediates salt tolerance in grapevines. *Journal of Experimental Botany*, 63(5), 2127–2139. <https://doi.org/10.1093/jxb/err426>

Jiao, Y., Xu, W., Duan, D., Wang, Y., & Nick, P. (2016).

A stilbene synthase allele from a Chinese wild grapevine confers resistance to powdery mildew by recruiting salicylic acid signaling for efficient defense. *Journal of Experimental Botany*, 67(19), 5841–5856. <https://doi.org/10.1093/jxb/erw351>

Jones, J., Dangl, J. (2006).

The plant immune system. *Nature* 444, 323–329. <https://doi.org/10.1038/nature05286>

Keylor, M. H., Matsuura, B. S., & Stephenson, C. R. J. (2015). Chemistry and Biology of

- Resveratrol-Derived Natural Products. *Chemical Reviews*, 115(17), 8976–9027.
<https://doi.org/10.1021/cr500689b>
- Kinoshita, T., & Shimazaki, K. I. (2001).** Analysis of the phosphorylation level in guard-cell plasma membrane H⁺-ATPase in response to fusicoccin. *Plant and Cell Physiology*, 42(4), 424–432. <https://doi.org/10.1093/pcp/pce055>
- Kumar, S. N., & Nambisan, B. (2014).** Antifungal activity of diketopiperazines and stilbenes against plant pathogenic fungi in vitro. *Applied Biochemistry and Biotechnology*, 172(2), 741–754. <https://doi.org/10.1007/s12010-013-0567-6>
- Labois, C., Wilhelm, K., Laloue, H., Tarnus, C., Bertsch, C., M.-L. G. & Chong, J. (2020).** Wood Metabolomic Responses of Wild and Cultivated Grapevine to Infection with *Neofusicoccum parvum*, a Trunk Disease Pathogen. *Metabolites*, 10(6), 232. <https://doi.org/doi:10.3390/metabo10060232>
- Langcake, P. (1981).** Disease resistance of *Vitis* spp. and the production of the stress metabolites resveratrol, ϵ -viniferin, α -viniferin and pterostilbene. *Physiological Plant Pathology*, 18(2), 213–226. [https://doi.org/10.1016/s0048-4059\(81\)80043-4](https://doi.org/10.1016/s0048-4059(81)80043-4)
- Leon, J., Shulaev, V., Yalpani, N., Lawton, M. A., & Raskint, I. (1995).** Benzoic acid 2-hydroxylase, a soluble oxygenase from tobacco, catalyzes salicylic acid biosynthesis (*Nicotiana tabacum*/tobacco mosaic virus/cytochrome P450/acquired resistance). *Plant Biology*, 92(October), 10413–10417.
- Liang, Z., Duan, S., Sheng, J., Zhu, S., Ni, X., Shao, J., ... Dong, Y. (2019).** Whole-genome resequencing of 472 *Vitis* accessions for grapevine diversity and demographic history analyses. *Nature Communications*, 10(1), 1–12. <https://doi.org/10.1038/s41467-019-09135-8>
- Lima, M. R. M., Machado, A. F., & Gubler, W. D. (2017).** Metabolomic Study of Chardonnay Grapevines Double Stressed with Esca-Associated Fungi and Drought. *Phytopathology*, 107(6), 669–680. <https://doi.org/http://dx.doi.org/10.1094/PHYTO-11->

16-0410-R

Livak K.J. & Schmittgen T.D. (2001). Analysis of relative gene expression data using real-time quantitative PCR and the $2(-\Delta\Delta C(T))$ method. *Methods* 25, 402–408. <https://doi.org/10.1006/meth.2001.1262>

Li, Y., & Trush, M. A. (1998). Diphenyleneiodonium, an NAD(P)H oxidase inhibitor, also potently inhibits mitochondrial reactive oxygen species production. *Biochemical and Biophysical Research Communications*, 253(2), 295–299. <https://doi.org/10.1006/bbrc.1998.9729>

Loeffler F. 1884. Untersuchung über die Bedeutung der Mikroorganismen für die Entstehung der Diphtherie beim Menschen, bei der Taube und beim Kalbe. *Mittheilungen kaiserl Gesundheitsamt* 2, 421–499.

Lorena, T., Calamassi. R, Bruno Mori, B., Mugnai, L. & Surcio, G. (2001). «Phaeomoniella chlamydospora»-Grapevine Interaction: Histochemical Reactions to Fungal Infection. *Phytopathologia Mediterranea*, 40(3) 400–406. [doi:10.14601/Phytopathol_Mediterr-1610](https://doi.org/10.14601/Phytopathol_Mediterr-1610)

Magnin-robert, M., Spagnolo, A., Boulanger, A., Cl, C., Abou-mansour, E., & Fontaine, F. (2016). Changes in Plant Metabolism and Accumulation of Fungal Metabolites in Response to Esca Proper and Apoplexy Expression in the Whole Grapevine. *Biochemistry and Cell Biology*, 106(6), 541–553. <https://doi.org/10.1094/PHYTO-09-15-0207-R>

Malerba, M., Contran, N., Tonelli, M., Crosti, P., & Cerana, R. (2008). Role of nitric oxide in actin depolymerization and programmed cell death induced by fusicoicin in sycamore (*Acer pseudoplatanus*) cultured cells. *Physiologia Plantarum*, 133(2), 449–457.

<https://doi.org/10.1111/j.1399-3054.2008.01085.x>

- Massonnet, M., Figueroa-Balderas, R., Galarneau, E. R. A., Miki, S., Lawrence, D. P., Sun, Q., ... Cantu, D. (2017).** Neofusicoccum parvum Colonization of the Grapevine Woody Stem Triggers Asynchronous Host Responses at the Site of Infection and in the Leaves. *Frontiers in Plant Science*, 8(June). <https://doi.org/10.3389/fpls.2017.01117>
- Moser, T. (2015).** Investigation of the transcriptional regulation of candidate genes of pathogen defense against *Plasmopara viticola* in grapevines. Dissertation, Julius Kühn-Institut, Germany. <https://doi.org/10.5073/dissjki.2015.004>
- Mugnai, L., Graniti, A., & Surico, G. (1999).** Esca (Black Measles) and Brown Wood-Streaking: Two Old and Elusive Diseases of Grapevines. *Plant Disease*, 83(5), 404–418. <https://doi.org/10.1094/pdis.1999.83.5.404>
- Mutawila, C., Fourie, P. H., Halleen, F., & Mostert, L. (2011).** Histo-pathology study of the growth of *Trichoderma harzianum*, *Phaeomoniella chlamydospora* and *Eutypa lata* on grapevine pruning wounds. *Phytopathologia Mediterranea*, 50(SUPPL.), 46–60. https://doi.org/10.14601/Phytopathol_Mediterr-8643
- Nick, P. (2014).** Schützen und nützen – von der Erhaltung zur Anwendung . Fallbeispiel Europäische Wildrebe. *Hoppea Denkschrift*, 159–173. Retrieved from www.regenburgische-botanische-gesellschaft.de
- Oh, C. S., Pedley, K. F., & Martin, G. B. (2010).** Tomato 14-3-3 protein 7 positively regulates immunity-associated programmed cell death by enhancing protein abundance and signaling ability of MAPKKK α . *Plant Cell*, 22(1), 260–272. <https://doi.org/10.1105/tpc.109.070664>

- Olivari, C., Meanti, C., De Michelis, M. I., & Rasi-Caldogno, F. (1998).** Fusicoccin Binding to Its Plasma Membrane Receptor and the Activation of the Plasma Membrane H⁺-ATPase: IV. Fusicoccin Induces the Association between the Plasma Membrane H⁺-ATPase and the Fusicoccin Receptor. *Plant Physiology*, 116(2), 529–537. <https://doi.org/10.1104/pp.116.2.529>
- Orozco-Cárdenas, M. L., Narváez-Vásquez, J., & Ryan, C. A. (2001).** Hydrogen peroxide acts as a second messenger for the induction of defense genes in tomato plants in response to wounding, systemin, and methyl jasmonate. *Plant Cell*, 13(1), 179–191. <https://doi.org/10.1105/tpc.13.1.179>
- Parage, C., Tavares, R., Rety, S., Baltenweck-Guyot, R., Poutaraud, A., Renault, L., ... Hugueney, P. (2012).** Structural, Functional, and Evolutionary Analysis of the Unusually Large Stilbene Synthase Gene Family in Grapevine. *Plant Physiology*, 160(3), 1407–1419. <https://doi.org/10.1104/pp.112.202705>
- Paolinelli-alfonso, M., Villalobos-escobedo, J. M., Rolshausen, P., Herrera-estrella, A., Galindo-sánchez, C., López-hernández, J. F., & Hernandez-martinez, R. (2016).** Global transcriptional analysis suggests *Lasiodiplodia theobromae* pathogenicity factors involved in modulation of grapevine defensive response. *BMC Genomics*, 1–20. <https://doi.org/10.1186/s12864-016-2952-3>
- Pescitelli, G., Masi, M., Reveglia, P., Baaijens-billones, R., Go, M., Savocchia, S., & Evidente, A. (2020).** Phytotoxic Metabolites from Three *Neofusicoccum* Species Causal Agents of *Botryosphaeria* Dieback in Australia, Luteopyroxin, Neoanthraquinone, and Luteoxepinone, a Disubstituted Furo- α -pyrone, a Hexasubstituted Anthraquinone, and a Trisubstituted Oxepi-2-. *Journal of Natural Products*, 83, 453–460. <https://doi.org/10.1021/acs.jnatprod.9b01057>
-

- Pezet, R., Gindro, K., Viret, O., & Spring, J. L. (2004).** Glycosylation and oxidative dimerization of resveratrol are respectively associated to sensitivity and resistance of grapevine cultivars to downy mildew. *Physiological and Molecular Plant Pathology*, 65(6), 297–303. <https://doi.org/10.1016/j.pmpp.2005.03.002>
- Pierron, R. J. G., Pouzoulet, J., Couderc, C., Judic, E., Compant, S., & Jacques, A. (2016).** Variations in Early Response of Grapevine Wood Depending on Wound and Inoculation Combinations with *Phaeoacremonium aleophilum* and *Phaeomoniella chlamydospora*. *Frontiers in Plant Science*, 7(March), 1–14. <https://doi.org/10.3389/fpls.2016.00268>
- Pietrowska, E., Różalska, S., Kaźmierczak, A., Nawrocka, J., & Malolepsza, U. (2014).** Reactive oxygen and nitrogen (ROS and RNS) species generation and cell death in tomato suspension cultures—*Botrytis cinerea* interaction. *Protoplasma*, 252(1), 307–319. <https://doi.org/10.1007/s00709-014-0680-6>
- Pap, D., Riaz, S., Dry, I. B., Jermakow, A., Tenschler, A. C., Cantu, D., ... Walker, M. A. (2016).** Identification of two novel powdery mildew resistance loci, Ren6 and Ren7, from the wild Chinese grape species *Vitis piasezkii*. *BMC Plant Biology*, 16(1), 1–19. <https://doi.org/10.1186/s12870-016-0855-8>
- Pouzoulet, J., Pivovarov, A. L., Santiago, L. S., & Rolshausen, P. E. (2014).** Can vessel dimension explain tolerance toward fungal vascular wilt diseases in woody plants? Lessons from dutch elm disease and esca disease in grapevine. *Frontiers in Plant Science*, 5(JUN), 1–11. <https://doi.org/10.3389/fpls.2014.00253>
- Pouzoulet, J., Scudiero, E., Schiavon, M., & Rolshausen, P. E. (2017).** Xylem vessel diameter affects the compartmentalization of the vascular pathogen *phaeomoniella chlamydospora* in grapevine. *Frontiers in Plant Science*, 8(August), 1–13. <https://doi.org/10.3389/fpls.2017.01442>

- Priyadarshan, P. M. (2019).** PLANT BREEDING: Classical to Modern (1st ed., p. 379-385). Springer Nature Singapore Pte Ltd. <https://doi.org/10.1007/978-981-13-7095-3>
- Qiao, F., Chang, X. L., & Nick, P. (2010).** The cytoskeleton enhances gene expression in the response to the Harpin elicitor in grapevine. *Journal of Experimental Botany*, 61(14), 4021–4031. <https://doi.org/10.1093/jxb/erq221>
- Ramírez-Suero, M., Bénard-Gellon, M., Chong, J., Laloue, H., Stempien, E., Abou-Mansour, E., ... Bertsch, C. (2014).** Extracellular compounds produced by fungi associated with Botryosphaeria dieback induce differential defense gene expression patterns and necrosis in Vitis vinifera cv. Chardonnay cells. *Protoplasma*, 251(6), 1417–1426. <https://doi.org/10.1007/s00709-014-0643-y>
- Rasclé, C., Loisel, E., Poussereau, N., Morgant, G., Héloir, M.-C., Viaud, M., ... Ferrarini, A. (2015).** Analysis of the Molecular Dialogue Between Gray Mold (*Botrytis cinerea*) and Grapevine (*Vitis vinifera*) Reveals a Clear Shift in Defense Mechanisms During Berry Ripening. *Molecular Plant-Microbe Interactions*, 28(11), 1167–1180. <https://doi.org/10.1094/mpmi-02-15-0039-r>
- Ridgway, H.J., Amponsah, N.T., Brown, D.S., Baskarathevan, J., Jones, E.E. and Jaspers, M.V. 2011.** Detection of botryosphaeriaceous species in environmental samples using a multi-species primer pair. *Plant Pathology*, 60: 1118-1127. <https://doi:10.1111/j.1365-3059.2011.02474.x>
- Romanazzi, G., Murolo, S., Pizzichini, L., & Nardi, S. (2009).** Esca in young and mature vineyards, and molecular diagnosis of the associated fungi. *European Journal of Plant Pathology*, 125(2), 277–290. <https://doi.org/10.1007/s10658-009-9481-8>
- Rudelle, J., Octave, S., Kaid-Harche, M., Roblin, G., & Fleurat-Lessard, P. (2005).**
-

- Structural modifications induced by *Eutypa lata* in the xylem of trunk and canes of *Vitis vinifera*. *Functional Plant Biology*, 32(6), 537. <https://doi.org/10.1071/fp05012>
- Schwarzerová, K., Zelenková, S., Nick, P., & Opatrný, Z. (2002).** Aluminum-induced rapid changes in the microtubular cytoskeleton of tobacco cell lines. *Plant and Cell Physiology*, 43(2), 207–216. <https://doi.org/10.1093/pcp/pcf028>
- Siebert, J.B. (2001).** “Eutypa: The economic toll on vineyards”. *Wines & Vines* (April),50-56.
- Singh, J., & Roberts, M. R. (2004).** Fusicoccin activates pathogen-responsive gene expression independently of common resistance signaling pathways, but increases disease symptoms in *Pseudomonas syringae*-infected tomato plants. *Planta*, 219(2), 261–269. <https://doi.org/10.1007/s00425-004-1234-5>
- Škalamera, D., & Heath, M. C. (1998).** Changes in the cytoskeleton accompanying infection-induced nuclear movements and the hypersensitive response in plant cells invaded by rust fungi. *Plant Journal*, 16(2), 191–200. <https://doi.org/10.1046/j.1365-313X.1998.00285.x>
- Slippers, B., & Wingfield, M. J. (2007).** Botryosphaeriaceae as endophytes and latent pathogens of woody plants: diversity, ecology and impact. *Fungal Biology Reviews*, 21(2–3), 90–106. <https://doi.org/10.1016/j.fbr.2007.06.002>
- Smertenko, A., & Franklin-Tong, V. E. (2011).** Organisation and regulation of the cytoskeleton in plant programmed cell death. *Cell Death and Differentiation*, 18(8), 1263–1270. <https://doi.org/10.1038/cdd.2011.39>
- Songy, A., Fernandez, O., Clément, C., Larignon, P., & Fontaine, F. (2019).** Grapevine trunk diseases under thermal and water stresses. *Planta*, 249(6), 1655–1679. <https://doi.org/10.1007/s00425-019-03111-8>

- Sosnowski, M. R., Creaser, M. L., Wicks, T. J., Lardner, R., & Scott, E. S. (2008).** Protection of grapevine pruning wounds from infection by *Eutypa lata*. *Australian Journal of Grape and Wine Research*, 14: 134-142. doi:10.1111/j.1755-0238.2008.00015.x
- Spagnolo, A., Larignon, P., Magnin-Robert, M., Hovasse, A., Cilindre, C., Van Dorselaer, A., ... Fontaine, F. (2014).** Flowering as the most highly sensitive period of grapevine (*Vitis vinifera* L. cv mourvèdre) to the *Botryosphaeria dieback* agents *neofusicoccum parvum* and *Diplodia seriata* infection. *International Journal of Molecular Sciences*, 15(6), 9644–9669. <https://doi.org/10.3390/ijms15069644>
- Stael, S., Kmicik, P., Willems, P., Van Der Kelen, K., Coll, N. S., Teige, M., & Van Breusegem, F. (2015).** Plant innate immunity - sunny side up? *Trends in Plant Science*, 20(1), 3–11. <https://doi.org/10.1016/j.tplants.2014.10.002>
- Steffens, B., & Sauter, M. (2009).** Epidermal cell death in rice is confined to cells with a distinct molecular identity and is mediated by ethylene and H₂O₂ through an autoamplified signal pathway. *Plant Cell*, 21(1), 184–196. <https://doi.org/10.1105/tpc.108.061887>
- Stempien, E., Goddard, M. L., Wilhelm, K., Tarnus, C., Bertsch, C., & Chong, J. (2017).** Grapevine *Botryosphaeria dieback* fungi have specific aggressiveness factor repertory involved in wood decay and stilbene metabolism. *PLoS ONE*, 12(12), 1–22. <https://doi.org/10.1371/journal.pone.0188766>
- Stempien, E., Goddard, M. L., Leva, Y., Bénard-Gellon, M., Laloue, H., Farine, S., ... Chong, J. (2018).** Secreted proteins produced by fungi associated with *Botryosphaeria dieback* trigger distinct defense responses in *Vitis vinifera* and *Vitis rupestris* cells. *Protoplasma*, 255(2), 613–628. <https://doi.org/10.1007/s00709-017-1175-z>

-
- Stevens, L. M., Sijbesma, E., Botta, M., Mackintosh, C., Obsil, T., Landrieu, I., ... Ottmann, C. (2018).** Modulators of 14-3-3 Protein-Protein Interactions. *Journal of Medicinal Chemistry*, 61(9), 3755–3778. <https://doi.org/10.1021/acs.jmedchem.7b00574>
- Svyatyna, K., Jikumar, Y., Brendel, R., Reichelt, M., Mithöfer, A., Takano, M., ... Riemann, M. (2014).** Light induces jasmonate-isoleucine conjugation via OsJAR1-dependent and -independent pathways in rice. *Plant, Cell and Environment*, 37(4), 827–839. <https://doi.org/10.1111/pce.12201>
- Tassoni, A., Fornalè, S., Franceschetti, M., Musiani, F., Michael, A. J., Perry, B., & Bagni, N. (2005).** Jasmonates and Na-orthovanadate promote resveratrol production in *Vitis vinifera* cv. Barbera cell cultures. *New Phytologist*, 166(3), 895–905. <https://doi.org/10.1111/j.1469-8137.2005.01383.x>
- Trujillo, M., Kogel, K. H., & Hüchelhoven, R. (2004).** Superoxide and hydrogen peroxide play different roles in the nonhost interaction of barley and wheat with inappropriate formae speciales of *Blumeria graminis*. *Molecular Plant-Microbe Interactions*, 17(3), 304–312. <https://doi.org/10.1094/MPMI.2004.17.3.304>
- Trouvelot, S., Varnier, A. L., Allègre, M., Mercier, L., Baillieul, F., Arnould, C., ... Daire, X. (2008).** A β -1,3 glucan sulfate induces resistance in grapevine against *Plasmopara viticola* through priming of defense responses, including HR-like cell death. *Molecular Plant-Microbe Interactions*, 21(2), 232–243. <https://doi.org/10.1094/MPMI-21-2-0232>
- Tu, M., Wang, X., Yin, W., Wang, Y., Li, Y., Zhang, G., ... Wang, X. (2020).** Grapevine VlbZIP30 improves drought resistance by directly activating VvNAC17 and promoting lignin biosynthesis through the regulation of three peroxidase genes. *Horticulture Research*, 7(1). <https://doi.org/10.1038/s41438-020-00372-3>
- Úrbez-Torres, J. R. (2011).** The status of Botryosphaeriaceae species infecting grapevines
-

-
- José. *Phytopathologia Mediterranea*, 50(4).
https://doi.org/https://doi.org/10.14601/Phytopathol_Mediterr-9316
- Úrbez-Torres, J. R., Haag, P., Bowen, P., & O’Gorman, D. T. (2013).** Grapevine Trunk Diseases in British Columbia: Incidence and Characterization of the Fungal Pathogens Associated with Black Foot Disease of Grapevine. *Plant Disease*, 98(4), 456–468.
<https://doi.org/10.1094/pdis-05-13-0524-re>
- Van Breusegem, F., & Dat, J. F. (2006).** Reactive oxygen species in plant cell death. *Plant Physiology*, 141(2), 384–390. <https://doi.org/10.1104/pp.106.078295>
- van de Wouwer, D., Vanholme, R., Decou, R., Goeminne, G., Audenaert, D., Nguyen, L., ... Boerjan, W. (2016).** Chemical genetics uncovers novel inhibitors of lignification, including p-iodobenzoic acid targeting CINNAMATE-4-HYDROXYLASE. *Plant Physiology*, 172(1), 198–220. <https://doi.org/10.1104/pp.16.00430>
- Van Doorn, W. G., Beers, E. P., Dangl, J. L., Franklin-Tong, V. E., Gallois, P., Hara-Nishimura, I., ... Bozhkov, P. V. (2011).** Morphological classification of plant cell deaths. *Cell Death and Differentiation*, 18(8), 1241–1246.
<https://doi.org/10.1038/cdd.2011.36>
- van Niekerk, J. M., Fourie, P. H., Halleen, F., & Crous, P. W. (2006).** Botryosphaeria spp. as grapevine trunk disease pathogens. *Phytopathologia Mediterranea*, 45(SUPPL. 1), 43–54.
- Vannozzi, A., Dry, I. B., Fasoli, M., Zenoni, S., & Lucchin, M. (2012).** Genome-wide analysis of the grapevine stilbene synthase multigenic family: genomic organization and expression profiles upon biotic and abiotic stresses. *BMC Plant Biology*, 12.
<https://doi.org/10.1186/1471-2229-12-130>
-

References

- Walker, S. E., & Lorsch, J. (2013).** RNA purification - Precipitation methods. *In Methods in Enzymology* (1st ed., Vol. 530). <https://doi.org/10.1016/B978-0-12-420037-1.00019-1>
- Wagschal, I., E. Abou-Mansour, A.-N. Petit, Clément C, Fontaine F. (2008).** Wood diseases of grapevine: A review on eutypa dieback and esca. In: *Plant Microbe Interactions* (eds. Bark EA, Clément C), pp 367-391
- Wang, L., & Nick, P. (2017).** Cold sensing in grapevine—which signals are upstream of the microtubular “thermometer.” *Plant Cell and Environment*, 40(11), 2844–2857. <https://doi.org/10.1111/pce.13066>
- Wang, R., (2019).** A New Actin-Dependent Pathway in Plant Defence -Aluminium Tolerance in Grapevine cells. PhD thesis. Karlsruhe Institute of Technology, Germany.
- Watanabe, N., & Lam, E. (2011).** Arabidopsis metacaspase 2d is a positive mediator of cell death induced during biotic and abiotic stresses. *Plant Journal*, 66(6), 969–982. <https://doi.org/10.1111/j.1365-313X.2011.04554.x>

7. Supplementary.

Method 1. Genomic DNA extraction by CTAB method

1. Wood samples were ground in liquid Nitrogen using sterilized mortars and pestles until they became fine powders. Afterwards, 120-150 mg of the fine wood powder were subject to the follow procedures;
2. Add 900 μ l boiled 1.5% Cetyltrimethylammonium bromide (CTAB) buffer and incubate for 1h at 65°C.
3. Add 630 μ l of Chloroform:isoamylalcohol solution (24:1), vortex and shake horizontally for 15 min at 75 rpm at room temperature.
4. Centrifuge at 15,000 rpm in a table centrifuge for 10 minutes.
5. Transfer the supernatant containing the nucleic acids into a new 2 ml reaction tube and precipitate DNA with 2/3 v/v ice-cold isopropanol (e.g. supernatant 700 μ l, isopropanol 450 μ l).
6. Incubation in – 20 degree for at least 20min. Shake gently and centrifuge at 15,000 rpm in 4 degree for additional 15 min.
7. Wash the precipitated nucleic acids with 1 ml 70% ethanol and spin at 15000 rpm in 4 degree for 10min and dried in a vacuum centrifuge for 15 min.
8. Dissolve DNA in 50 μ l 1/10 nucleus free water containing 5 μ g RNase A for RNA digestion. Keep the sample 2 hours at room temperature before freezing at -20°C.

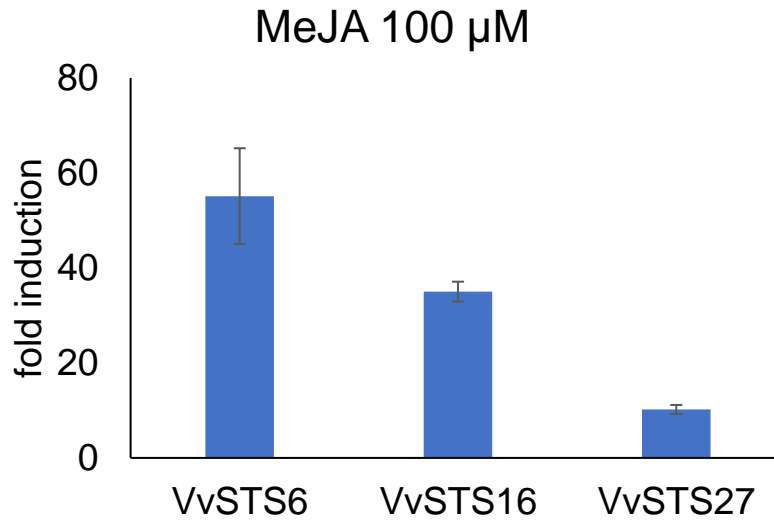
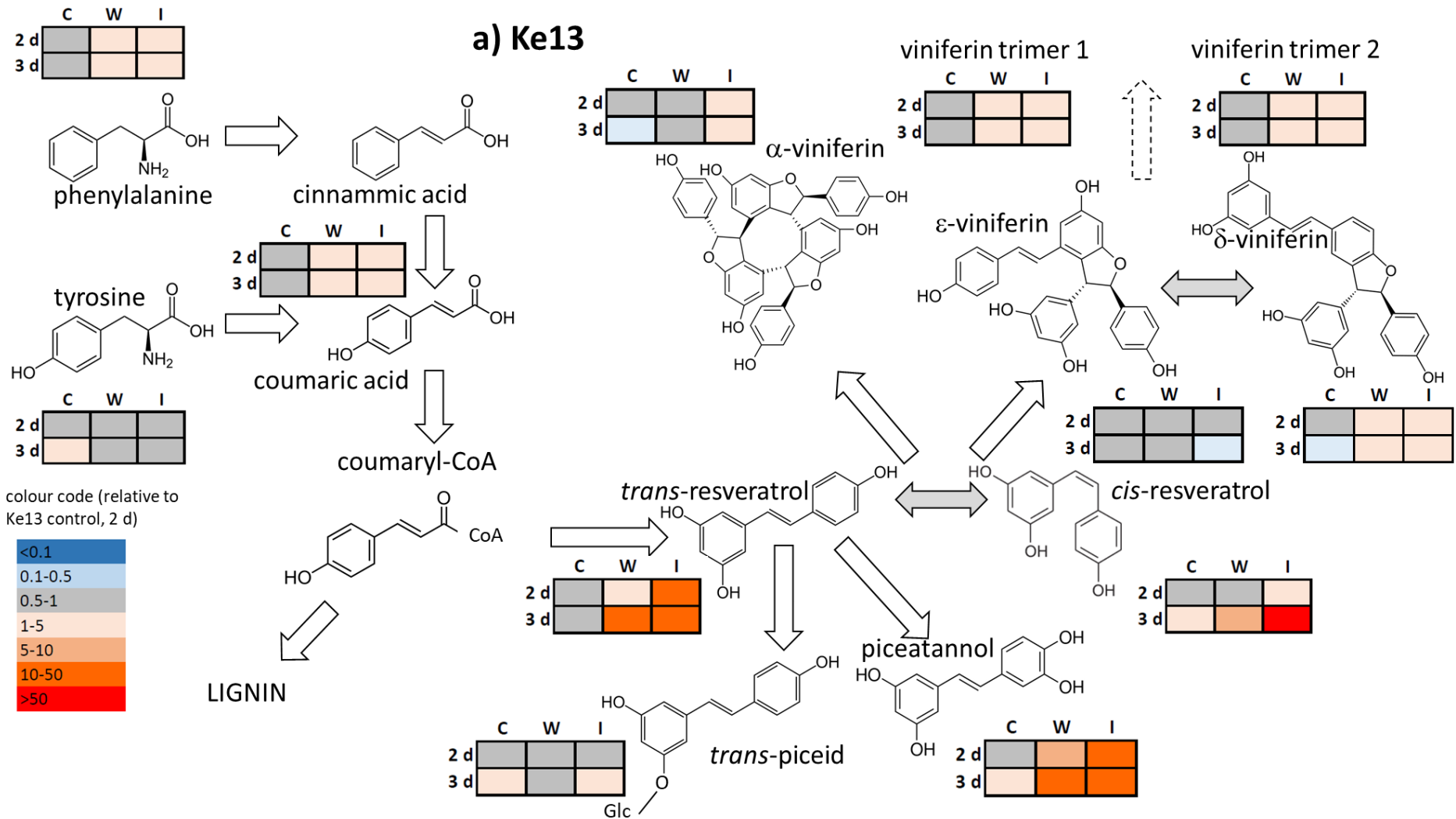
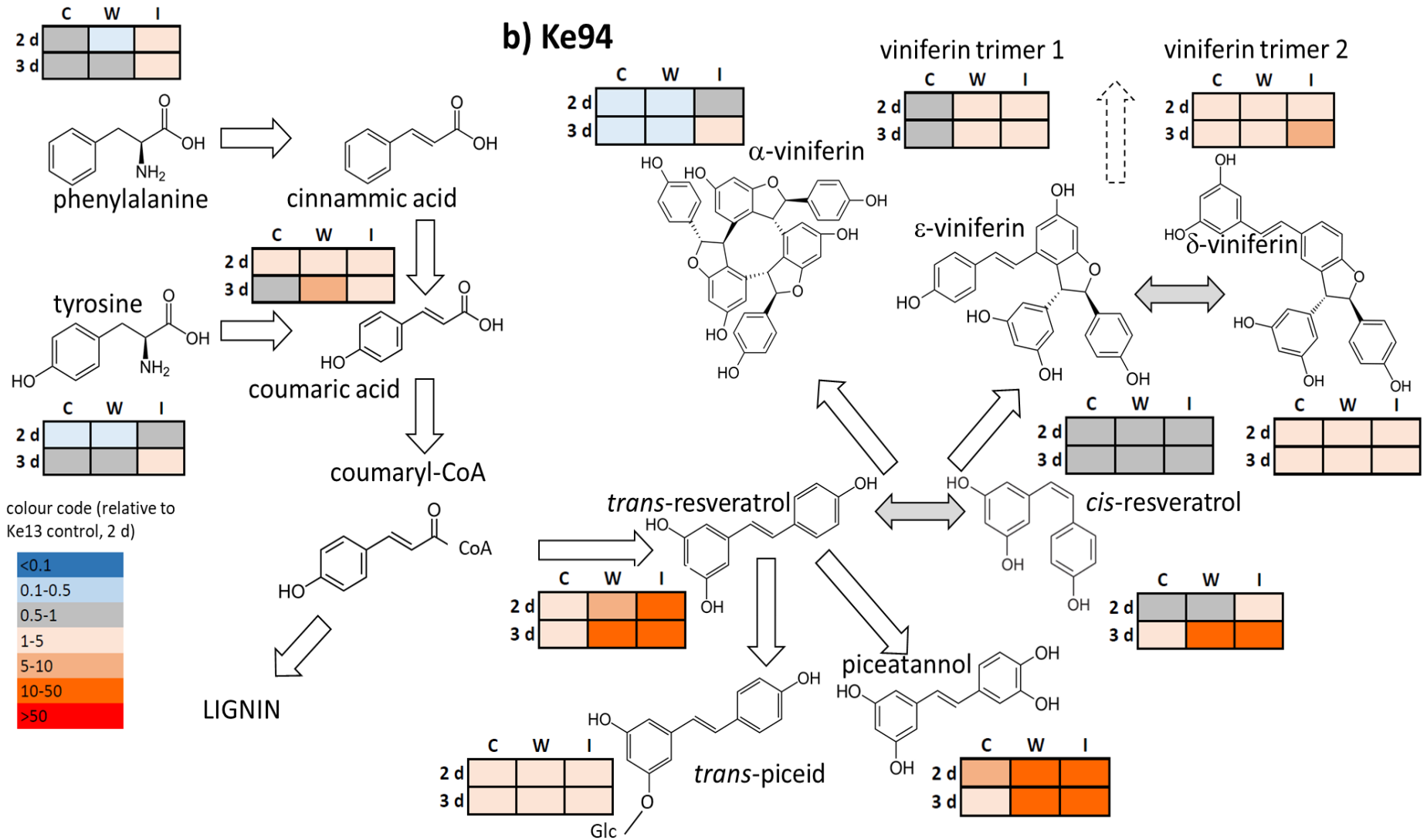
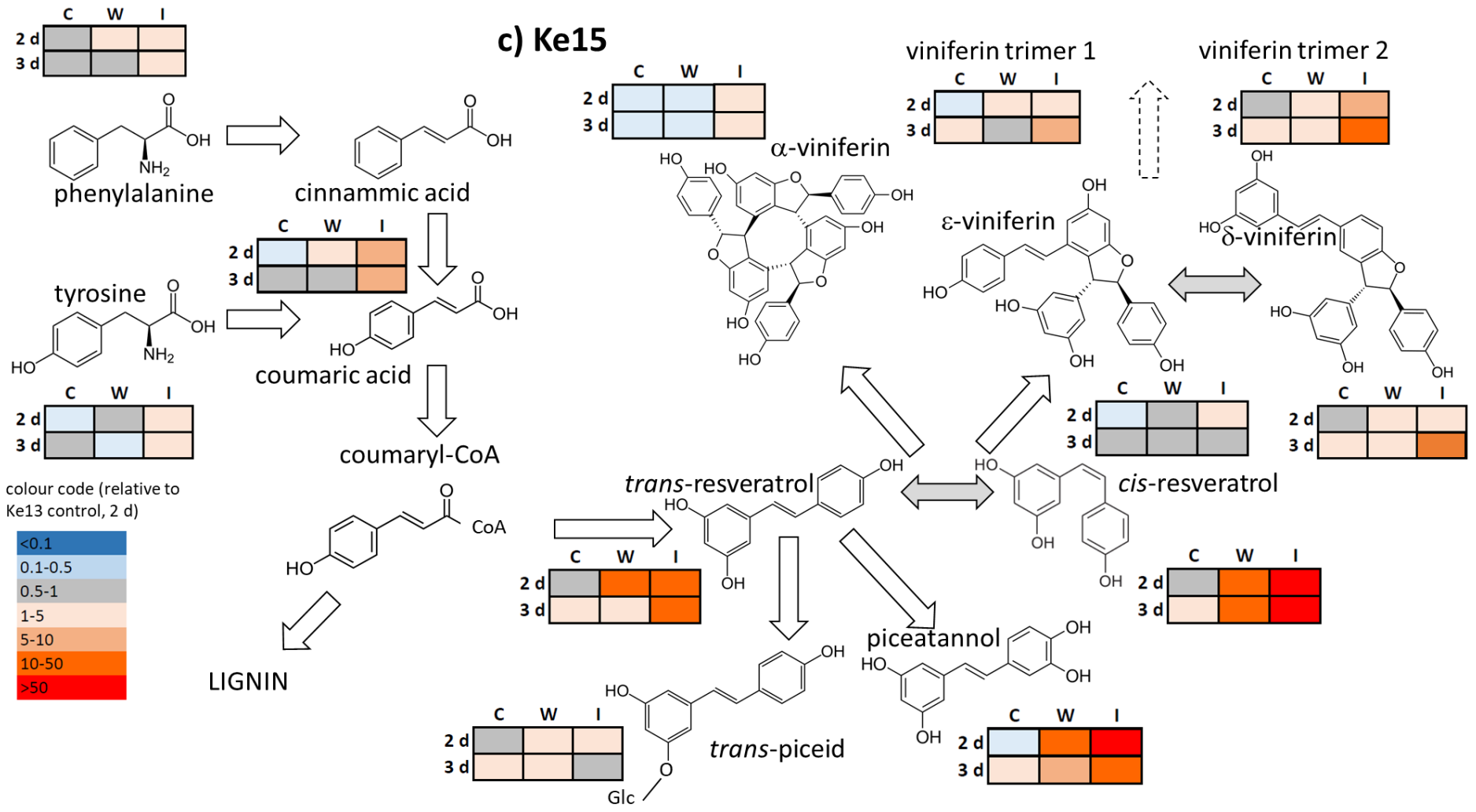


Fig. S1. Steady-state transcripts levels for three stilbene synthases in suspension cells of *Vitis rupestris* in response to exogenous methyl jasmonate (100 μ M) for 1 h. Fold induction refers to the expression levels of the respective transcript in control cells. Data represent means and SE from three biological replicates. Published data in Khattab et al., *New Phytologist* (2020).







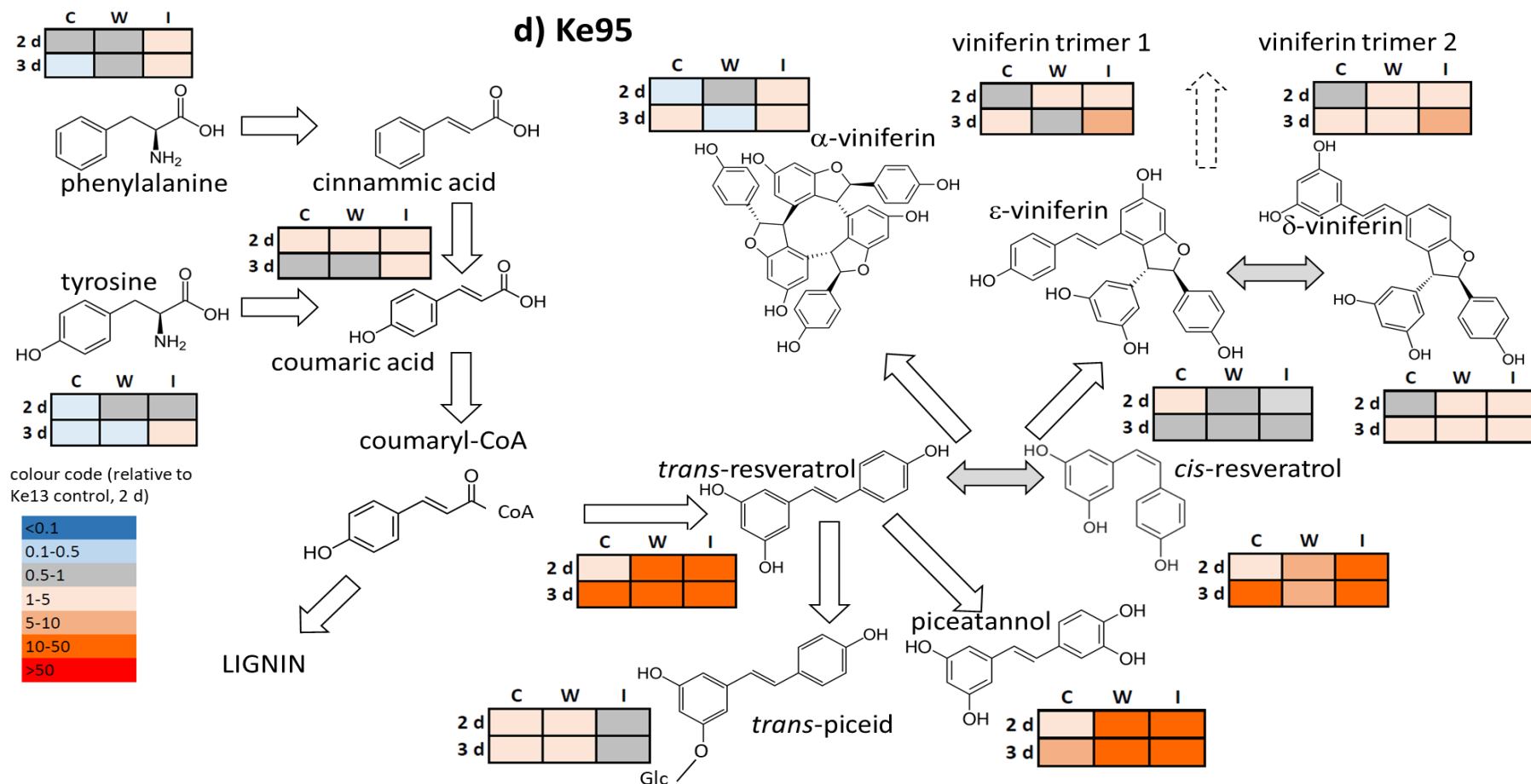


Fig. S2. Heat map of metabolite abundance under 3 different conditions; control (C), wound, non-infected plants (W) and infection (I) in four *sylvestris* accessions. **(a, b)** Two genotypes belong to the piceid chemotype (Ke13, Ke94). **(c, d)** Two genotypes (Ke15, Ke95) represent resveratrol-viniferin chemotype. Wood samples were collected after the infection with *Neofusicoccum parvum* strain Bt-67 from the centre of the internodes at 2 and 3 dpi. The final result of the respective metabolite was normalized to the metabolite abundance in the control plants of Ke13 at day 2. Colour code represent fold changes. Data represent mean values of 3 or 4 biological replicates for each genotype and time point. Statistical analysis was performed using Tukey's test, with p-value ≤ 0.05 . Published data in Khattab et al., New Phytologist (2020).

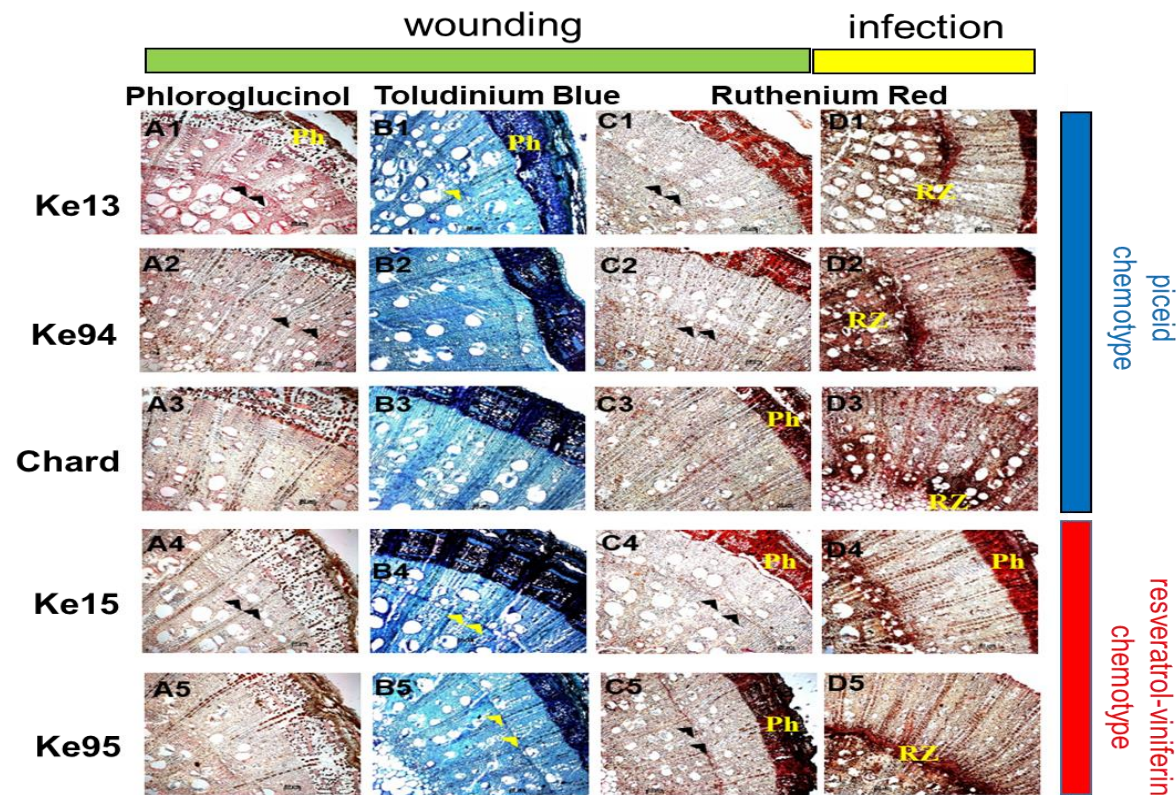


Fig. S3. Genotypic differences in lignin and pectin metabolism using histochemical labelling. (A-B) Lignin intensity in wood cross-sections in response to wounding. (C) Effect of wounding on pectic poly saccharides content as compared to infection with *Neofusicoccum parvum* strain Bt-67 (D). Sections of 20 μm thickness obtained from the central region of the treated internode were either with Phloroglucinol-HCl staining lignin in light red or rose color (A1-5), Toluidine Blue staining lignin in blue, and pectic polysaccharides in violet (B1-5), or Ruthenium Red staining pectic polysaccharides red-brown (C1-5). For comparison, sections obtained from infected canes were stained with Ruthenium Red as well (D1-5). Here, the reaction zone of plant-fungal interaction is indicated by RZ. Arrowheads indicate the annual rings, and Ph the position of the phloem in the cross sections. Size bar 100 μm . Published data in Khattab et al., *New Phytologist* (2020).

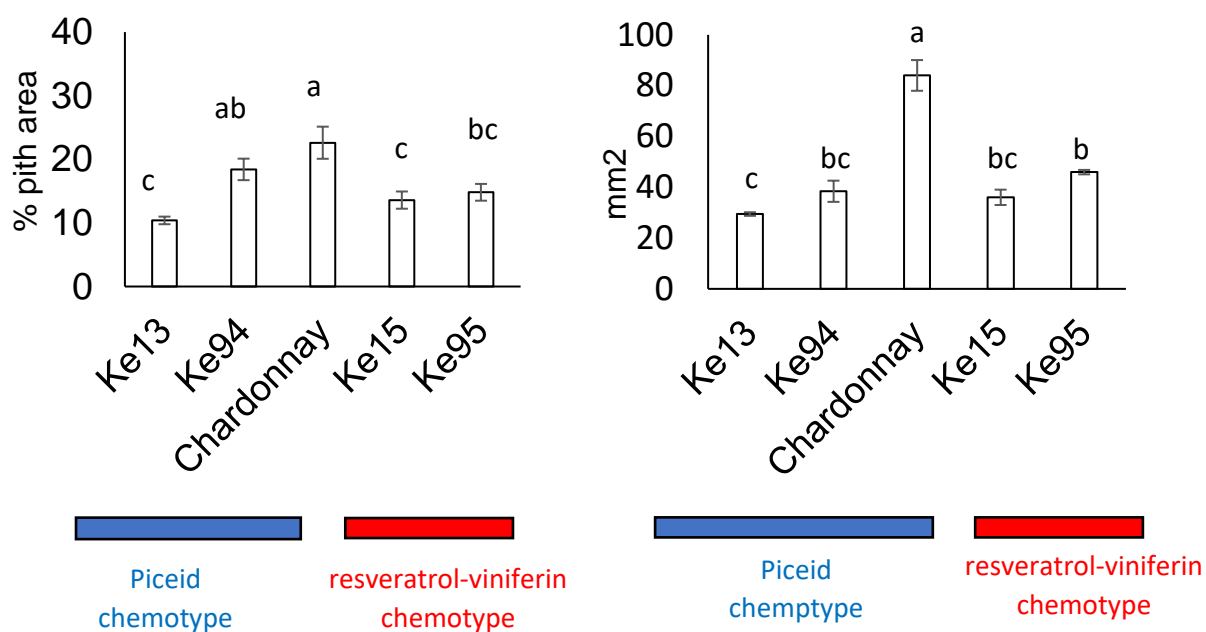


Fig. S4. Genotypic differences in wood structure **(a)** Relative cross area covered by pith parenchyma. **(b)** Stem cross area readouts in the area used for histology and CryoSEM. Data represent mean and standard errors obtained from 5 biological replicates and statistically differentiated. Statistical differences were determined using Duncan's test. Published data in Khattab et al., *New Phytologist* (2020).

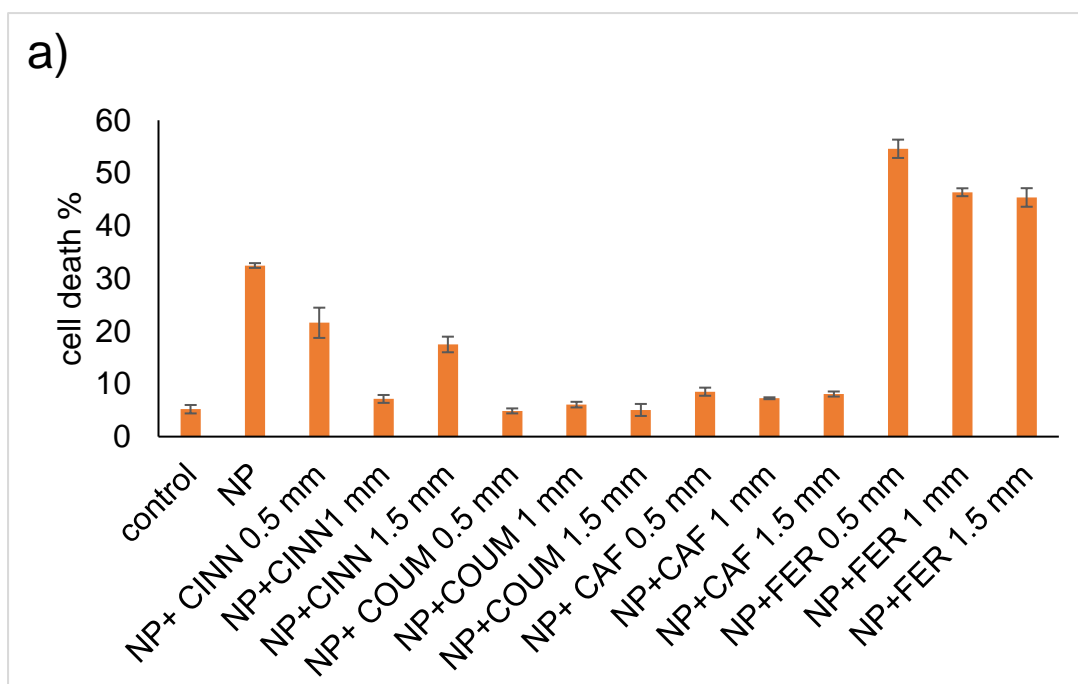
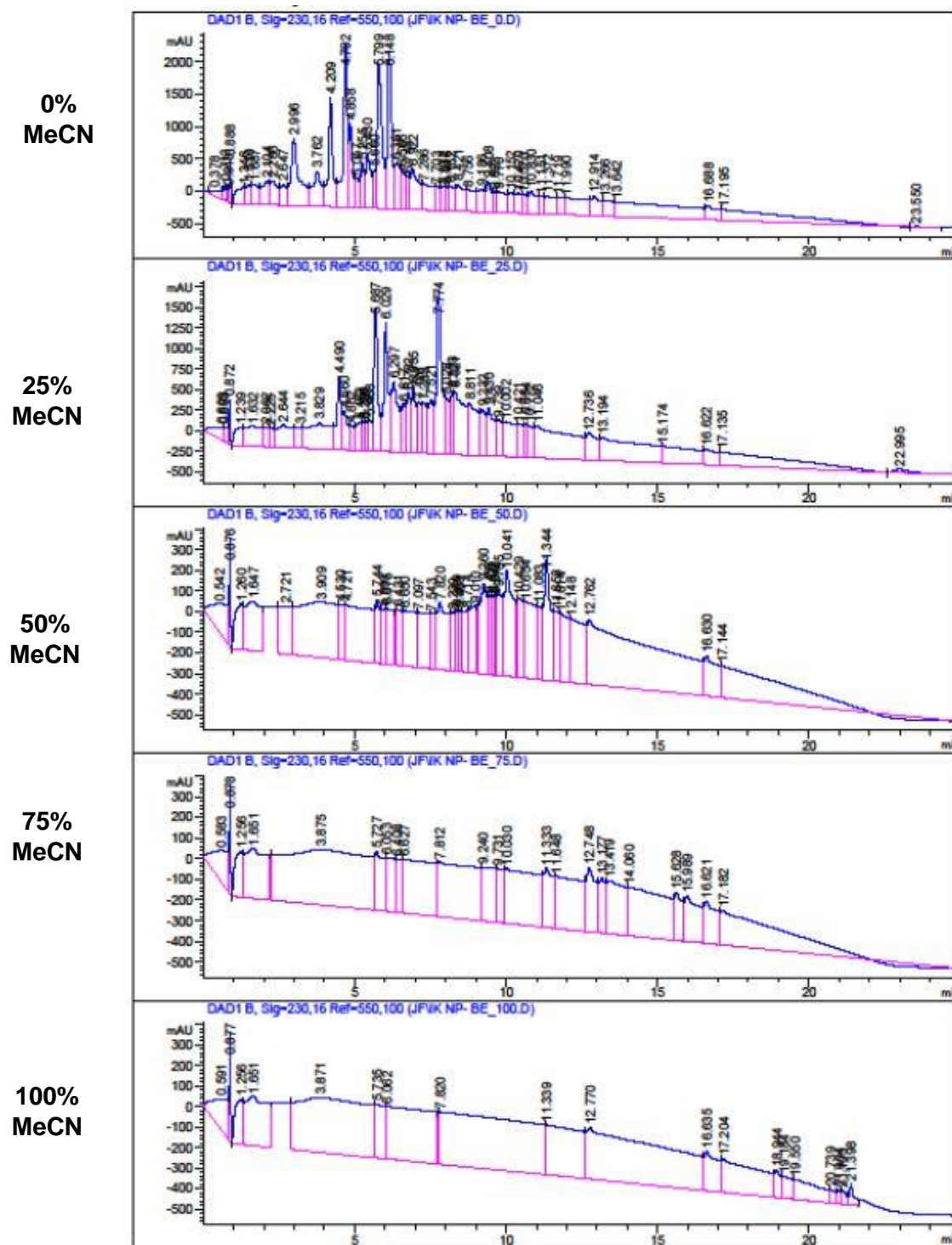


Fig. S5. Percentage of dead cells in *V. rupestris* cell line after 24 hr treatments of sterilized *Neofusicoccum parvum* Bt-67 culture filtrates (35 µl/ 1 ml Vitis cells) fermented separately for 2 weeks with (0.5:1,5) mM of 4 lignin precursors (cinnamic acid, *p*-coumaric acid, caffeic acid, ferulic acid).



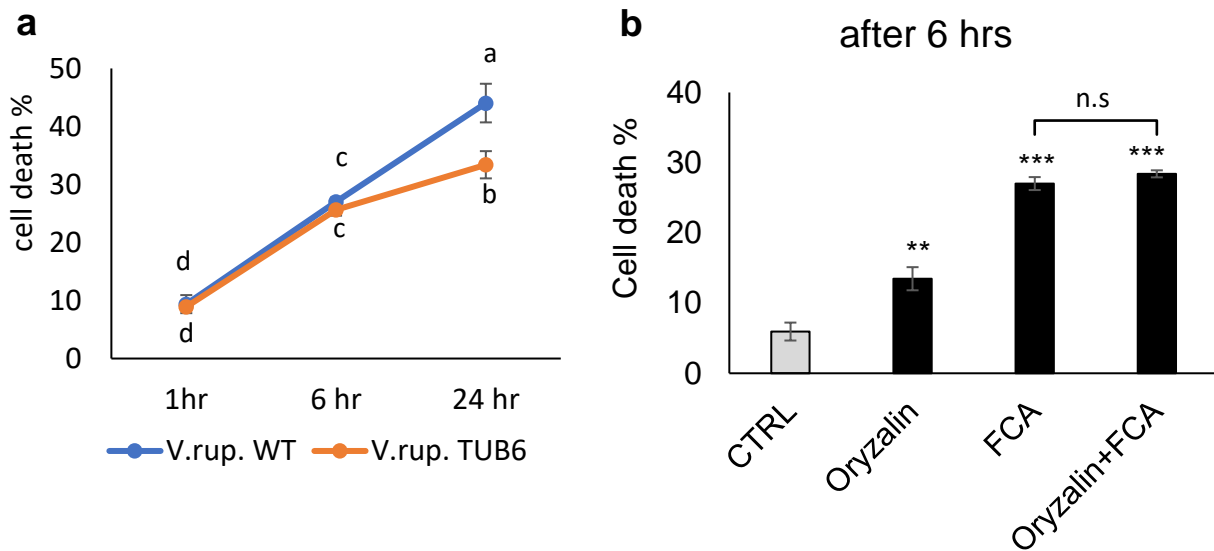


Fig. S7. Effect of Microtubules manipulation on the mortality driven by toxic polyketide, fusiccocin A. **a)** Overexpression of microtubules in the *Vitis rupestris* cell line *AtTUB6*-GFP led to less cell death rates due Fusicocin A treatment comparing to *Vitis rupestris* wild type. **b)** Cell death rates by 6 hrs of 6 μ M Fusicocin A after depleting the microtubules by 10 μ M Oryzalin. Asterisks and different letters indicate statistical differences based on LSD and Duncan's test with significant levels $P < 0.05$ (*), $P < 0.01$ (**), and $P < 0.001$ (***)

Supplementary. Table 1; Genetic details and the sequences of the primers for the targeted genes;

Gene	Accession nr.	Primer type	Primer sequence (5'-3')	Reference
VvEF1- α	XM_002284888	VvEF1- α -F	GAAGTGGGTGCTTGATAGGC	(Spagnolo et al., 2017)
		VvEF1- α -R	AACCAAATATCCGGAGTAAAAGA	
VvUBQ	XR_002030723	VvUBQ-F	GAGGGTCGTCAGGATTTGGA	Moser (2014)
		VvUBQ-R	GCCCTGCACTTACCATCTTTAAG	
VvPAL	XM_002268220	VvPAL-F	TCCTCCCGGAAAACAGCTG	(Spagnolo et al., 2017)
		VvPAL-R	TCCTCCAAATGCCTCAAATCA	
VvSTS27	X76892	VvSTS27-F	CCCAATGTGCCACTTTAAT	Duan et al. (2015)
		VvSTS27-R	CTGGGTGAGCAATCCAAAAT	
VvSTS6	XM_002271335	VvSTS6-F	GTTGTGCTGCATAGCGTTGC	Vannozzi et al., (2012)
		VvSTS6-R	GATTTAATTGGAAATTGTCCCCTTC	
VvSTS16	XM_019226034	VvSTS16-F	CTTTTGACCAATTGGAATCAAC	Vannozzi et al., (2012)
		VvSTS16-R	TGACATGTTCCCATATTTCACTTAG	
VvSTS47	AF274281	VvRS1. F	TGGAAGCAACTAGGCATGTG	Duan et al. (2015)
		VvRS1. R	GTGGCTTTTCCCCCTTTAG	
VvCAOMT	NM_001281171	VvCAOMT-F	GGACTGGAGCCACCCTTAAC	This paper
		VvCAOMT-R	CAACATGCTCCACACCAGGA	
VvCAD	XM_002269320	VvCAD-F	GAGAACGGTGAAGGGAAGCA	This paper
		VvCAD-R	TCATTGTTTGCAAGGCGCTC	
VvJAZ1	JF900329	VvJAZ1-F	TGCAGTCTGTTGAGCCAATACATA	Ismail et al., (2012)
		VvJAZ1-R	CACGTTTCCGGACTTCTTTACAC	
VvJAZ4	XM_002272363.2.	VvJAZ4-F	TTCAGGAAATCGGCAACAACAGA	Zhang <i>et al.</i> , (2012)
		VvJAZ4-R	CCCTTGCGGCTAATAGCATG	
VvJAZ9	XM_002277157.1.	VvJAZ9-F	TTTACCGGGCAGAGAGCGCC	Zhang <i>et al.</i> , (2012)
		VvJAZ9-R	GATTCGGGCGTGCCGTTTCC	
VvICS	XM_019226638	VvICS-F	CTCCGCCATCTCCCACTTGAAATC	Wang (2019)
		VvICS-R	TCTTGTTGAGCGTGGAGCCAATC	
VvNPR1	GSVIVT00031933001	VvNPR1-F	GCAGGAAACAAACAAGGACAGGAT	Hou, et al. (2013)
		VvNPR1-R	CAGCCATTGTTGGTGAAGAGATTG	
VvPR1	XM_002273752	VvPR1-F	TGCTAACAGAGATTGGCGATTG	Wang (2019)
		VvPR1-R	CGCATCGGTGCCTGTCAATGAA	
VvPR10	AJ291705	VvPR10-F	CTGTGGTTGACGGAGATGTT	(Ramírez-Suero et al., 2014)
		VvPR10-R	CCCTTAACGTGCTCTTCAGAG	
VvCu.SOD1	VIT_202s0025g04830.1	VvCu.SOD1-F	GGAGCTCCTGACAGAGTTTATG	(Hu, <i>et al.</i> , 2019)
		VvCu.SOD1-R	ACCGAGAACCCTGACTACTT	
VvCu.SOD2	VIT_206s0061g00750.1	VvCu.SOD2-F	CGACTGTCTCTGTTCCGATTAC	(Hu, <i>et al.</i> , 2019)
		VvCu.SOD2-R	GGATTGAAATGTGCTCCTGTTG	
VvCu.SOD3	VIT_208s0007g07280.1	VvCu.SOD3-F	AGTGGGCAGCATTCCATT	(Hu, <i>et al.</i> , 2019)
		VvCu.SOD3-R	ACCAGCATTCCCAGTTGTT	
Vv.Mn.SOD1	VIT_00032675001	VvMn.SOD1-F	CGGAGGTCATGTCAACCACT	This paper
		VvMn.SOD1-R	ACCCAGTGAACCTTTTGGGG	
Vv.Mn.SOD1	VIT_213s0067g02990.1	VvMn.SOD2-F	GGTGGTTGAACTACTGCAAATC	(Hu, <i>et al.</i> , 2019)
		VvMn.SOD2-R	GTAATCCGGCCTCACATTCTT	
BOT	MT645701	BOT.100F	AAACTCCAGTCAGTRAAC	Ridgway et al. (2011)
		BOT.472R	TCCGAGGTCAMCCTTGAG	

8. Publications;

- Khattab, I. M., Sahi, V. S., Baltenweck, R., Maia-Grondard, A., Hugueney, P., Bieler, E., Dürrenberger, M., Riemann, M. & Peter Nick (2020). Ancestral chemotypes of cultivated grapevine with resistance to Botryosphaeriaceae-related dieback allocate metabolism towards bioactive stilbenes. *New Phytologist*, 229(2), 1133–1146. <https://doi.org/10.1111/nph.16919>
- Khattab, I. M., Fischer, J., Kazmierczak, A., Thines, E. & Peter Nick (2021). Hunting the plant surrender signal activating transition to apoplexy in Botryosphaeria related Dieback of grapevines. Submitted soon.

Note: There are parts of the thesis published in Khattab et al., *New Phytologist* (2020), including 9 figures (**Fig. 3 to Fig. 10**) and the visual model of **Fig. 25**. All experiments were performed by Islam M. Khattab. LC-MS analysis was conducted in collaboration with partners; in Philippe Hugueney lab, INRAE institute- University of Strasbourg, France, for plant metabolomics, and in Eckhard Thines lab, Institut für Biotechnologie und Wirkstoff-Forschung, Kaiserslautern (IBWF) for fungal metabolomics. All partners agree to publish the data in the thesis. The publication (Khattab et al., *New Phytologist* (2020)) was written by Islam Khattab, reviewed by co-authors and complemented by Prof. Dr. Peter Nick.

Curriculum Vitae

Islam M. Khattab, MSc.



📍 Fritz-Haber*-Weg. 4, Gbd. 30.43, (5. OG). **Postcode, 76131** Karlsruhe, Germany.

☎ +49115732506433 📠 +201116734430

✉ islam.khattab@agr.dmu.edu.eg

islam.khattab@kit.edu

khattab.islamm@gmail.com

Educational experience

• *From Sept 2006 to June 2010*

• **BSc. in Agricultural Sciences.**

Faculty of Agriculture, Alexandria University-Damanhour Branch- Egypt.

• *From Sept 2011 to June 2015*

• **MSc. In Agricultural Sciences.**

Department of Horticulture, Faculty of Agriculture, Damanhour University, Egypt.

• *From April 2017 to February 2021*

• **PhD candidate in Molecular cell biology.**

Nick lab, Botanical Institute I, Karlsruhe Institute of Technology, Germany.

Publications

- **Khattab, I. M., Fischer, J., kazmierczak, A., Thines, E. & Peter Nick. 2021.** Hunting the plant surrender signal activating transition to apoplexy in Botryosphaeria Dieback of grapevines. Submitted soon.
- **Khattab, I. M., Sahi, V. S., Baltenweck, R., Maia-Grondard, A., Huguene, P., Bieler, E., Dürrenberger, M., Riemann, M. & Peter Nick. 2020.** Ancestral chemotypes of cultivated grapevine with resistance to Botryosphaeria Dieback allocate metabolism towards bioactive stilbenes. *New Phytologist* (229) 1133–1146. doi:10.1111/nph.16919
- **Karim, M. F., Khattab, I. M., Elsapagh, A. S. & Neven M. N. Nagy. 2017.** The Effect of Controlled Deprivation of Nitrogen, Potassium and Ringing the Bearing Branches on the Incidence of Misshapen Navel Disorder and Fruit Quality in “Washington” Navel Oranges. *Assiut Journal of Agricultural Sciences*, 47(6–2), 533–545. <https://doi.org/10.21608/ajas.2017.2766>
- **Karim, M. F., Elsapagh, A. S., Neven M. N. Nagy & Khattab, I. M. 2015.** Alleviating the misshapen navel disorder in mature green fruits of “Washington” navel oranges by limited deprivation of Nitrogen, Potassium and Ringing positions. *Journal of Agricultural & Environmental Science*. (14)1